PhD Thesis

PRIMARY BIORECEPTIVITY OF GRANITIC ROCKS TO PHOTOTROPHIC BIOFILMS. DEVELOPMENT OF A BIORECEPTIVITY INDEX

Daniel Vázquez Nion

PROGRAMA DE MEDIO AMBIENTE E RECURSOS NATURAIS

DEPARTAMENTO DE EDAFOLOXÍA E QUÍMICA AGRÍCOLA

FACULTADE DE FARMACIA

SANTIAGO DE COMPOSTELA

2016

USC
UNIVERSIDADE
DE SANTIAGO
DE COMPOSTELA

AUTORIZACIÓN DO DIRECTOR DA TESE

Beatriz Prieto Lamas e Benita Silva Hermo, profesoras titulares do Departamento de Edafoloxía e Química Agrícola da Universidade de Santiago de Compostela

Como directoras da Tese de Doutoramento titulada “Primary bioreceptivity of granitic rocks to phototrophic biofilms. Development of a bioreceptivity index”, presentada por Daniel Vázquez Nion, alumno do Programa de Doutoramento Medio Ambiente e Recursos Naturais, autorizan a presentación da tese indicada, considerando que reúne os requisitos esixidos no artigo 34 do regulamento de Estudos de Doutoramento, e que como Directoras da mesma non incurren nas causas de abstención establecidas na lei 30/1992.

En Santiago de Compostela, a 1 de Setembro de 2016.

Asinado: Dra. Beatriz Prieto Lamas Dra. Benita Silva Hermo

USC
UNIVERSIDADE
DE SANTIAGO
DE COMPOSTELA

A mis padres

USC
UNIVERSIDADE
DE SANTIAGO
DE COMPOSTELA

Este trabajo fue financiado por:

Programa de axudas predoutorais financiadas polos grupos de investigación da Universidade de Santiago de Compostela no marco do Estatuto do Persoal de Investigación en Formación. Referencia: 2011/ AX461.

USC
UNIVERSIDADE
DE SANTIAGO
DE COMPOSTELA

RESUMEN

La biorreceptividad, término acuñado por Guillitte (1995), se define como 'la aptitud de un material para ser colonizado por uno o varios grupos de organismos, sin que necesariamente se produzca un biodeterioro'. Esto implica una relación ecológica entre el material y los organismos colonizadores, por lo que la biorreceptividad también puede ser definida como 'la totalidad de las propiedades de un material que contribuyen al establecimiento, fijación y desarrollo de flora y/o fauna'. Guillitte (1995) estableció diferencias dependiendo del grado de alteración del material estudiado. Así, cuando un material todavía no ha sido expuesto a la colonización, de modo que sus propiedades permanecen muy similares o idénticas a aquellas de su estado inicial, la biorreceptividad se manifiesta con la aparición de los primeros organismos colonizadores, a lo cual denominó 'biorreceptividad primaria'. Cuando las propiedades de un material evolucionan a lo largo del tiempo debido a la acción de los organismos colonizadores u otros factores ambientales, surge el concepto de 'biorreceptividad secundaria', mientras que si las propiedades de un material son modificadas de manera artificial, se podría inducir una 'biorreceptividad terciaria'. Finalmente, si se tienen en cuenta las partículas o sustancias que se pueden depositar y acumular sobre un material, podemos hablar de 'biorreceptividad extrínseca' para describir la situación en que dichos depósitos exógenos modifiquen de manera sustancial la biorreceptividad, de 'biorreceptividad semi-extrínseca' cuando la biorreceptividad depende simultáneamente de las propiedades del material y de los depósitos exógenos, y de 'biorreceptividad intrínseca' cuando la colonización depende principalmente de las características propias del material, independientemente de las contribuciones externas.

La biorreceptividad es un concepto fundamental para la conservación del patrimonio construido, la ingeniería civil y la industria de la piedra ornamental, ya que la minimización de la colonización biológica que, de manera inexorable, sufren las estructuras expuestas al ambiente, es una estrategia clave para la prevención de su subsiguiente biodeterioro, con lo que ello conlleva en términos de reducción de costes de limpieza y/o rehabilitación. En Galicia, la práctica totalidad del patrimonio monumental y la arquitectura tradicional están construidas en granito. Además, la industria granitera gallega constituye actualmente un importante recurso económico para la región, incluyendo un elevado número de canteras de extracción e industrias

manufactureras, que la convierten en un referente del sector tanto a nivel nacional como internacional. El estudio de la biorreceptividad del granito es por lo tanto de especial relevancia para Galicia.

El conocimiento actual sobre la biorreceptividad de las rocas es incompleto y está fragmentado, por lo que la influencia de las propiedades intrínsecas de las rocas sobre su biorreceptividad requiere de una mayor investigación. Según algunos autores, la colonización biológica de las rocas está principalmente asociada con sus características físicas, mientras que otros encuentran una mayor relación con su composición química. En una reciente revisión del tema, Miller et al. (2012) llegaron a la conclusión de que, de manera general, la caracterización de algunas propiedades como la rugosidad superficial, la porosidad y la composición mineralógica debe ser considerada esencial para la evaluación de la biorreceptividad de las rocas. Los estudios de biorreceptividad primaria relacionados específicamente con el granito son relativamente escasos. Prieto & Silva (2005) hallaron que el grado de colonización alcanzado por varios tipos de granito estaba principalmente influenciado por la rugosidad superficial de la roca, además de por cuatro propiedades intrínsecas de la misma: el pH de abrasión, la densidad aparente, la porosidad abierta y la absorción de agua por capilaridad. Tiano et al. (1995) llevaron a cabo un estudio en el que se observó un granito con una elevada biorreceptividad en comparación con varias calizas, mármoles y areniscas, lo cual fue atribuido a la heterogeneidad de su composición química. En un trabajo realizado por Miller et al. (2006), en cambio, se encontró un granito poco susceptible a la colonización biológica en comparación con otras rocas carbonatadas, y la presencia de elementos tóxicos para los microorganismos fue sugerido como posible causa. Marques et al. (2015) estudiaron un granito con una baja biorreceptividad respecto a varios esquistos, los cuales mostraron un menor pH de abrasión y coeficiente de capilaridad y una mayor densidad aparente que el granito. Aunque estos estudios han proporcionado información muy valiosa sobre algunas de las características que influyen en la susceptibilidad del granito a ser colonizado y han establecido las primeras comparaciones con otros tipos de rocas, es claramente necesario ampliar la investigación para superar muchas incógnitas aún no resueltas. Esto permitiría minimizar (o maximizar en determinados casos) la colonización sufrida por edificios y monumentos construidos con granito mediante la selección de los materiales en función

de su biorreceptividad, lo cual, como ya se ha mencionado, se puede considerar como una estrategia clave en la prevención de su posterior biodeterioro.

El principal objetivo de la presente tesis doctoral es precisamente profundizar en el conocimiento de la biorreceptividad primaria de las rocas graníticas, con el fin de desarrollar un índice de biorreceptividad que pueda ser utilizado como herramienta para la selección de granitos en trabajos de construcción. El cumplimiento de este objetivo requiere de un estudio complejo en el que se deben tener en cuenta varias consideraciones clave. Así, el cultivo biológico utilizado como inóculo para los experimentos de biorreceptividad debe representar lo más fielmente posible a una colonización natural de estas rocas, por lo que debería estar formado por una comunidad microbiana compleja de colonizadores pioneros capaces de formar biofilms subaéreos, principalmente algas verdes (clorófitas) y cianobacterias, los cuales sirven de base para el posterior establecimiento de organismos heterótrofos. Las condiciones experimentales para la formación y crecimiento de estos biofilms fotótroficos en laboratorio deben ser óptimas, de modo que las propiedades intrínsecas de las rocas, relacionadas con su biorreceptividad, puedan ser evaluadas de manera eficiente. Las técnicas utilizadas para la cuantificación del crecimiento de los biofilms deben ser escogidas, y desarrolladas si fuera necesario, para producir información útil y veraz sobre el proceso de colonización de la roca. Además, la aplicación de un experimento de biorreceptividad estandarizado permitiría el desarrollo de un índice de biorreceptividad, el cual todavía no ha sido establecido para ningún material, y que proporcionaría la posibilidad de clasificar las rocas en una escala de acuerdo a su susceptibilidad a la colonización biológica.

Teniendo en cuenta estas consideraciones metodológicas, el desarrollo experimental del presente trabajo comenzó con el análisis de cinco biofilms subaéreos desarrollados de forma natural sobre la superficie de edificios históricos construidos con granito en la ciudad de Santiago de Compostela, con el fin de conocer su composición y diversidad microbiana. El estudio de estos biofilms se llevó a cabo mediante ‘environmental barcoding’, utilizando para ello técnicas de secuenciación de próxima generación (Pacific Biosciences). El análisis de los resultados reveló la presencia de comunidades microbianas complejas, compuestas principalmente por especies de algas clorófitas y de hongos ascomicetos, colonizadores habituales de sustratos rocosos. La riqueza específica y diversidad estimadas resultaron mayores para las comunidades de

hongos que para las de algas, y asimismo, los hongos mostraron una mayor heterogeneidad entre las diferentes muestras. Los datos obtenidos confirmaron la idea general de que los biofilms subaéreos son ecosistemas con una diversidad de algas relativamente baja, así como la ubicuidad de muchas de las especies más comunes. El alto número de OTUs (por sus siglas en inglés, unidades taxonómicas operacionales) sin identificar obtenidos también puso en evidencia la necesidad de incrementar la representación de los microorganismos formadores de biofilms subaéreos en las bases de datos de secuenciación de ADN.

Las muestras de los biofilms naturales recogidas fueron a su vez cultivadas en medio de cultivo BG11 líquido, especialmente diseñado para el desarrollo de organismos fototróficos, con el fin de obtener inóculos para ser utilizados en el posterior experimento de biorreceptividad de los granitos. Fue necesario un año de incubación para la obtención de cultivos con comunidades microbianas estables. Los cultivos fototróficos multiespecie finalmente obtenidos mostraron una composición microbiana bastante diferente de los biofilms naturales de los que provenían. Esto no es sorprendente, ya que el medio de cultivo empleado propició la proliferación de los organismos fotótrofos, por lo que en ninguno de los cinco cultivos fueron detectadas especies fúngicas. Además, al realizar el cultivo en medio líquido, los organismos tuvieron que adaptarse desde un estado en forma de biofilm a un estado planctónico, lo que sin duda produjo que unas especies proliferaran en detrimento de otras. Así, la caracterización taxonómica de los cultivos reveló que estos estaban formados principalmente por especies de algas clorófitas y cianobacterias. Aunque estas especies no conformaban una parte significativa de los biofilms naturales muestreados, sí que son consideradas como colonizadores pioneros habituales de rocas en edificios y monumentos, incluyendo los construidos con granito, por lo que se concluyó que los cultivos son adecuados para ser utilizados como inóculos para reproducir una colonización de estas rocas en laboratorio.

El siguiente paso fue el diseño de un procedimiento experimental para un óptimo crecimiento de biofilms subaéreos sobre granito en laboratorio. Esto permitiría, por una parte, una evaluación eficaz de las propiedades del granito que influyen en su biorreceptividad, y en segundo lugar, la estandarización de un protocolo experimental para el desarrollo de biofilms. Con este fin, se realizó la inoculación de probetas de granito con los diferentes cultivos en fase de crecimiento exponencial y estas se

sometieron a condiciones ambientales controladas dentro de una cámara climática. Las condiciones ensayadas, consistentes en una temperatura de 23ºC, una luz de ~20 µmol photon m^{-2} s^{-1} en un fotoperiodo luz/oscuridad de 12 horas, proporcionada por lámparas fluorescentes, una humedad relativa del ~95% y un aporte permanente de agua a las probetas por capilaridad, resultaron ser adecuadas para el desarrollo de biofilms en un periodo de tres meses.

Para evaluar el potencial de cada uno de los cultivos estudiados, con el fin de ser utilizados como inóculos en experimentos de biorreceptividad, se tuvieron en cuenta unos determinados criterios. En primer lugar, el cultivo debe estar formado por una comunidad microbiana compleja capaz de adaptarse al sustrato granítico y emular una colonización natural. Además, el tiempo necesario para que el biofilm formado alcance un estado estacionario debe ser razonablemente corto, ya que esta fase de crecimiento es la más adecuada para la comparación de muestras en un estudio de biorreceptividad. Por último, es importante que el grado de colonización alcanzado sea el mayor posible, ya que un cultivo capaz de formar biofilms densamente poblados mejoraría la sensibilidad a la hora de establecer comparaciones entre diferentes muestras. Los resultados obtenidos de los biofilms desarrollados a partir de los diferentes cultivos señalaron a uno de ellos (cultivo C5) como el idóneo para su uso en experimentos de biorreceptividad. Este cultivo, compuesto de varias especies que incluyen briófitas (protonemas de *Syntrichia ruralis*), carófitas (*Klebsormidium* sp.), clorófitas (*Bracteacoccus* sp., *Chlamydomonas* sp., *Chlorella* sp. y *Stichococcus bacillaris*) y cianobacterias (*Aphanocapsa* sp. y *Leptolyngbya cebennensis*), demostró ser especialmente adecuado para este propósito debido principalmente a su riqueza microbiana, su rápida adaptabilidad al sustrato y su alta capacidad de colonización. De este modo, se obtuvo un inóculo capaz de emular una colonización natural del granito y se desarrolló un protocolo estandarizado para la formación de biofilms, requisitos considerados como esenciales para poder avanzar en el estudio de la biorreceptividad.

Paralelamente a estas tareas, se diseñó un método para la extracción de EPS de biofilms desarrollados sobre rocas, ya que actualmente no existen referencias sobre ningún protocolo al respecto. Es importante contar con un procedimiento de extracción eficiente que permita la caracterización y cuantificación de los EPS en este tipo de biofilms, ya que sería de gran utilidad para mejorar el conocimiento del proceso de colonización de las superficies rocosas. Con este propósito, se analizó la eficacia de dos

extractantes, NaOH y H_2SO_4, a diferentes concentraciones, temperaturas y tiempos de extracción, para obtener EPS de biofilms subaéreos multiespecie desarrollados sobre probetas de granito en laboratorio. Se utilizaron dos diseños experimentales para cada extractante: un diseño Box-Behnken, considerando la concentración de extractante, la temperatura y el tiempo de extracción como variables independientes, y un diseño factorial completo, considerando solamente la concentración y el tiempo como variables independientes, a una temperatura constante de 4ºC, ya que el calentamiento podría provocar la disrupción de los EPS y/o la lisis celular. La eficiencia de las extracciones llevadas a cabo fue evaluada analizando los contenidos de carbohidratos y proteínas en los extractos, principales componentes de los EPS, así como el contenido en ADN, indicativo de lisis celular a altas concentraciones. Los resultados obtenidos demostraron que el H_2SO_4 no resultó un extractante adecuado, ya que provocó una lisis celular excesiva, principal problema encontrado en el desarrollo del método. En cambio, utilizando una extracción con NaOH a baja temperatura se consiguió minimizar la lisis celular a niveles aceptables mediante metodología de superficie de respuesta.

El protocolo de extracción finalmente desarrollado se resume a continuación. La probeta de granito con biofilm se coloca sobre una placa Petri con la superficie colonizada hacia abajo. Se mantiene un nivel de agua destilada suficiente para asegurar un contacto completo con el biofilm y se añaden 6 µL mL^{-1} de formaldehído (37% en peso). La placa Petri se sella y se mantiene a 4ºC durante 60 min. Posteriormente, se añade 0.2 mL mL^{-1} de una solución de NaOH 2.5 mol L^{-1} y se mantiene a 4ºC durante 120 min. El extracto obtenido se centrifuga a 5000 rpm durante 20 min y el sobrenadante se filtra a través de discos de 0.20 µm de tamaño de poro. El filtrado con los EPS extraídos se recoge para la realización de los análisis químicos correspondientes.

Se llevaron a cabo experimentos para comprobar la validez del protocolo optimizado, obteniéndose así los primeros datos cuantitativos de EPS extraídos de biofilms subaéreos sobre sustrato rocoso. Los resultados mostraron una relación PN/PS con valores entre 0,06 y 0,60. Estos valores son mucho menores que los encontrados en otros tipos de biofilms por otros autores, lo que sugiere que los biofilms subaéreos pueden producir mayores cantidades de carbohidratos para favorecer la retención de agua y así permitir su supervivencia en periodos de desecación. Posteriormente, el protocolo diseñado se aplicó a biofilms desarrollados sobre diferentes variedades de

granitos y utilizando diferentes cultivos como inóculo, lo que permitió llegar a una serie de conclusiones relevantes. Las cantidades de EPS producidos por los biofilms subaéreos dependen principalmente de los requerimientos y/o características de los organismos formadores del biofilm, y no de la biorreceptividad del sustrato, ya que ni el tipo de granito ni la rugosidad superficial afectaron significativamente a la cantidad de EPS encontrados. En cambio, el uso como inóculo de diferentes cultivos, formados por diferentes comunidades microbianas, sí produjo cantidades significativamente diferentes de EPS. Además, se observó que los contenidos de EPS no varían significativamente con el tiempo a partir del primer mes de incubación de los biofilms, lo que sugiere que los microorganismos producen los EPS requeridos para su desarrollo al comienzo de la colonización de la roca, y su producción no aumenta significativamente durante su posterior crecimiento. Estos resultados tienen una especial relevancia para comprender el proceso de biodeterioro de la piedra debido a organismos formadores de biofilms, en el cual los EPS tienen un papel central, ya que los ciclos de humectación y secado que habitualmente ocurren en las superficies de los edificios provocan el hinchamiento y contracción de la matriz de EPS, lo cual ejerce presiones mecánicas en la estructura de la roca, y lleva finalmente a la aparición de fisuras y a su desagregación.

Una vez puesta a punto la metodología necesaria, se llevó a cabo el experimento central de la tesis, el cual consistió en un estudio completo de la biorreceptividad primaria de once variedades de rocas graníticas, utilizadas habitualmente como materiales de construcción y/o rocas ornamentales. Uno de los granitos fue además sometido a cuatro acabados superficiales diferentes, con el fin de estudiar el efecto de la rugosidad superficial de la roca sobre la biorreceptividad. El cultivo fototrófico multiespecie utilizado como inóculo (cultivo C5), así como el procedimiento experimental estandarizado diseñado para el desarrollo de biofilms en laboratorio, permitieron además utilizar los datos obtenidos para el desarrollo un índice de biorreceptividad para rocas graníticas. La fluorescencia clorofílica y las medidas de color, técnicas utilizadas para la monitorización del crecimiento de los biofilms subaéreos en el experimento, proporcionaron información complementaria relativa a dos aspectos de la colonización biológica. La fluorescencia clorofílica permitió estimar la biomasa fototrófica de los biofilms formados, así como evaluar su estado fisiológico, mientras que las medidas de color permitieron cuantificar el impacto estético que los biofilms provocaron sobre la superficie de los granitos, lo que demostró estar

correlacionado con la claridad inicial de la roca y no con el grado de colonización alcanzado.

Los contenidos de chl *a* encontrados en los biofilms, derivados de las medidas de fluorescencia clorofílica, mostraron diferencias significativas en el grado de colonización alcanzado para las diferentes variedades de granito, así como para las rugosidades superficiales analizadas. Los granitos estudiados también mostraron diferencias significativas en sus propiedades físicas y químicas, por lo que fue posible establecer relaciones entre estas propiedades y la biorreceptividad de las rocas. Los resultados obtenidos mediante el tratamiento estadístico de los datos permitieron concluir que la biorreceptividad primaria de las rocas graníticas está determinada en mayor grado por las propiedades físicas que por la composición química de la roca. El crecimiento de los biofilms fototróficos sobre las probetas fue potenciado en gran medida por valores altos de porosidad abierta, contenido de agua capilar y rugosidad superficial. La porosidad y capilaridad están relacionadas con el movimiento y almacenamiento de agua dentro de la roca, un recurso imprescindible para el desarrollo biológico, mientras que la rugosidad favorece el anclaje y establecimiento de los microorganismos sobre la superficie de la misma. De este modo, los granitos que presentaron un cierto grado de alteración mineral, lo cual está asociado con valores elevados de estas propiedades, mostraron una mayor biorreceptividad que los granitos considerados sanos.

Las consideraciones metodológicas tenidas en cuenta a lo largo del estudio permitieron el desarrollo de un índice de biorreceptividad (*BI*, por sus siglas en inglés) robusto y fundamentado, cumpliendo así el principal objetivo de la presente tesis. El *BI* propuesto está formado por dos componentes: BI_{growth}, diseñado para cuantificar el grado de colonización de los granitos, y BI_{colour}, diseñado para cuantificar el cambio de color producido en la roca como consecuencia de dicha colonización, y que puede ser considerado como la biorreceptividad perceptible al ojo humano. La ecuación propuesta para el cálculo del *BI* es la siguiente:

$$BI = \frac{2 \cdot BI_{growth} + BI_{colour}}{3}$$

siendo:

$$BI_{growth} = 10 \cdot \frac{chl\ a\ (\mu g\ cm^{-2})}{4.14\ \mu g\ cm^{-2}} \qquad BI_{colour} = 10 \cdot \frac{\Delta E^*_{ab}}{24.25}$$

donde chl *a* y ΔE^*_{ab} son los valores de clorofila *a* y diferencia de color, respectivamente, producidos por el biofilm formado sobre la roca en estudio tras la realización del experimento de biorreceptividad estandarizado. Los valores de *BI*, así como los de BI_{growth} y BI_{colour}, fueron ajustados a una escala 0-10, la cual puede ser usada para clasificar cualitativamente los granitos en función de su biorreceptividad primaria, como se muestra en la siguiente tabla:

Índice de biorreceptividad (*BI*)	Asignación cualitativa
$BI \leq 2$	Biorreceptividad muy baja
$2 < BI \leq 4$	Biorreceptividad baja
$4 < BI \leq 6$	Biorreceptividad media
$6 < BI \leq 8$	Biorreceptividad alta
$BI > 8$	Biorreceptividad muy alta

En cuanto a los resultados del *BI* calculado para los diferentes granitos estudiados, todos ellos con un acabado superficial apomazado, se encontró que el Silvestre AM fue el único clasificado con biorreceptividad muy alta. A continuación se situaron los granitos Silvestre Ribadavia, Silvestre Ingemar, Rosa Porriño, Blanco Castilla, Blanco Cristal, Mondariz y Rosavel, con una biorreceptividad media, y Grissal y Labrador Claro con una biorreceptividad baja. El Negro Sudáfrica fue el único que mostró una biorreceptividad muy baja. Es preciso mencionar que tanto el Labrador Claro como el Negro Sudáfrica no pueden ser petrológicamente clasificados como granitos, sino que se clasifican como monzonita y gabro, respectivamente, pero fueron incluidos de todos modos en el estudio debido a que son comercializados bajo la denominación de granitos en el ámbito de las rocas ornamentales. En el caso del granito Silvestre Ingemar, que fue sometido a diferentes acabados superficiales, se observó un incremento del *BI* desde una biorreceptividad baja (con acabado pulido) hasta una biorreceptividad muy alta (con acabado arenado) como consecuencia de un incremento de la rugosidad superficial, lo que refleja la fuerte influencia de esta propiedad. La porosidad abierta y el contenido en agua capilar, características que también afectan en gran medida a la biorreceptividad, son propiedades inherentes a la roca y por lo tanto no pueden ser manipuladas. Sin

embargo, la rugosidad superficial puede ser modificada dependiendo del acabado superficial aplicado, por lo que la selección de acabados lisos podría ayudar a minimizar la colonización biológica de granitos muy biorreceptivos.

Las consideraciones metodológicas que deben ser tenidas en cuenta en el cálculo del *BI* para nuevas rocas, con el fin de clasificarlas dentro de la escala propuesta, se pueden resumir de la siguiente manera. Las probetas deberán ser inoculadas con un cultivo fototrófico multiespecie capaz de adaptarse al sustrato y emular una colonización natural, y la cantidad inoculada deberá ser lo más parecida posible a la empleada en el presente estudio (1.51 mg de biomasa seca en fase de crecimiento exponencial para una superficie de 16 cm^2, o equivalente). Las probetas inoculadas deberán ser sometidas a las condiciones de crecimiento estandarizadas descritas (23ºC de temperatura, iluminación con lámparas fluorescentes a ~20 µmol fotón m^{-2} s^{-1} en un fotoperiodo de luz/oscuridad de 12h, ~95% de humedad relativa y acceso a agua permanente por capilaridad) durante tres meses. Los valores del contenido en chl *a* (µg cm^{-2}) y ΔE^*_{ab} de los biofilms formados al final del periodo de colonización podrán ser entonces utilizados para el cálculo del *BI*.

Los resultados obtenidos en la presente tesis doctoral ofrecen nuevas posibilidades de investigación relativas al estudio de la biorreceptividad de las rocas. La principal perspectiva de futuro derivada de este trabajo es la aplicación del protocolo desarrollado para el cálculo del *BI* a tantos litotipos como sea posible, tanto granitos como otros tipos de rocas, lo que permitiría la creación de una base de datos sobre la biorreceptividad primaria de estos materiales. En este sentido, el concepto de *BI* propuesto, así como los valores obtenidos, deberán ser exportados a los usuarios finales (p.ej. conservadores/restauradores, arquitectos, ingenieros y distribuidores de rocas ornamentales y de construcción) para su aplicación práctica. La fácil comprensión de los valores del *BI*, que clasifica las rocas en una escala 0-10 asociada a su biorreceptividad, permitiría entonces su aplicación como herramienta para la toma de decisiones en la selección de materiales adecuados para su uso en nuevas construcciones y/o sustituciones en estructuras existentes.

Palabras clave

Biofilm; biorreceptividad; cultivo multiespecie; EPS; granito; índice de biorreceptividad.

Referencias

Guillitte O. 1995. Bioreceptivity: a new concept for building ecology studies. Science of the Total Environment 167: 215-220.

Marques J, Vázquez-Nion D, Paz-Bermúdez G, Prieto B. 2015. The susceptibility of weathered versus unweathered schist to biological colonization in the Côa Valley Archaeological Park (north-east Portugal). Environmental Microbiology 17: 1805-1816.

Miller A, Dionísio A, Macedo MF. 2006. Primary bioreceptivity: a comparative study of different Portuguese lithotypes. International Biodeterioration & Biodegradation 57: 136-142.

Miller AZ, Sanmartín P, Pereira-Pardo L, Dionísio A, Saiz-Jimenez C, Macedo MF, Prieto B. 2012. Bioreceptivity of building stones: A review. Science of the Total Environment 426: 1-12.

Prieto B, Silva B. 2005. Estimation of the potential bioreceptivity of granitic rocks from their intrinsic properties. International Biodeterioration & Biodegradation 56: 206-215.

Tiano P, Accolla P, Tomaselli L. 1995. Phototrophic biodeteriogens on lithoid surfaces: an ecological study. Microbial Ecology 29: 299-309.

USC
UNIVERSIDADE
DE SANTIAGO
DE COMPOSTELA

CONTENTS

USC
UNIVERSIDADE
DE SANTIAGO
DE COMPOSTELA

SUMMARY

The main objective of this PhD thesis was to undertake a comprehensive study of the primary bioreceptivity to phototrophic biofilms in various types of granitic rock commonly used as building material and/or ornamental stone, thus enabling development of a bioreceptivity index.

The microbial communities forming the subaerial biofilms that grow naturally on several granite historic buildings in Santiago de Compostela (NW Spain) were characterised using next-generation sequencing (Pacific Biosciences) techniques for environmental barcoding. This revealed complex microbial communities mainly comprising species of Chlorophyta (green algae) and Ascomycota (fungi) that are commonly associated with rocky substrata. The estimated species richness and diversity were higher for the fungal assemblages than for algae, and fungal samples were more heterogeneous. The data supported the assumption that subaerial biofilms are ecosystems with relatively low algal diversity and that many of the species common to the biofilms are ubiquitous.

Multi-species phototrophic cultures derived from biofilms comprising common pioneer colonisers of granite rocks were found to be capable of forming subaerial biofilms on granite in a clearly defined, laboratory-based experimental protocol. One of the cultures proved particularly suitable for bioreceptivity studies, mainly owing to its microbial richness, rapid adaptability to the substratum and high capacity for colonization. An inoculum capable of inducing environmental-like colonisation of

granite and a standardised laboratory protocol for biofilm formation (both essential for correct assessment of bioreceptivity) were successfully developed.

A method for extracting EPS from subaerial biofilms growing on stone surfaces was also designed and optimized. Application of this method revealed that the amounts of EPS produced by subaerial biofilms mainly depended on the requirements and/or characteristics of the biofilm-forming microorganisms rather than on the bioreceptivity of the substratum. Moreover, microorganisms were found to produce the amounts of EPS they require at the initial stage of establishment on the stone surface, independently of subsequent biomass development.

Finally, a comprehensive evaluation of the primary bioreceptivity of several varieties of granite was carried out. Chlorophyll fluorescence analysis enabled estimation of the phototrophic biomass of subaerial biofilms formed and assessment of their photosynthetic performance. Colour measurements enabled quantification of the aesthetic impact of biofilm growth on granite surfaces, which was more closely correlated with the initial lightness of the stone than with the final biomass of the biofilm. The bioreceptivity of the granites was more strongly affected by the physical characteristics of the stones than by their chemical composition. Growth of phototrophic biofilms was strongly enhanced by high open porosity, capillary water content and surface roughness, and the bioreceptivity of weathered granites was higher than that of sound granites.

The findings of the study enabled us to develop a robust and well-founded bioreceptivity index (*BI*) for granitic rocks. The proposed *BI* has two components: BI_{growth}, which quantifies the extent of the biological growth, and BI_{colour}, which quantifies the colour change undergone by the stone due to the colonisation and which can be considered the bioreceptivity perceptible by the human eye. The values of *BI*, BI_{growth} and BI_{colour} were fitted to a scale of 0-10, thus enabling qualitative classification of the lithotypes according to their primary bioreceptivity. The index can therefore be used as a decision-making tool for selection of appropriate lithotypes for building and/or ornamental purposes.

CHAPTER 1
GENERAL INTRODUCTION

Freshly exposed rock surfaces are rapidly colonised by microbial communities that can form subaerial biofilms. Biofilm formation begins with adhesion of the microorganisms to the rock substrate. The primary colonisers associate with cells of the same and of metabolically cooperative species to form aggregates via secretion of extracellular polymeric substances (EPS) (Costerton 2007). The EPS matrix, which is mainly composed of polysaccharides, proteins, nucleic acids and lipids, provides mechanical stability to biofilms, mediates their adhesion to surfaces and forms a cohesive, three-dimensional polymeric network that interconnects and transiently immobilizes biofilm cells. The biofilm matrix also acts as an external digestive system by keeping extracellular enzymes close to the cells, enabling them to metabolize dissolved, colloidal and solid biopolymers. The EPS matrix thus contributes to making biofilms the most successful forms of life on Earth (Fleming & Wingender 2010).

Subaerial biofilms on rocky substrata are ubiquitous, self-sufficient microbial ecosystems that are in direct contact with the atmosphere and solar radiation. The microbial communities in subaerial biofilms are composed of a variety of microorganisms, mainly algae, cyanobacteria, bacteria and fungi (Figure 1.1). According to several authors (e.g. Ortega-Calvo et al. 1991, Tiano et al. 1995, Crispim & Gaylarde 2005), cyanobacteria and green algae (chlorophyta) are considered pioneer taxa in the colonisation of stone. These phototrophic organisms build up a visible protective biofilm enriched with inorganic compounds and organic biomass on the stone surface, thus providing an excellent nutrient base for subsequent growth of

heterotrophic microflora (Warscheid & Braams 2000). Inhabitants of subaerial biofilms are in close contact with one another and cooperate extensively, especially to avoid loss of energy and nutrients, in a process resembling symbiosis. The metabolic activity of subaerial biofilms centres on retaining water, thus protecting the cells from fluctuating environmental conditions and solar radiation as well as prolonging their vegetative life (Gorbushina 2007).

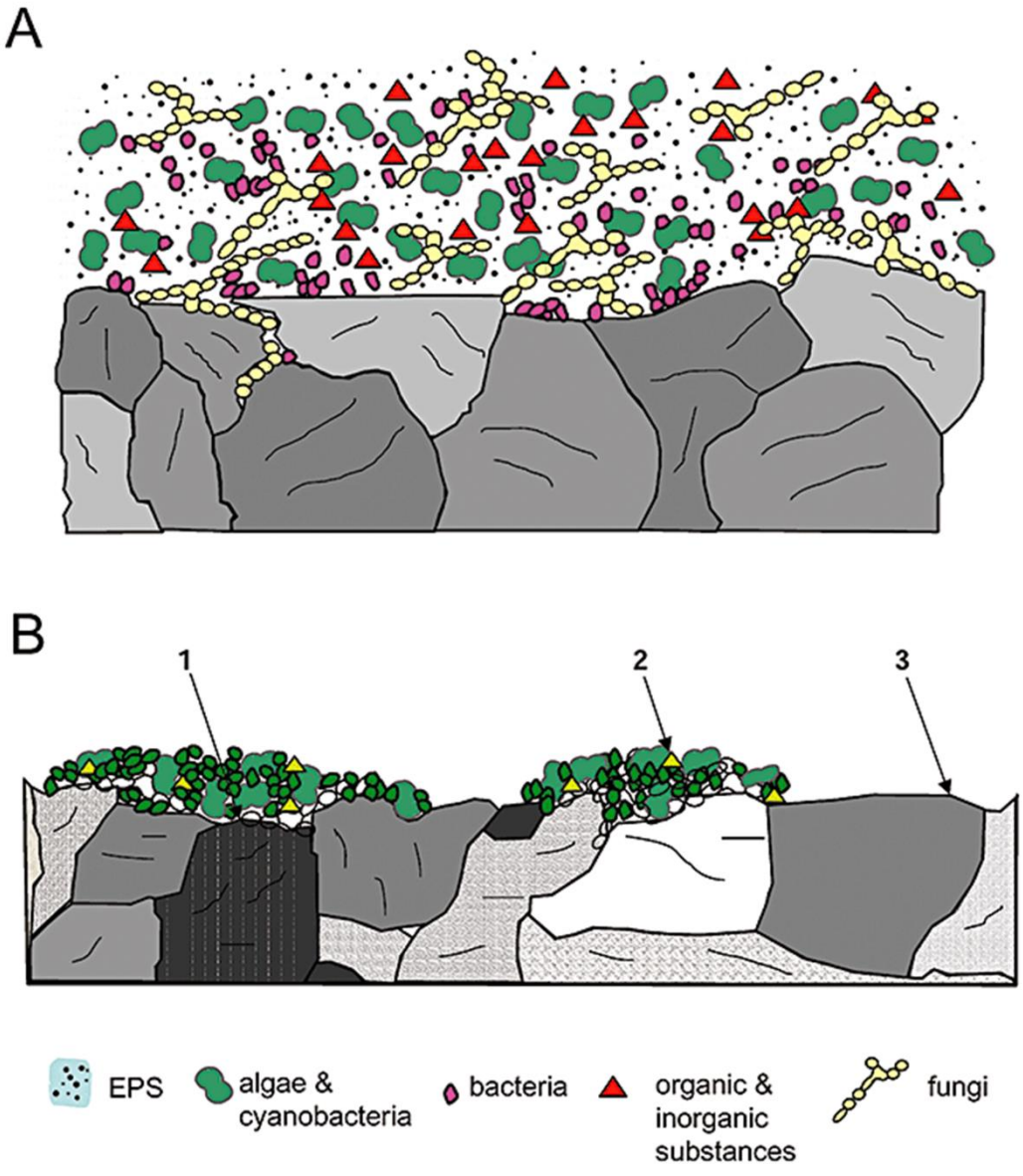

Figure 1.1 Schematic representation of subaerial biofilms and their interactions (adapted from Gorbushina 2007). A) Microorganisms are embedded in EPS and form a miniature microbial ecosystem including both heterotrophic and phototrophic settlers. B) Subaerial biofilms act as coupling agents between the lithosphere and atmosphere. Effects seen at the interface include 1) biofilm-substrate interactions; 2) biofilm-atmosphere interactions; 3) atmosphere-substrate interactions.

In urban habitats, the surfaces of many stone buildings are exposed to full sunlight, and the organisms growing on such surfaces are therefore frequently subjected to extremely high levels of light irradiance and UV radiation and extreme dehydration (Crispim & Gaylarde 2005). Most urban habitats are also strongly affected by pollutants such as gases (SO_2, CO, NO_X, hydrocarbons, ozone), aerosols, dusts and heavy metals. As a result of the negative effects of the combination of these different factors, urban buildings can be considered extreme environments (Rindi 2007). Vital biofilm connections at the atmosphere-rock interface are stimulated by the stresses that all members have to bear (Gorbushina & Broughton 2009). If these stresses persist, microbes will dominate the biomass, while under more favourable conditions, macroscopic vegetation will succeed (Chertov et al. 2004).

Biological colonisation of rocks can lead to weathering, precipitation of minerals and protection of surfaces from erosion. Microbial life therefore plays a central role in many geomorphological processes and has an important influence on shaping the surface of the Earth (Viles 2012). When the colonisation takes place on man-made stone surfaces such as buildings and monuments, microbial growth often leads to aesthetic and/or physico-chemical decay. Damage to stone produced by microorganisms is often referred to as biodeterioration (see Warscheid & Braams 2000, McNamara & Mitchell 2005 and Scheerer et al. 2009 for reviews), which can severely alter stone structures. Hence, while rock weathering in the natural environment is unquestionably essential for life on Earth (e.g. for soil formation), biodeterioration of stone buildings may result in high conservation and repair costs and also in irretrievable loss of heritage and history represented by culturally significant stone artefacts (Warscheid & Braams 2000, Prieto & Sanmartín 2016, Villa et al. 2016; Figure 1.2A). In this context, minimization of the colonisation undergone by stone structures should be considered a key strategy for preventing biodeterioration. The extent to which a stone surface is biologically colonised depends on environmental factors and also on the intrinsic properties of the material (i.e. two different types of stone may undergo different degrees of colonisation under the same environmental conditions; Miller et al. 2012). The choice of lithotype used for construction and/or replacement of material in stone-made heritage should therefore take into account the susceptibility of the stone to being colonised. On the other hand, microbial colonisation of buildings is sometimes considered to be aesthetically desirable (Figure 1.2B), to provide protection against some types of

weathering (Viles & Cutler 2012, Bartoli et al. 2014) and to be beneficial to the environment (Pérez et al. 2014, Manso et al. 2015). The choice of the lithotype may therefore also focus on enhancing the susceptibility to colonisation.

Figure 1.2 Biological colonisation of facades: A) View of the Cathedral of Santiago de Compostela (Spain) during restoration work to remove extensive lichen colonisation; B) Wall colonised by living plants in Madrid (Spain).

1.1 BIORECEPTIVITY: BASIC DEFINITIONS

The term 'bioreceptivity' was introduced by Guillitte (1995) as an alternative to the term 'susceptibility' for use in the field of building ecology. It is defined as 'the aptitude of a material to be colonised by one or several groups of living organisms without necessarily undergoing any biodeterioration', which implies an ecological relationship between the material and the colonizing organisms. Bioreceptivity can therefore also be defined as 'the totality of material properties that contribute to the establishment, anchorage and development of fauna and/or flora'.

Guillitte (1995) also established differences that depend on the degree of alteration of the material under study. Hence, when a material has not yet been exposed to colonisation, so that its properties remain very similar or identical to those in the initial state, the bioreceptivity will only be expressed during appearance of the first colonizing organisms and is termed 'primary bioreceptivity'. In stone, primary bioreceptivity

indicates the initial potential of freshly cut quarry rocks to be colonised. When the properties of a material evolve over time under the action of colonizing organisms or other environmental factors, it may result in a different kind of bioreceptivity, called 'secondary bioreceptivity', involving weathered rocks. When the properties of the material are modified by artificial treatment, such as the coatings or consolidation treatments commonly used on rocks, 'tertiary bioreceptivity' can be induced.

Taking into account that particles or substances can be deposited and accumulate on a material (e.g. soil, dust or pollutants), the term 'extrinsic bioreceptivity' can be used to describe the situation in which these exogenous deposits substantially modify the conditions of bioreceptivity. 'Semi-extrinsic bioreceptivity' describes a type of bioreceptivity that depends directly and simultaneously on the properties of the material and on the deposits of exogenous substances, e.g. when the vegetation colonizing the material is colonised by epiphytes or is parasitized by other organisms. Finally, when colonisation mainly depends on the properties of the material, irrespective of exogenous contributions, the term 'intrinsic bioreceptivity' is proposed. Figure 1.3 shows a schematic overview of the definition and variants of the bioreceptivity concept developed by Guillitte (1995).

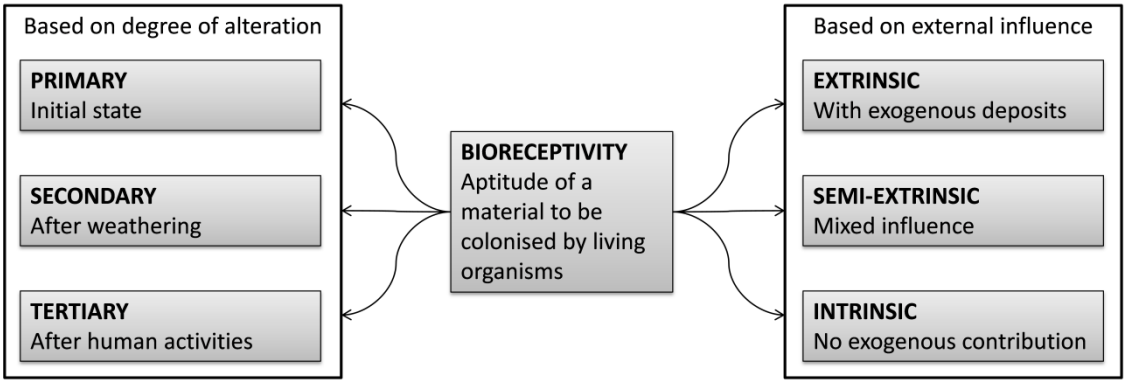

Figure 1.3 Bioreceptivity concepts

1.2 METHODOLOGICAL CONSIDERATIONS FOR THE STUDY OF BIORECEPTIVITY

According to Guillitte (1995), bioreceptivity expresses the colonisation potential as defined by the characteristics of the material under study, regardless of the colonisation potential of the environment in which the material is found. Both the bioreceptivity of

the material and the environmental conditions will determine whether colonisation will occur, and the absence of some factors will hamper or prevent colonisation. Settlement and growth of subaerial biofilms are affected by environmental factors such as water availability, temperature, light, wind and presence of atmospheric pollutants, which can in turn be affected by parameters such as the orientation of the stone surface, shading and proximity to the ground or contamination sources. The presence of water is essential for the development of any organism. In any experimental set-up designed for studying bioreceptivity, optimal water input will enable properties related to the absorption and movement of water through the stone pore structure to be evaluated, and the bioreceptivity of the stone will thus be taken into account. For an integrated approach to evaluating the potential colonisation of materials, bioreceptivity will be best expressed under optimal environmental conditions for the development of organisms.

In order to assess the bioreceptivity of a material to a particular type of microorganism, Guillitte (1995) proposed inoculating the material with diaspores of the microorganism and then incubating the inoculated material under optimal environmental conditions. As most types of colonisation occur as part of a synergistic process, colonisation by a single type of organism may either become impossible or completely atypical. The bioreceptivity of materials can thus be determined with species belonging to the major biological groups that colonise the material under study. A practical approach for evaluating the bioreceptivity of several building materials (including natural rocks, mortars and bricks) was applied by Guillitte & Dreesen (1995), who used a mixture of cyanobacteria, green algae, diatoms and mosses as inoculum and quantified the surface colonisation over a 9-month period.

Finally, Guillitte (1995) recommended carrying out integrated multidisciplinary studies under standardized (as far as possible) experimental conditions, using bioreceptivity tests similar to those used to determine the physico-chemical properties of materials. Development of a bioreceptivity index, which could be included in a scale, was encouraged. The bioreceptivity index of a material would provide users with information about the colonisation risk and help them choose a material depending on whether or not colonisation is desirable. Such an index could also provide information about the effectiveness of different treatments or could be used to provide weighted biotic indices determined using different materials. More recently, Miller et al. (2012) also indicated the need to standardise laboratory protocols. This would enable

generation of a database concerning the primary bioreceptivity of lithotypes used in building construction, as well as the definition of bioreceptivity index that could be included in ornamental rock catalogues and could be used as a decision-making tool for selecting appropriate lithotypes for use in new constructions and replacement of materials in existing structures.

1.3 STONE BIORECEPTIVITY EXPERIMENTS

Several studies have investigated the bioreceptivity of stone materials (see Miller et al. 2012 for a review). Most of these have been carried out under laboratory conditions in order to assess the primary bioreceptivity of different types of construction material, as proposed by Guillitte (1995). Studies focused on laboratory-based primary bioreceptivity tests are summarised in Table 1.1.

Table 1.1 Laboratory-based primary bioreceptivity experiments carried out by different researchers. Adapted and updated from Miller et al. (2012).

Lithotypes studied	Organisms tested	Biomass quantification technique used	Reference
Limestone, mortar, brick	Mixture of cyanobacteria, green algae, diatoms and mosses	Surface area covered (%) by macroscopic observation and optical microscopy	Guillitte & Dreesen (1995)
Limestone, marble, dolomite, travertine, sandstone, granite, brick	*Pleurococcus* sp. (green alga), *Lyngbya* sp. (cyanobacterium)	Surface area covered (%) by chlorophyll fluorescence	Tiano et al. (1995)
Limestone, sandstone, mortar	*Gloeothece* sp. (cyanobacterium)	Chlorophyll a extraction	Saiz-Jimenez et al. (1995)
Limestone, dolomite	Natural mixed microbial populations (bacteria)	Viable counts of bacteria, visualization by staining and colorimetric techniques	Papida et al. (2000)
Limestone, marble, sandstone	*Apatococcus* sp. (green alga), *Lyngbya* sp. (cyanobacterium)	Surface area covered (%) by chlorophyll fluorescence	Tomaselli et al. (2000)
Mortar	*Cladosporium sphaerospermum* (fungus)	Visual and microscopic observation	Shirakawa et al. (2003)
Granite	*Nostoc* sp., *Oscillatoria* sp., *Scytonema* sp. (cyanobacteria)	Chlorophyll a extraction	Prieto & Silva (2005)
Limestone, marble, granite	*Stichococcus bacillaris* (green alga)	Surface area covered (%) by macroscopic observation, in vivo chlorophyll fluorescence	Miller et al. (2006)

Table 1.1 (Continued)

Lithotypes studied	Organisms tested	Biomass quantification technique used	Reference
Cement	*Alternaria alternata*, *Aspergillus niger* (fungi)	Visual inspection	Wiktor et al. (2006)
Cement	*Chroococcidiopsis* sp. (cyanobacterium), *Chlorella* sp., *Chlorhormidium* sp. (green algae)	Surface area covered (%) by image analysis, colorimetric techniques, chlorophyll a extraction	Escadeillas et al. (2007, 2009)
Mortar	Fungal, bacterial and algal suspensions	Light and epifluorescence microscopy	Urzì & De Leo (2007)
Limestone, calcarenite	Natural multi-species phototrophic culture	Surface area covered (%) by image analysis, chlorophyll a extraction, chlorophyll fluorescence	Miller et al. (2009a, 2010a, 2010b)
Limestone, marble	*Bagliettoa baldensis*, *Bagliettoa marmoreal* (lichens)	Microscopic observation of stained preparations	Favero-Longo et al. (2009)
Concrete	*Chlorella vulgaris* (green alga)	Surface area covered (%) by image analysis, colorimetric techniques	De Muynck et al. (2009a)
Mortar	Individual and mixed fungal isolates	Surface area covered (%) by image analysis	Giannantonio et al. (2009)
Cement	*Alternaria alternate*, *Exophiala* sp., *Coniosporium uncinatum* (fungi)	Microscopic observation of stained preparations	Wiktor et al. (2009, 2011)
Mortar	*Klebsormidium flaccidum* (green alga)	Surface area covered (%) by image analysis, colorimetric techniques	Tran et al. (2012, 2014)
Brick	*Chlorella mirabilis* (green alga), *Chroococcidiopsis fissurarum* (cyanobacterium)	Colorimetric techniques, confocal laser scanning microscopy	D'Orazio et al. (2014)
Cement	*Chlorella vulgaris* (green alga)	Colorimetric techniques, chlorophyll fluorescence by PAM-fluorometry	Manso et al. (2014a)
Schist, granite	*Nostoc* spp., *Scytonema* sp. (cyanobacteria)	Colorimetric techniques, chlorophyll a extraction	Marques et al. (2015)
Glass tile	*Chlorella vulgaris* (green alga)	Chlorophyll a extraction	Ferrándiz-Mas et al. (2016)

Artificial materials (e.g. mortar, cement and brick) are the most commonly studied types of substrate, followed by calcareous rocks (mainly limestones and marbles). Granite has only been considered in four laboratory-based primary bioreceptivity studies (Tiano et al. 1995, Prieto & Silva 2005, Miller et al. 2006, Marques et al. 2015). Despite being widely used in civil engineering, granite is not as extensively present in

stone cultural heritage as other lithotypes such as calcareous rocks (McNamara & Mitchell 2005, Macedo et al. 2009).

In most bioreceptivity experiments, samples have been inoculated with phototrophic microorganisms, particularly green algae and/or cyanobacteria, which are considered pioneering colonisers of stone surfaces (Ortega-Calvo et al. 1991, Tiano et al. 1995, Crispim & Gaylarde 2005). In other studies, artificial colonisation has been carried out with fungi, bacteria and lichens. In all of these studies, single species or a mixture of isolated strains were used to inoculate the stone. However, as already mentioned, microorganisms develop naturally on stone in complex microbial communities embedded in an EPS matrix forming subaerial biofilms. Therefore, tests carried out with a single type of organism may not represent natural conditions, as the competition and/or synergy between colonising microorganisms are not taken into account. Miller et al. (2009a, 2010a, 2010b) performed a laboratory-induced colonisation experiment by inoculating limestones with a phototrophic community previously collected from a limestone monument and cultured under laboratory conditions (Miller et al. 2008, 2009b). Use of this multi-species community culture yielded phototrophic biofilms similar to those found naturally on stone surfaces. Prieto et al. (2005, 2006a) also produced a multi-species liquid culture composed of organisms adapted to the conditions of quartz-rich substrata, mainly cyanobacteria, bacteria and bryophytes. These researchers then used the culture as an inoculum to induce biofilm formation on open rock faces of a quartz quarry, with the aim of reducing the visual impact generated by quartz mining, thus demonstrating the usefulness of these cultures for field applications.

Some researchers have attempted to develop standardised laboratory tests based on the procedure used by Guillitte & Dreesen (1995) for assessing the bioreceptivity of stone materials. Shirakawa et al. (2003) proposed an experimental set-up relying on characterization of stone samples, isolation of microorganisms, growth of isolated organisms, inoculation, incubation and quantification of biomass. Guillitte & Dreesen (1995), Prieto & Silva (2005) and Miller et al. (2008) have also developed techniques for inoculating stone samples and incubating phototrophic biofilms in growth chambers. Such laboratory experiments are crucial for addressing temporal and spatial variability and enhancing statistical data. Moreover, the incubation chambers can be used to simulate natural environmental conditions, such as changing moisture, temperature and

nutrient regimes on replicate samples, thus evaluating both bioreceptivity and biodeterioration (Miller et al. 2012). The incubation conditions used by several authors for the laboratory-based development of subaerial biofilms on stone are summarised in Table 1.2.

Table 1.2 Laboratory conditions for the development of subaerial biofilms on stone used in different studies.

Dimensions of stone blocks	Air humidity	Water supply	Temperature	Light intensity	Duration of incubation	Reference
5x5x5 cm^3	80-90 %	Periodic sprinkling	25-30 °C	NC/NS	9 months	[1]
5x5x0.5 cm^3	NC/NS	NC/NS	30 °C	100 µmol photon m^{-2} s^{-1}	1 month	[2]
diameter 3.8 cm x 1 cm	NC/NS	NC/NS	27 °C	NC/NS	21 days	[3]
25 cm^2	NC/NS	NC/NS	28 °C	50 µmol photon m^{-2} s^{-1}	1 month	[4]
4x4x0.5 cm^3	95 %	NC/NS	25 °C	800 lux	2 months	[5]
diameter 4.4 cm x 1 cm	Ambient	Capillary absorption	Ambient (18-22 °C)	Ambient	4 months	[6]
~3x2x0.3 cm^3	NC/NS	NC/NS	13-15 °C	NC/NS	12 months	[7]
diameter 4.4 cm x 1 cm	NC/NS	Capillary absorption	18-22 °C	1200 lux	3 months	[8]
4x4x1 cm^3	95 %	NC/NS	22 °C	1600 lux	4 months	[9]

[1] Guillitte & Dreesen (1995), [2] Tiano et al. (1995), [3] Papida et al. (2000), [4] Tomaselli et al. (2000), [5] Prieto & Silva (2005), [6] Miller et al. (2006), [7] Favero-Longo et al. (2009), [8] Miller et al. (2009a, 2010a, 2010b), [9] Marques et al. 2015. NC/NS: not controlled/not specified.

Various different methods have been used to quantify microbial growth on artificially colonised surfaces. The most common techniques used are quantification of the surface area covered (by macro or microscopic observations and image analysis), chlorophyll *a* extraction, chlorophyll fluorescence and colorimetric measurements (Table 1.1). Image analysis techniques have been successfully developed for calculating the surface area covered by biofilms growing on relatively homogeneous materials, such as cements and carbonate rocks (Escadeillas et al. 2009, De Muynck et al. 2009a, Giannantonio et al. 2009, Miller et al. 2010a, Tran et al. 2012). However, to our

knowledge, these techniques have not been yet used with granite, as the heterogeneous minerals contained in granite may cause difficulties in image processing. Chlorophyll *a* is a photosynthetic pigment present in all photoautotrophic microorganisms, including cyanobacteria and green algae, and it is thus reliable and commonly used to estimate the photosynthetic biomass present in subaerial biofilms (e.g. Saiz-Jimenez et al. 1995, Prieto & Silva 2005, Escadeillas et al. 2009, Miller et al. 2010b, Marques et al. 2015). Quantification of chlorophyll *a* by extraction with organic solvents involves destruction of the sample. This process has many disadvantages, e.g. repeated analysis of the same samples is not possible and the experimental procedure is very laborious and time consuming. Use of chlorophyll fluorescence techniques enables the non-destructive estimation of photosynthetic biomass, as calibrations relating the amounts of chlorophyll *a* in phototrophic biofilms and the basal fluorescence signals have been successfully achieved (Eggert et al. 2006, Gregor et al. 2008, Gustavs et al. 2009). Finally, colour measurement has been demonstrated to be a reliable non-destructive method for monitoring biofilm growth on stone surfaces (Prieto et al. 2004, Escadeillas et al. 2009, De Muynck et al. 2009, Sanmartín et al. 2012, Manso et al. 2014, Marques et al. 2015). Prieto et al. (2010) developed a protocol for measuring the colour of granite in order to overcome the difficulties associated with the mineral heterogeneity of this type of rock. The main advantage of this technique is that, in addition to estimating biological growth on surfaces, it enables simultaneous quantification of the aesthetic impact of the colonisation, which is very important from the point of view of the biodeteriorative effect.

The use of different methods of quantifying biological colonisation may significantly affect the results, thus hampering comparison of the findings of different studies. Miller et al. 2012 highlighted the need to compare the efficiency of various methods of estimating biofilm biomass on stone for each type of microorganisms and try to establish the most suitable method (or methods) of monitoring bioreceptivity.

1.4 STONE PROPERTIES RELATED TO BIORECEPTIVITY

The intrinsic properties of stone related to bioreceptivity assessed by several authors in laboratory-based primary bioreceptivity experiments are shown in Table 1.3. The mineral and chemical composition and open porosity are the characteristics most commonly evaluated by researchers in relation to the bioreceptivity of stone. Physical

properties related to movement of water through the rock matrix (e.g. open porosity, capillary water, permeability) and the chemical composition of the material are the main properties that seem to affect the colonisation of stones (Miller et al. 2012). However, the conclusions reached by different authors vary greatly. For example, Miller et al. (2006) suggested that the differences in the bioreceptivity were mainly related to the chemical composition of the substrata, rather than to physical characteristics. On the other hand, Tiano et al. (1995) demonstrated that preferential colonisation was primarily correlated with the stone structure, rather than with the chemical composition of the lithotypes under study. Other properties, such as surface roughness, were also found to be important for microorganism growth. Hence, rough surfaces are usually colonised more rapidly than smooth surfaces, as the irregularities in the surface may form anchoring sites and micro-refuges enabling microorganisms to attach and become established (Tomaselli et al. 2000, Prieto & Silva 2005, Miller et al. 2009a). Overall, there is no clear correlation between the potential bioreceptivity of stone materials and their physical or chemical characteristics, although properties such as roughness, porosity and mineralogical nature are considered key factors (Miller et al., 2012).

Table 1.3 Stone properties related to bioreceptivity, evaluated in various different studies. Adapted and updated from Miller et al. (2012).

Property	[1]	[2]	[3]	[4]	[5]	[6]	[7]	[8]	[9]
Texture / mineralogy	•	•	•			•	•	•	•
Chemical composition	•	•	•		•	•	•	•	•
Abrasion pH		•			•			•	•
Surface roughness		•		•	•			•	
Bulk density					•				•
Dry density			•						
Open porosity	•	•	•	•	•	•	•	•	•
Water content			•		•				•
Capillary water					•	•		•	•
Permeability								•	

[1] Guillitte & Dreesen (1995), [2] Tiano et al. (1995), [3] Papida et al. (2000), [4] Tomaselli et al. (2000), [5] Prieto & Silva (2005), [6] Miller et al. (2006), [7] Favero-Longo et al. (2009), [8] Miller et al. (2009a, 2010a, 2010b), [9] Marques et al. 2015.

In bioreceptivity studies including granite, Prieto & Silva (2005) demonstrated that the bioreceptivity of several types of granite varies due to the differences in some

physical properties. The extent of colonisation was mainly related to the surface roughness, in addition to four intrinsic properties: abrasion pH, bulk density, open porosity and capillary water. These researchers developed a simple and rapid method of investigating the potential bioreceptivity of granite to cyanobacteria without biological experiments, based on the characterisation of these four intrinsic properties and use of the following equation:

$$\mu g\ chlorophyll\ a/cm^2 = -206.397 - 1.708\,pH - 6.965\,OP + 84.977\,BD + 21.362\,Wc$$

where *OP* is open porosity, *BD* is bulk density and *Wc* is the amount of water absorbed by capillarity.

Comparison of the bioreceptivity of granitic stones with that of other lithotypes has not yielded clear results. Tiano et al. (1995) attributed the relatively high bioreceptivity of granite (in comparison with several limestones, sandstones and marbles) to the highly heterogeneous chemical composition of the material. However, Miller et al. (2006) suggested that the weak colonisation observed on granite, relative to that on carbonate rocks, was due the sensitivity of the inoculating microorganisms to the possible presence of toxic elements as minor components of the stone. Marques et al. (2015) observed that only a small portion of the inoculated cyanobacteria was able to establish on the samples of granite and did not develop considerably in comparison with schist samples, which showed lower abrasion pH and capillarity coefficients and higher bulk density than the granite.

USC
UNIVERSIDADE
DE SANTIAGO
DE COMPOSTELA

CHAPTER 2

FRAMEWORK OF THE THESIS

2.1 SCOPE OF THE RESEARCH

Bioreceptivity is a fundamental concept in the ornamental stone industry and in the fields of cultural heritage and civil engineering to help understand the susceptibility of stone constructions to biological colonisation and subsequent biodeterioration. In Galicia (NW Spain), traditional houses and the stone cultural heritage are built almost entirely of granite. Moreover, the Galician granite industry nowadays comprises an important economic resource, including many extraction quarries and manufacturing industries, which offer a great variety of ornamental granites. According to the main business association of the sector in Spain (the 'Cluster del Granito'), 92 % of the granite extracted in Spain and 85% of the granite processed in the country are done so in Galicia. The Galician granite industry generated 123 million € of benefits from exportation in 2015, reaching the 5th position on the international market. These data indicate the importance of studying the primary bioreceptivity of granitic rocks in Galicia.

As explained in the previous chapter, knowledge about stone bioreceptivity is fragmentary and the influence of the intrinsic properties of stone on its bioreceptivity must be clarified. According to some authors, biological colonisation is primarily associated with physical characteristics, while others claim that this is mainly determined by the chemical composition of the stone. However, characterization of some stone properties such as surface roughness, porosity and mineralogical composition can be considered essential for evaluation of the bioreceptivity of the stone

(Miller et al. 2012). Primary bioreceptivity studies on granite are relatively scarce (Tiano et al. 1995, Prieto & Silva 2005, Miller et al. 2006, Marques et al. 2015). The aforementioned studies have provided very valuable information concerning some of the stone characteristics influencing the susceptibility of granite to colonisation and have established the first comparisons with other lithotypes; however, further research is clearly needed to overcome many remaining uncertainties.

Correct design and standardisation of a laboratory-based experimental set-up is undoubtedly required to enable comprehensive assessment of the primary bioreceptivity of granitic rocks. For this purpose, several key features should be taken into account:

a) The biological culture used as the inoculum should emulate as closely as possible environmental-like colonisation of granite under laboratory conditions, so that the results obtained can be extrapolated to the real environment.
b) The experimental conditions during formation and growth of subaerial biofilms in laboratory should be optimised, so that the intrinsic properties of the stone related to its bioreceptivity can be efficiently assessed.
c) A sufficiently representative number and type of granites should be tested to include a wide range of stone properties for a valid assessment of the effects on bioreceptivity.
d) The granite properties analysed should be carefully selected on the basis of the results of previous bioreceptivity studies, to prevent loss of valuable information.
e) The most suitable techniques for quantifying biomass should be chosen, and if necessary developed, in order to produce valuable and reliable information about the stone colonisation process.
f) The data should be carefully compiled and statistically treated in order to maximize the information obtained and to enable correct interpretation of the results.

Following these criteria, the uncertainties involving the bioreceptivity of granitic rocks can be resolved. One practical application of standardised laboratory-based bioreceptivity experiments is to establish a bioreceptivity index (Guillitte 1995, Miller et al. 2012). This index would enable classification of different granitic rocks on a scale according to their susceptibility to biological colonisation. The index could therefore be transferred to end-users (e.g. conservators/restorers, architects, engineers) as a decision-making tool for selecting appropriate lithotypes for use in new constructions and to

replace materials in existing structures. The definition of such an index has not yet been established for any stone material as this requires a complex study analysing a wide variety of types of granite used in construction. Moreover, development of a bioreceptivity index for granitic rocks through standardised laboratory-based experiments will enable the application or adaptation of such an index to other lithotypes.

2.2 OBJECTIVES

The main objective of this PhD thesis is to provide a comprehensive evaluation of the primary bioreceptivity of granitic rocks used as building materials and/or ornamental stone, thus enabling development of a bioreceptivity index. A complex study is required to accomplish this goal, for which the following specific objectives are proposed:

1) Characterisation of the microbial communities in subaerial biofilms growing naturally on the surfaces of granite buildings in Santiago de Compostela (Galicia, NW Spain) and comparison of these with previously described microbial communities.
2) Production of stable phototrophic multi-species cultures, derived from natural subaerial biofilms and representative of the actual microbial diversity, and assessment of their potential suitability for use as inocula for investigating the bioreceptivity of granite under reproducible and environmentally realistic conditions.
3) Development of a method of extracting the EPS from subaerial biofilms grown on rocky substrata. No such protocol has yet been established for this purpose and it could provide very valuable information about the microbial colonisation of stone surfaces.
4) Design of a laboratory-based experimental set-up with optimal environmental conditions for the formation and growth of subaerial biofilms on granite, in an attempt to standardise the protocols used in the bioreceptivity studies.
5) Monitoring of the growth of the subaerial biofilms on different granites by using techniques that enable accurate quantification of biomass and other useful parameters related to the colonisation process.

6) Assessment of the influence of the intrinsic stone properties on their susceptibility to biological colonisation and establishment of any differences between the primary bioreceptivity of the granitic rocks studied.
7) Development of a bioreceptivity index, based on the results obtained in primary bioreceptivity experiments, to enable classification of the different granitic rocks studied on a scale according to their susceptibility to biological colonisation.

2.3 WORK STRATEGY

The experimental work carried out in order to accomplish the above mentioned objectives is structured in this PhD thesis as shown below (Figure 2.1).

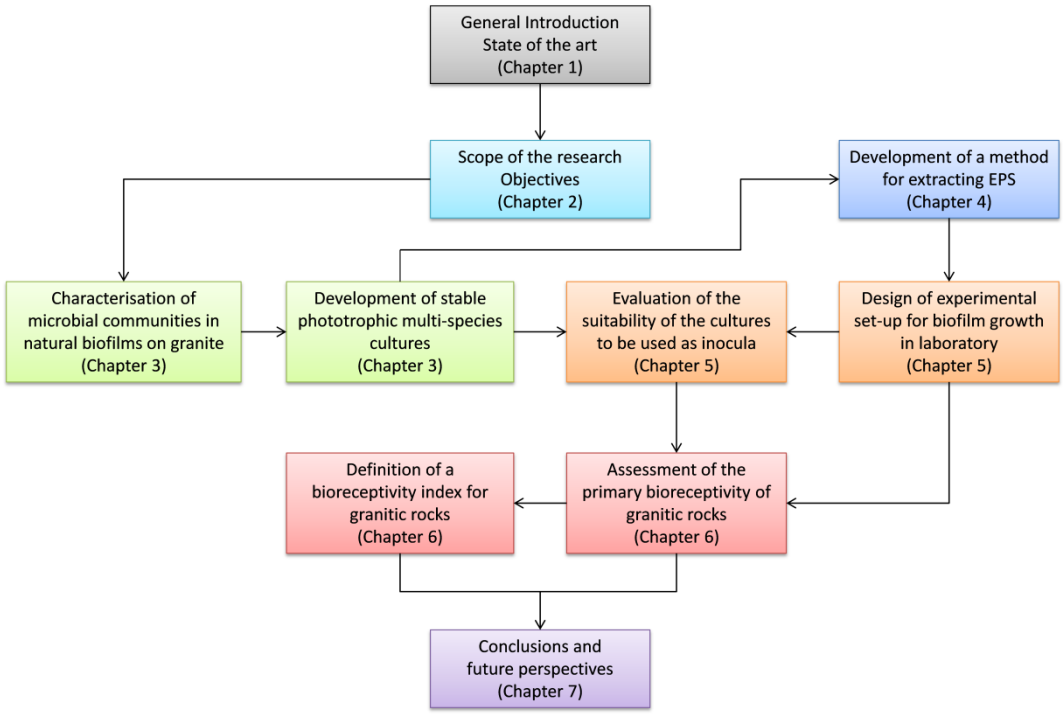

Figure 2.1 Outline of the thesis.

The thesis is divided into seven chapters. A brief introduction to the topic and a description of the state of the art concerning primary bioreceptivity studies were presented in Chapter 1. The current chapter, Chapter 2, outlines the scope of the research study and the proposed objectives.

The first part of the experimental work is presented in Chapter 3. Microbial communities of natural subaerial biofilms developed on historical granite buildings in Santiago de Compostela (Galicia, NW Spain) were characterised by environmental barcoding and next-generation sequencing. Phototrophic multi-species cultures derived from these biofilms were also characterised for use as inocula in further stone colonisation experiments.

Chapter 4 focuses on the development of a method for extracting the EPS from subaerial biofilms grown on rocky substrata, as a literature review revealed that no protocol had yet been established for this purpose. Use of such a protocol could provide very valuable information concerning the microbial colonisation of stone surfaces.

Chapter 5 concerns the design of an experimental set-up using the previously obtained multi-species phototrophic cultures to grow biofilms on granite under laboratory conditions. The colonising capacity of each culture was monitored by different techniques and their suitability for use as inocula in bioreceptivity experiments was assessed.

Once the experimental conditions were established (i.e. inoculum, growth conditions and measurement techniques), an in-depth evaluation of the primary bioreceptivity of several types of granite used in construction was carried out, as reported in Chapter 6. The results were used to develop a bioreceptivity index for granitic rocks.

Finally, in Chapter 7 the main conclusions reached as a result of this research are summarised and future research perspectives are presented.

USC
UNIVERSIDADE
DE SANTIAGO
DE COMPOSTELA

CHAPTER 3

SUBAERIAL BIOFILMS ON GRANITIC HISTORIC BUILDINGS: MICROBIAL DIVERSITY AND DEVELOPMENT OF PHOTOTROPHIC MULTI-SPECIES CULTURES[1]

3.1 INTRODUCTION

Inhabitants of subaerial biofilm communities are in close contact with one another. According to several authors (Ortega-Calvo et al. 1991, Tiano et al. 1995, Crispim & Gaylarde 2005), cyanobacteria and green algae (chlorophyta) are considered pioneer taxa in the colonization of stone, providing an excellent organic nutrient base for subsequent heterotrophic microflora. Heterotrophs and autotrophs grow in thin films that develop into associations that resemble symbioses. Vital biofilm connections at the atmosphere-rock interface are stimulated by the extreme physical and nutritional stresses that all members have to bear (Gorbushina & Broughton 2009). If these stresses persist, microbes will dominate the biomass, while under more favourable conditions, macroscopic vegetation could succeed (Chertov et al. 2004).

Because of the complexity of the microbial composition of most subaerial biofilms, understanding their development requires knowledge of all the components (aerobic heterotrophs, lithotrophs, oxygenic phototrophs, and even heterotrophic phagotrophs) (Gorbushina 2007). Some research has been focused on characterizing the microbial composition of biofilms growing on historic buildings, mainly from the point of view of their biodeterioration potential. Gaylarde & Gaylarde (2005) analysed the major microbial biomass of 230 biofilms developed on building surfaces, concluding that

[1]The content of this chapter has been published in:
Vázquez-Nion D, Rodríguez-Castro J, López-Rodríguez MC, Fernández-Silva I, Prieto B. 2016. Subaerial biofilms on granitic historic buildings: microbial diversity and development of phototrophic multi-species cultures. Biofouling 32: 657-669. doi: 10.1080/08927014.2016.1183121.

cyanobacteria, followed by fungi, were most common in Latin America, whereas green algae, followed by cyanobacteria, were most frequently present as major biomass in Europe. Macedo et al. (2009) compiled an inventory of the most common taxa of green algae and cyanobacteria reported on cultural heritage of various lithotypes in the Mediterranean Basin, which highlights the value of these data for ecological studies on stone colonization by facilitating the selection of single species or mixed communities of microorganisms and stone substrata for laboratory experiments.

Since natural biofilm communities are often difficult to investigate *in situ*, laboratory studies may increase knowledge of the processes involved in the formation and growth of biofilms on stone surfaces. Several laboratory-based stone colonization studies have been carried out, but in most of these experiments, individual community members were studied separately (Tiano et al. 1995, Shirakawa et al. 2003) or in artificially mixed cultures (Guillitte & Dreesen 1995, Prieto & Silva 2005, Seiffert et al. 2014, Marques et al. 2015, Villa et al. 2015). These inocula can be useful in many laboratory studies owing to their simplicity and high degree of experimental control, but their low microbial diversity may limit the ability to study complex processes involving an environmental community structure.

The use of cultures that resemble the microbial communities of natural subaerial biofilms, especially if they include pioneer colonizers such as green algae and cyanobacteria, could lead to a better simulation of environmental biofilm development as well as to a standardised methodology in these types of studies. In this regard, Miller et al. (2008, 2009b) developed a multi-species phototrophic culture composed of cyanobacteria and green algae from a natural biofilm growing on a Portuguese limestone monument. Colonization experiments of carbonate rocks carried out under laboratory conditions using this complex microbial community (Miller et al. 2008, 2010a) highlighted the advantage of simulating competition and/or synergy among colonizing microorganisms and enhanced understanding of the microbial processes occurring on stone cultural heritage assets. Prieto et al. (2005, 2006a) developed a multi-species liquid culture comprised of organisms adapted to the conditions of quartz-rich substrata, mainly cyanobacteria, bacteria and bryophytes, which they applied as an inoculum to induce biofilm formation on open rock faces of a quartz quarry in order to reduce the visual impact generated by quartz mining, demonstrating the usefulness of these cultures for field applications.

Considering the potential of these types of cultures for improving knowledge of subaerial biofilms, the aims of the present study were: (1) to identify the microorganisms present in natural biofilms on granitic historic buildings in Santiago de Compostela (Galicia, NW Spain) using environmental barcoding through next-generation sequencing (Pacific Biosciences); and (2) to obtain well-characterized stable phototrophic multi-species cultures that are representative of the actual microbial diversity present in those biofilms, to be used in further colonization experiments on granitic stone under reproducible and environmental-like conditions.

3.2 MATERIALS AND METHODS

3.2.1 Biofilm sampling

Five environmental samples of subaerial biofilms were taken from the outer walls of granitic historic buildings in Santiago de Compostela (Table 3.1, Figure 3.1), declared a World Heritage Site by UNESCO since 1985. Sampling areas of ~25 cm^2 were scraped using a sterile scalpel. Samples were collected in sterile vials and immediately transported to the laboratory. A portion of each sample (named B1 to B5) was stored at -80°C until being processed for identification of microbial communities and another portion was used for culturing procedures.

Table 3.1 Location and description of natural biofilm samples.

Sample	Biofilm location	Sample description
B1	Cathedral of Santiago de Compostela, entrance stairs	Green biofilm, 0.2 m above ground level, easily removable, east orientation
B2	Palace of Xelmírez, entrance hall	Light green biofilm, 0.3 m above ground level, firmly attached, south orientation
B3	Palace of Xelmírez, entrance hall	Dark green biofilm, 0.3 m above ground level, firmly attached, north orientation
B4	Monastery of San Martín Pinario, cloister	Green biofilm, 2 m above ground level, easily removable, north orientation
B5	Monastery of San Martín Pinario, cloister	Green biofilm, 2 m above ground level, easily removable, east orientation

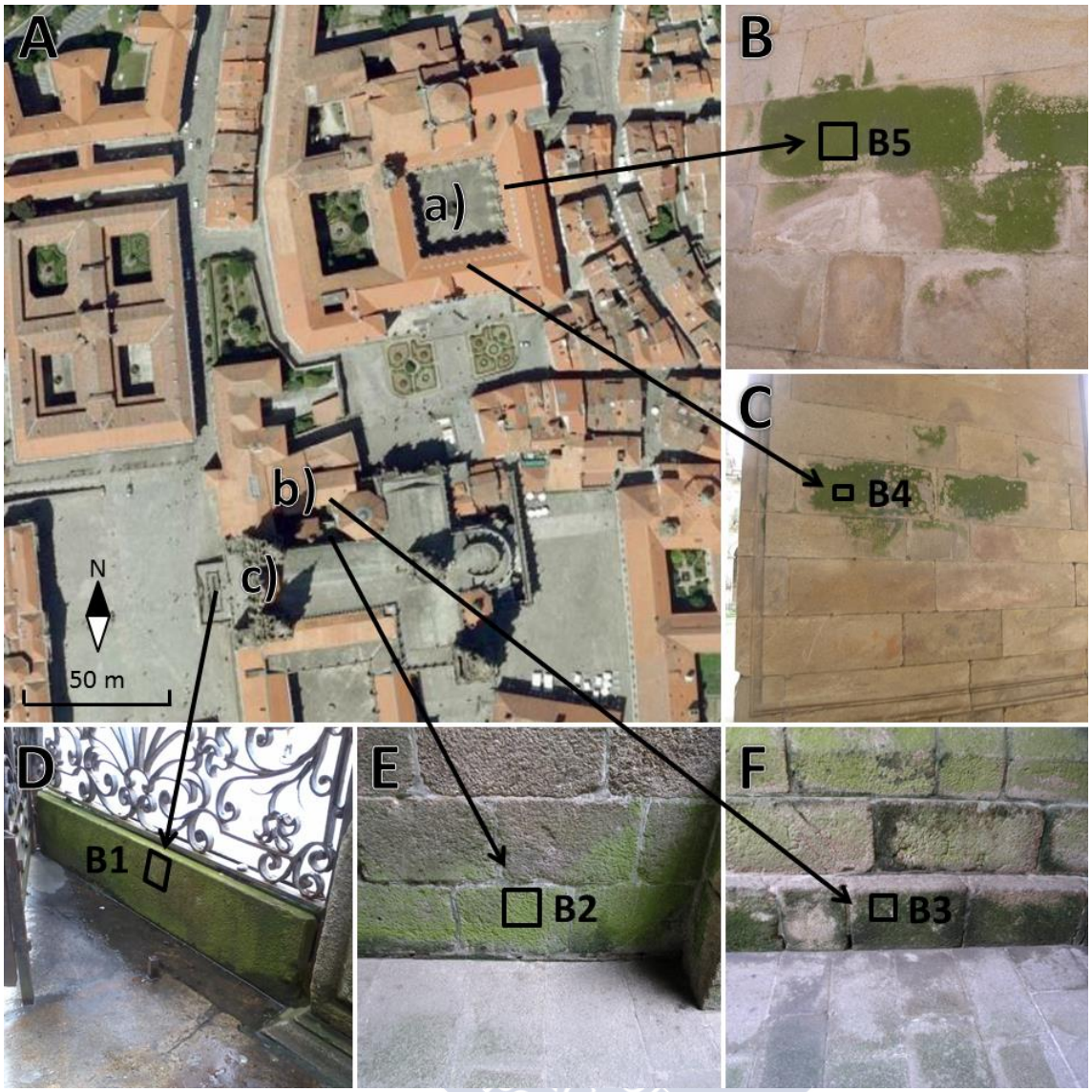

Figure 3.1 (A) Location of monuments where biofilm samples were collected: a) Monastery of San Martín Pinario; b) Palace of Xelmírez; c) Cathedral of Santiago de Compostela. (B, C, D, E, F) Sampling areas of biofilms B5, B4, B1, B2 and B3, respectively.

3.2.2 Cultivation of biofilms

In order to obtain phototrophic multi-species cultures, a portion of each sampled biofilm was inoculated into flasks containing 200 mL of BG11 liquid medium (Rippka et al. 1979) and grown with aeration in a controlled chamber at 23°C under a 12 h light/dark photoperiod (~20 μmol photon m^{-2} s^{-1}). After one month, cultures were transferred to flasks containing 1 L of BG11 medium and kept under the same conditions for two more months (Figure 3.2). A cultivation period of three months was chosen because this was demonstrated to be enough time for the establishment of the

microbial components of the community in the phototrophic multi-species culture developed by Miller et al. (2008). After that time, an aliquot of each culture (named C1 to C5) was filtered through sterile nitrocellulose filter disks (0.2 μm pore) and stored at -80°C until processed for DNA extraction. Fresh BG11 medium was periodically added to the cultures (ca. once a month) in order to maintain them in a healthy state.

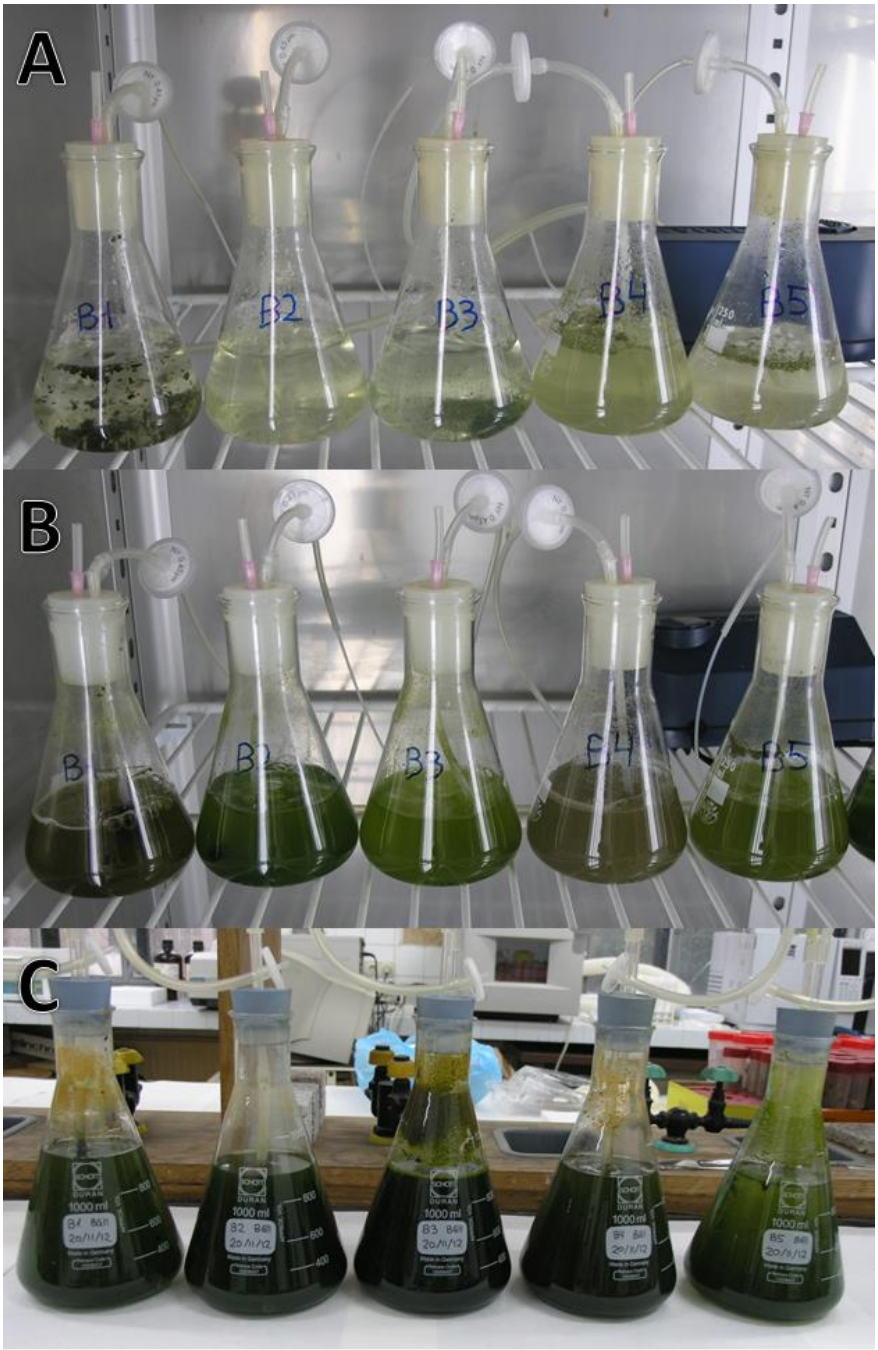

Figure 3.2 Biofilm cultures (A) after inoculation, (B) after one month and (C) after three months of incubation. From left to right: cultures of sample B1, B2, B3, B4 and B5 (named in the present work as C1, C2, C3, C4 and C5, respectively).

3.2.3 Characterization of biofilm communities by environmental barcoding

Total DNA was extracted both from environmental biofilm samples (B1, B2, B3, B4 and B5) and their liquid cultures (C1, C2, C3, C4 and C5, respectively) after incubation for three months. Extractions were carried out using the PowerSoil DNA Isolation Kit (MoBio Laboratories Inc.), according to the manufacturer's protocol. The quality of the DNA was checked on agarose gels and DNA isolates were stored at -20°C until further processing.

Given the expected biodiversity of the taxa present in the biofilms, various primer combinations targeting the ITS, 18S SSU rRNA and 23S LSU rRNA barcoding genes were used, which have been previously shown to have good phylogenetic resolution in the target groups (Table 3.2 and references therein). In order to combine several PCR reactions in a single sequencing run, the 5′-end of the primers was modified by adding a 6 bp indexing sequence (five different indexes for each of the environmental biofilms and five for the cultures). PCR amplification reactions were conducted with primers 18S1.2F (Whiting 2002) and ALG2R (Cutler et al. 2012), which were designed to amplify a ~1,000 bp region of the 18S SSU rRNA gene in green algae in 50 µL reactions containing 50 ng of extracted DNA, 0.3 µM of each primer, 0.2 mM of each dNTP, 5 µL of 10× reaction buffer, 2.5 mM $MgCl_2$ and 2.5 U of AmpliTaq DNA polymerase (Applied Biosystems). PCR cycling conditions were as follows: 2 min pre-denaturation at 94°C, followed by 35 cycles of denaturation at 95°C for 30 s, annealing at 54°C for 30 s, and extension at 72°C for 1 min 15 s. PCRs with the primer pair p23SrV_f1/p23SrV_r1 (Sherwood & Presting 2007), which was designed to target a ~400 bp-fragment of the 23S LSU rRNA gene in multiple eukaryotic algal and cyanobacterial groups, were carried out in 50 µL-reactions containing 50 ng of extracted DNA, 0.4 µM of each primer, 0.2 mM of each dNTP, 5 µL of 10× reaction buffer, 2.5 mM $MgCl_2$ and 1 U of AmpliTaq DNA polymerase. PCR cycling conditions consisted of pre-denaturation for 2 min at 94°C, followed by 35 cycles of denaturation at 94°C for 20 s, annealing at 55°C for 30 s and extension at 72°C for 30 s, followed by final extension at 72°C for 10 min. Finally, PCR reactions with primers ITS1F (Gardes & Bruns 1993) and ITS4 (White et al. 1990), designed to amplify a ~700 bp segment of the fungal intergenic spacer region containing the two internal transcribed spacers (ITS) and the 5.8S rRNA gene (ITS1-5.8S-ITS2), were conducted in 50 µL containing 50 ng of extracted DNA, 0.3 µM of each primer, 0.2 mM of each dNTP, 5 µL of 10× reaction

buffer, 2.5 mM $MgCl_2$ and 2.5 U of AmpliTaq DNA polymerase. The thermocycling program was: pre-denaturation for 2 min at 94°C, followed by 35 cycles of denaturation at 95°C for 30 s, annealing at 53°C for 30 s and extension at 72°C for 1 min. All the amplification reactions were performed in a GeneAmp PCR System 9700 (Applied Biosystems). PCR products with amplified DNA fragments were purified with GenElute PCR Clean-Up Kit (Sigma-Aldrich Co.) in accordance with the manufacturer's instructions, pooled at equimolar concentrations and then sent to Yale Center for Genome Analysis (West Haven, CT, USA). Sequencing libraries were prepared following Pacific Biosciences' DNA Template Prep Kit and sequenced in a SMRT cell of a Pacific Biosciences RS system.

Table 3.2 Primers used in this study.

Primer	Sequence (5'→3')	Target group	Reference
18S1.2F	TGCTTGTCTCAAAGATTAAGC	Green algae	Whiting 2002
ALG2R	CTTCCGTCAATTCCTTTAAGT		Cutler et al. 2012
p23SrV_f1	GGACAGAAAGACCCTATGAA	Eukaryotic algae and Cyanobacteria	Sherwood & Presting 2007
p23SrV_r1	TCAGCCTGTTATCCCTAGAG		
ITS1F	CTTGGTCATTTAGAGGAAGTAA	Fungi	Gardes and Bruns 1993
ITS4	TCCTCCGCTTATTGATATGC		White et al. 1990

FASTAQ formatted circular consensus sequences were processed using QIIME v.1.9.0 (Caporaso et al. 2010). Reads were demultiplexed, barcodes and primers sequences were trimmed and reads with low quality or anomalous length were excluded. Remaining sequences were clustered into operational taxonomic units (OTUs) based on a 97% identity cutoff using the UCLUST algorithm (Edgar 2010). Representative sequences of each OUT were then taxonomically classified using Mothur (Wang et al. 2007; Schloss et al. 2009) against the SILVA (Quast et al. 2013) and UNITE (Kõljalg et al. 2013) databases. These sequence data have been submitted to the GenBank database under accession numbers KU579398-KU585897.

Community richness (Chao1) and diversity (Shannon index) were calculated for all biofilm samples using QIIME. To compare the communities among sampled biofilms, as well as with their respective cultures, the phylogenetically based weighted (using sequence abundance data, only qualitatively) and unweighted (using presence-absence data) UniFrac metrics (Lozupone & Knight 2005) were used. For this purpose,

sequences were previously aligned with MUSCLE (Edgar 2004) and phylogenetic trees were built using FastTree 2.1.3 (Price et al. 2010). The resulting distance matrices were visualized using principal coordinates analysis (PCoA).

3.2.4 Light microscope identification

The five BG11 liquid cultures derived from natural biofilms were examined under light microscopy the 12th and 14th month after the beginning of cultivation, in order to assess the stability of their microbial communities over time. Culture samples were fixed with a solution of formaldehyde (5% v/v), glacial acetic acid (3% v/v) and glycerin (20% v/v). The morphological characterization of the phototrophic microorganisms present in cultures was performed using an Olympus BX61 microscope equipped with differential interference contrast (DIC, Nomarski) and the Olympus DP12 microscope digital camera system. Taxonomic identification of the observed specimens was carried out according to Ettl and Gärtner (1995), Komárek and Anagnostidis (1999, 2005) and Komárek (2013). The species observed were qualitatively classified as dominant (≥ 5% of total cell count) or accessory (< 5% of total cell count), according to their relative abundance in each culture.

3.3 RESULTS

3.3.1 Pacific Biosciences sequencing

Sequencing data from both natural biofilms and three-month-old cultures revealed a total of 568 OTUs: 62 OTUs corresponding to the amplification of algal 18S (primers 18S1.2F and ALG2R), 207 OTUs to algal 23S (primers p23SrV_f1 and p23SrV_r1), and 299 OTUs to fungal ITS (primers ITS1F and ITS4).

Richness and diversity estimates from the five environmental biofilm samples are shown in Table 3.3, where differences in the number of OTUs among samples are shown. The number of OTUs identified in each simple ranged from three OTUs in B1 to 17 in B2 for algal 18S sequencing; from four OTUs in B5 to 24 in B3 for algal 23S; and from 11 fungal ITS OTUs in B5 to 89 in B4. Differences between samples become greater if Chao1 was used to describe richness, due to the high proportion of singletons in the total number of OTUs (53% of algal 18S OTUs were singletons, 61% of algal

23S OTUs and 56% of fungal ITS OTUs). Shannon diversity follows the same trend as richness, showing differences among samples, with low values for algae (mean Shannon index: 1.75 for 18S and 1.54 for 23S) and higher values for fungi (mean Shannon index: 3.43).

Table 3.3 Number of OTUs, richness (Chao1) and diversity (Shannon index) derived from Pacific Biosciences data of the five environmental biofilm samples.

Biofilm sample	Algal 18S[a]			Algal 23S[b]			Fungal ITS[c]		
	OTUs	Chao1	Shannon	OTUs	Chao1	Shannon	OTUs	Chao1	Shannon
B1	3	3.0	1.21	12	21.3	1.54	13	18.3	3.21
B2	17	95.0	2.55	12	15.0	1.47	66	178.8	4.49
B3	5	8.0	1.39	24	42.3	2.55	61	226.0	3.78
B4	10	38.0	1.53	6	12.0	1.04	89	254.0	4.06
B5	6	7.0	2.09	4	5.0	1.12	11	32.0	1.62

Sequences obtained from primers 18S1.2F/ALG2R[a], p23SrV_f1/p23SrV_r1[b] and ITS1F/ITS4[c].

Taxonomic classification of Pacific Biosciences sequencing data derived from the five environmental biofilm samples revealed the presence of algae and fungi in all of them (Table 3.4). Eukaryotic algae were represented by the phyla Charophyta and Chlorophyta. Within the Charophyta only two species belonging to the same genus were identified: *Klebsormidium flaccidum*, identified in sample B1 through both 18S and 23S (chloroplast) algal barcoding sequences, and *Klebsormidium nitens*, found in B1 and B3. Chlorophyta proved to account for most of the species diversity, with representative taxa present in the five biofilms sampled, such as *Apatococcus lobatus*, *Prasiola furfuracea* and *Stichococcus* spp., in addition to several OTUs only resolved to the family or phylum level. Unexpectedly, Cyanobacteria were only detected in biofilm B3 and could not be identified. Regarding fungi, members of the phylum Ascomycota (i.e. *Capnobotryella* sp., *Cladosporium* sp., *Devriesia* spp. or *Rhinocladiella* spp.) were found in all biofilm samples, whereas Basidiomycota (i.e. *Cryptococcus* spp.) were only detected in biofilms B2 and B3, both sampled on the same building. According to the algal taxa found in relation to the building sampled (Table 3.1), *Prasiola furfuracea* and *Stichococcus bacillaris* were only detected in samples from the Palace of Xelmírez (B2 and B3), whereas *Apatococcus lobatus* was found in the two samples from the Monastery of San Martín Pinario (B4 and B5). Regarding fungi, the species *Cladosporium* sp. and *Teratosphaeria knoxdavesii* were common to samples B2 and B3 (Palace of Xelmírez). When samples with the same biofilm orientation are compared,

the only match is the presence of *Devriesia stirlingiae* on the north orientated walls (B3 and B4). Clustering of biofilm samples in the PCoA plots based on UniFrac distances (Figure 3.3) are in accordance with these observations.

Table 3.4 Most abundant taxa (non-singleton) identified in environmental biofilm samples derived from Pacific Biosciences sequencing.

	Marker	Occurrence in biofilm samples				
		B1	B2	B3	B4	B5
ALGAE						
Charophyta						
Klebsormidium flaccidum	Algal 18S/Algal 23S	●				
Klebsormidium nitens	Algal 18S	●		●		
Chlorophyta						
Apatococcus lobatus	Algal 18S				●	●
Coccomyxa subellipsoidea	Algal 23S	●				
Desmococcus sp.	Algal 18S	●				
Phyllosiphon arisari	Algal 18S		●			
Prasiola furfuracea	Algal 18S		●	●		
Pseudomuriella aurantiaca	Algal 18S				●	
Stichococcus bacillaris	Algal 23S		●	●		
Stichococcus jenerensis	Algal 18S		●			
Stichococcus sp.	Algal 18S		●			
Trentepohlia sp.	Algal 18S		●			
Other unidentified Trebouxiophyceae	Algal 18S		●	●	●	●
Other unidentified Chlorophyta	Algal 23S	●	●	●	●	●
Cyanobacteria						
Unidentified Cyanobacteria	Algal 23S			●		
FUNGI						
Ascomycota						
Acremonium tubakii	Fungal ITS			●		
Capnobotryella sp.	Fungal ITS				●	
Cladosporium sp.	Fungal ITS		●	●		
Debaryomyces prosopidis	Fungal ITS			●		
Devriesia stirlingiae	Fungal ITS			●	●	
Devriesia xanthorrhoeae	Fungal ITS		●		●	
Devriesia spp.	Fungal ITS		●	●	●	
Engyodontium album	Fungal ITS			●		
Penicillium chermesinum	Fungal ITS			●		
Penicillium sp.	Fungal ITS			●		
Penidiella sp.	Fungal ITS			●		
Pseudeurotium hygrophilum	Fungal ITS	●				
Rhinocladiella spp.	Fungal ITS	●	●			
Teratosphaeria knoxdavesii	Fungal ITS		●	●		
Other unidentified Ascomycota	Fungal ITS	●	●	●	●	●
Basidiomycota						
Cryptococcus spp.	Fungal ITS			●		
Other unidentified Basidiomycota	Fungal ITS		●			

Table 3.5 Most abundant taxa (non-singleton) identified in BG11 culture samples after three months of cultivation derived from Pacific Biosciences sequencing.

	Marker	Occurrence in culture samples				
		C1	C2	C3	C4	C5
PLANTAE						
Bryophyta						
Syntrichia ruralis	Algal 23S					●
ALGAE						
Charophyta						
Klebsormidium flaccidum	Algal 23S	●				
Klebsormidium subtilissimum	Algal 23S	●				
Chlorophyta						
Bracteacoccus spp.	Algal 18S	●	●	●	●	
Chlamydomonas nivalis	Algal 23S	●		●		
Chlorella sp.	Algal 18S					●
Chloromonas macrostellata	Algal 18S	●				
Chloromonas radiata	Algal 23S	●				
Coccomyxa subellipsoidea	Algal 23S	●				
Coelastrum astroideum	Algal 18S	●				
Desmococcus sp.	Algal 18S		●			
Friedmannia israeliensis	Algal 18S /Algal 23S					●
Haematococcus spp.	Algal 18S /Algal 23S	●				
Pseudomuriella aurantiaca	Algal 18S			●		
Scenedesmus obliquus	Algal 23S	●	●		●	
Scenedesmus sp.	Algal 18S	●				
Stichococcus bacillaris	Algal 23S		●	●		
Stichococcus jenerensis	Algal 18S					●
Other unidentified Chlorophyceae	Algal 18S	●				●
Other unidentified Trebouxiophyceae	Algal 18S					●
Other unidentified Chlorophyta	Algal 23S	●	●	●	●	●
Cyanobacteria						
Leptolyngbya sp.	Algal 23S	●				
Microcoleus sp.	Algal 23S	●				
Synechococcus sp.	Algal 23S	●		●		
Other unidentified Chroococcales	Algal 23S	●			●	
Other unidentified Nostocales	Algal 23S	●				
Other unidentified Oscillatoriales	Algal 23S	●			●	
Other unidentified Cyanobacteria	Algal 23S	●			●	
FUNGI						
Ascomycota						
Acremonium nepalense	Fungal ITS	●	●			●
Capnobotryella sp.	Fungal ITS				●	
Cyphellophora laciniata	Fungal ITS		●			
Cyphellophora reptans	Fungal ITS		●	●		
Devriesia spp.	Fungal ITS		●		●	
Engyodontium album	Fungal ITS		●	●	●	
Exophiala psychrophila	Fungal ITS		●			
Fusarium sp.	Fungal ITS	●				
Penicillium restrictum	Fungal ITS		●			
Other unidentified Ascomycota	Fungal ITS	●	●	●	●	●
Basidiomycota						
Trametes versicolor	Fungal ITS		●	●		
Other unidentified Basidiomycota	Fungal ITS				●	

The microbial diversity of the five BG11 cultures derived from the natural biofilm samples was studied through environmental barcoding after cultivation for three months. Considering the sum of the observed OTUs in the five samples and compared to the natural biofilms, liquid cultures showed almost the same number of algal 18S OTUs (36 in cultures and 41 in biofilms), an increased number of algal 23S OTUs (178 in cultures and 58 in biofilms) and a decrease in fungal ITS OTUs (107 in cultures and 240 in biofilms). Shannon diversity estimates show the same trend; BG11 cultures harboured a higher diversity of algae (mean Shannon index: 1.90 for 18S and 2.33 for 23S) and a lower diversity of fungi (mean Shannon index: 2.14) compared to the diversity found in natural biofilms. Furthermore, taxonomic classification of OTUs revealed the presence of algae and fungi in all cultures (Table 3.5). The algal phylum Charophyta was represented by *Klebsormidium* spp., only found in culture C1 (derived from natural biofilm B1), while Chlorophyta showed a wider diversity in the five cultures, including species of several common genera such as *Bracteacoccus*, *Chlorella*, *Scenedesmus* or *Stichococcus*. In contrast to the lack of Cyanobacteria sampled from natural biofilms, the cyanobacterial genera *Leptolyngbya*, *Microcoleus* and *Synechococcus*, and other taxa classified only to the order or phylum level, were identified in cultures C1, C3 and C4. Fungi were represented by the phyla Ascomycota (i.e. *Acremonium nepalense*, *Cyphellophora* spp., *Devriesia* spp. or *Engyodontium album*), present in all the five culture samples, and Basidiomycota (i.e. *Trametes versicolor*), with taxa found in cultures C2, C3 and C4. The presence of the moss (Bryophyta) *Syntrichia ruralis* identified through 23S (chloroplast) sequences in culture C5 should also be noted.

As seen in a comparison of Tables 3.4 and 3.5, not much overlap between the taxa identified to the species or genus level in natural biofilms and their respective three-month-old cultures in BG11 medium was found, with a few exceptions (i.e. *Klebsormidium flaccidum* in samples B1 and C1 and *Stichococcus bacillaris* in samples B2, C2, B3 and C3). Similarly, pairs of biofilm-culture samples did not cluster together in the PCoA plots (Figure 3.3). However, PCoA plots do show a certain degree of clustering between culture samples, and a certain degree of clustering between biofilm samples, particularly when richness and not abundance is taken into account (i.e. plots are based on unweighted UniFrac distances). Fungal distance matrices showed a higher heterogeneity among samples than the algal ones.

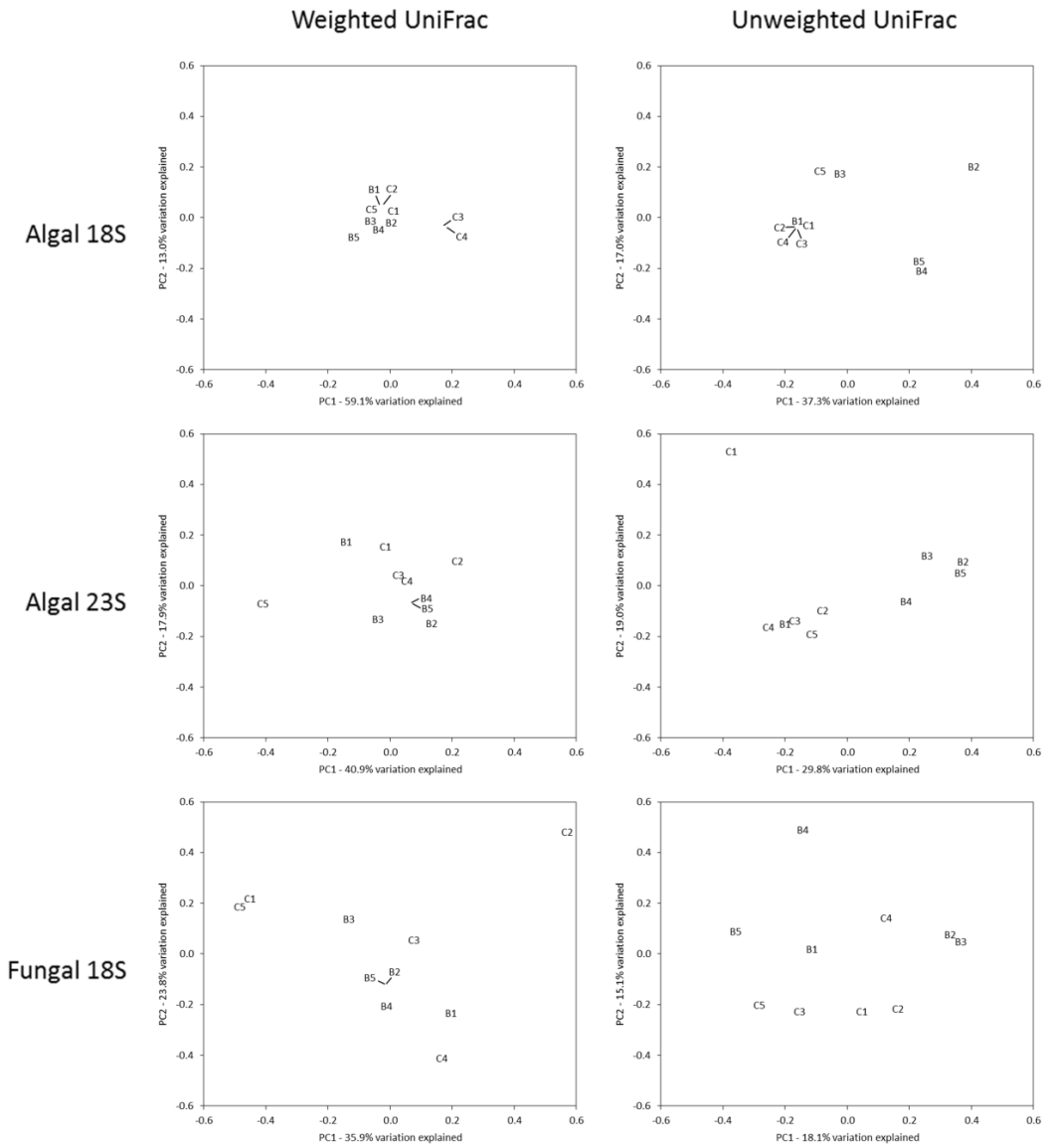

Figure 3.3 Principal coordinate plots of weighted (abundance data, left) and unweighted (presence-absence data, right) UniFrac distances between the ten samples (five natural biofilms and their respective five cultures) for the three primer pairs used.

3.3.2 Morphological identification

The light microscope observation of the five cultures derived from natural biofilms after incubation for 12 and 14 months allowed identification of the major microorganisms (Table 3.6) and assessment of the community stability. C1 proved to be a culture quite different from the others, dominated by several Cyanobacteria and *Monodus chodatii* (Figure 3.4B), the only alga found from the phylum Ochrophyta, not detected by molecular methods. Microscopy only revealed the presence of

Bracteacoccus minor (Figure 3.4C) in culture C2, while the main species found in C3 were two Chlorophyta (*Chlorella* sp. and *Stichococcus bacillaris*, Figure 3.4D,E) and two Cyanobacteria from the genus *Gloeocapsa*. Culture C4 showed *Bracteacoccus* sp. as dominant and several accessory Cyanobacteria. The microbial composition of C5 appeared to be rather more complex, dominated by three members of the Chlorophyta (*Bracteacoccus* sp., *Chlorella* sp. and *Stichococcus bacillaris*), one cyanobacterium (*Aphanocapsa* sp.) and protonemata of a Bryophyta from the genus *Syntrichia* (Figure 3.4F). No fungal hyphae were detected in any of the five cultures. In both the twelfth and fourteenth month of cultivation, the same species composition in each culture was observed, which indicated that this time was sufficient for the establishment of the species able to withstand the culture conditions.

Table 3.6 Phototrophic microorganisms identified in the five BG11 cultures after one year of cultivation through microscopic observations.

	Occurrence in cultures					Reference[a]
	C1	C2	C3	C4	C5	
PLANTAE						
Bryophyta						
Syntrichia sp. (protonema)[b]					+	
ALGAE						
Charophyta						
Klebsormidium sp.[b]	-				-	Rifón-Lastra & Nogerol-Seoane (2001)
Chlorophyta						
Bracteacoccus minor[b]		+				Rifón-Lastra & Nogerol-Seoane (2001)
Bracteacoccus sp.[b]				+	+	Rifón-Lastra & Nogerol-Seoane (2001)
Chlamydomonas sp.[b]	-				-	
Chlorella sp.[b]			+		+	Rifón-Lastra & Nogerol-Seoane (2001)
Kirchneriella sp.	-					
Stichococcus bacillaris[b]	-		+		+	Rifón-Lastra & Nogerol-Seoane (2001)
Ochrophyta						
Monodus chodatii	+					
Cyanobacteria						
Aphanocapsa fuscolutea			-			Anagnostidis et al. (1991)
Aphanocapsa sp.	-				+	Anagnostidis et al. (1991)
Chamaesiphon sp.	+					Zurita et al. (2005)
Chlorogloeopsis cyanea	+					Keshari & Adhikary (2014)
Chroococcus sp.				-		Zurita et al. (2005)
Gloeocapsa aeruginosa			+			Miller & Macedo (2006)
Gloeocapsa punctata			+			Miller & Macedo (2006)
Gloeocapsa sp.	-					Miller & Macedo (2006)
Hassallia byssoidea	+					Keshari & Adhikary (2014)
Isocystis sp.			-	-		
Leptolyngbya cebennensis[b]					-	Miller et al. (2009b)
Phormidium terebriforme	+					Ortega-Calvo et al. (1991)
Pseudocapsa dubia				-		

Observed species are qualitatively classified as dominant (+) or accessory (-) as a function of their relative abundance in the cultures.

[a]Previous published studies reporting the presence of the genus on stone building surfaces, including granite (underlined).

[b]Genus detected in the three-months-old cultures through environmental barcoding.

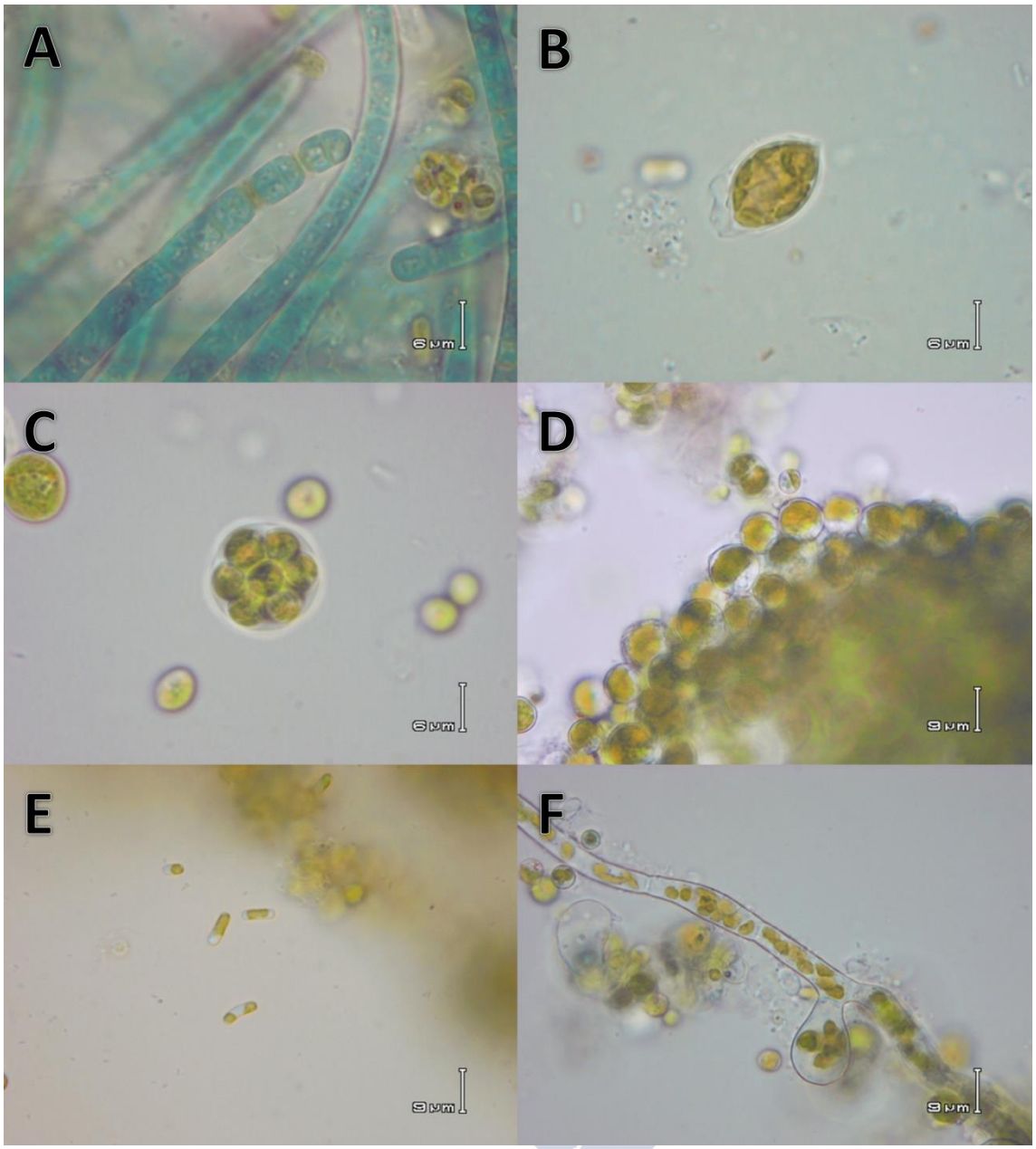

Figure 3.4 Images of different morphotypes observed in cultures by light microscopy. (A) Filaments of *Phormidium terebriforme* and (B) single cell of *Monodus chodatii*, found in culture C1. (C) Autospore of *Bracteacoccus minor* in C2. (D) Agglomeration of *Chlorella* sp. and (E) cells of *Stichococcus bacillaris*, morphotypes observed in both C3 and C5. (F) Protonema of *Syntrichia* sp. found in culture C5.

3.4 DISCUSSION

3.4.1 The microbial diversity of natural biofilms

Pacific Biosciences sequencing data of the five biofilms sampled revealed microbial communities mainly composed of Chlorophyta (green algae) and Ascomycota (fungi), which are considered, along with Cyanobacteria, to represent the major

microbial biomass of biofilms on building stone surfaces (Gaylarde & Gaylarde 2005). The only previous work, to the authors' knowledge, that applied next-generation sequencing to the analyses of the microbial communities of this type of biofilm (Cutler et al. 2013) found similar patterns of richness and diversity; analyses of pyrosequencing data revealed that subaerial biofilms on sandstone buildings in Belfast (UK) were also dominated by Chlorophyta and Ascomycota and that fungal communities were richer and more heterogeneous than algal assemblages. Their Shannon diversity estimates from algal assemblages were almost identical to those reported here (1.11–2.47 vs 1.21–2.55 in the present work; Table 3.3), but slightly lower for fungi (1.84–2.77 vs 1.62–4.49 in the present work). The present results support the view of Cutler et al. (2013), who pointed to the potential of epilithic algal communities as experimental models (e.g. to study the impact of climate change) owing to their relative simplicity, whereas the more heterogeneous fungal communities would be less suitable.

With regard to the taxonomic composition of the five biofilms studied, some of the algal species commonly associated with stone surfaces of European buildings were found, such as *Klebsormidium flaccidum* and *Desmococcus* sp. in B1, *Trentepohlia* sp. in B2, *Stichococcus bacillaris* in B2 and B3 or *Apatococcus lobatus* in B4 and B5 (Rindi 2007, Macedo et al. 2009; Table 3.4). An analysis of biofilms on granite walls of 50 buildings in the same region as the present work (Galicia, NW Spain) (Rifón-Lastra & Noguerol-Seoane 2001) classified as 'typical' species subaerial green algae belonging to genera *Apatococcus*, *Desmococcus*, *Klebsormidium*, *Stichococcus* or *Trentepohlia*, all of which were identified in the biofilms in the present study. Thus, the data support the assumption that subaerial biofilms are ecosystems with low algal diversity, as well as the ubiquity of many of their common species. Regarding fungi, despite a higher heterogeneity among samples, all were dominated by Ascomycota, and most of the genera identified in the biofilms (e.g. *Acremonium*, *Cladosporium*, *Engyodontium*, *Penicillium* or *Rhinocladiella*) can be considered as common on rock substrata (Burford et al. 2003).

The present study also underlines the limited representation of subaerial biofilm forming microorganisms in DNA sequence databases and the necessity of systematic studies of these organisms to enhance the production of high-quality molecular datasets. Cyanobacteria were detected only in biofilm B3, which could only be classified to the phylum level. This low taxonomic resolution was also observed in eukaryotic algae and

fungi, with many OTUs only resolved above genus level. Moreover, the datasets obtained with the two different molecular markers for algae (18S SSU and 23S LSU rRNA genes) revealed only a few cases of OTUs assigned to the same taxon (*Klebsormidium flaccidum*, *Friedmannia israeliensis* and *Haematococcus* spp.), highlighting their complementarity and therefore the benefit of increasing the number of molecular markers available.

The absence of Cyanobacteria in sequencing data of four of the five biofilms studied was unexpected, since they are considered one of the major contributors of microbial biomass to subaerial biofilms (Gaylarde & Gaylarde 2005), although a relatively low number of taxa was reported on granitic stone (Macedo et al. 2009). However, the detection in subsequent cultures (Tables 3.5 and 3.6) of Cyanobacteria and other taxa of eukaryotic algae and fungi that were not detected in the environmental samples suggests that not all the biofilm diversity was captured. The rarefaction analyses of richness accumulation (results not shown) and the gap between the number of OTUs and the Chao1 values (which represent the 'true' richness of the samples) observed in almost every sample and primer pair combination (Table 3.3) further support this observation. The biofilms sampled must contain low numbers of individuals of other species, whose sequences were not present in the data derived from environmental DNA. It seems reasonable to assume that when environmental conditions changed during the cultivation of biofilms samples in BG11 liquid medium, some of these undetected species proliferated to the detriment of others.

3.4.2 Multi-species cultures derived from natural biofilms

A macroscopically visible growth, characterized by a bright green colour and a disaggregated appearance (Figure 3.2), was observed in the five cultures during the cultivation of biofilms for three months in BG11 liquid medium, previous to the collection of samples for sequencing purposes. As seen in Tables 3.4 and 3.5, an alteration in the microbial community composition occurred when biofilm samples were cultivated in liquid BG11 medium. This was not surprising, as microorganisms were moved from a biofilm to a planktonic state, which certainly promoted the growth of some taxa and limited the growth of others. During the time which elapsed from the collection of culture samples for sequencing purposes (three-month-old cultures) to the microscopic observations (12-month-old cultures), changes in the microbial

composition were also noticed (Tables 3.5 and 3.6). This leads to the consideration that the three-month-old cultures were in a transient state where the microbial community was not yet completely adapted to the culture conditions, in contrast to the culture developed by Miller et al. (2008). However, microscopic observations after cultivation for 12 and 14 months did not reveal substantial changes in species composition in any of the five cultures, suggesting that the establishment of stable microbial communities had been achieved after a 12-month period.

The five cultures finally obtained showed a microbial composition quite different from the natural biofilms from which they originated (Figure 3.3, Tables 3.4 and 3.6). BG11 medium is specially designed for green algae and Cyanobacteria (Rippka et al. 1979). As expected, this promoted the proliferation of phototrophic organisms, so that no fungal hyphae were detected in any of the five cultures after the 12-month cultivation period. The taxa found in the cultures are considered common pioneer colonizers of stone surfaces, including granite buildings (Table 3.6 and references therein). Taking this into account, it can be assumed that the phototrophic multi-species cultures obtained can be used as inocula to reliably reproduce natural colonization of granitic stone. Most of the stone colonization studies under laboratory conditions (e.g. Tiano et al. 1995, Prieto & Silva 2005, Seiffert et al. 2014, Marques et al. 2015, Villa et al. 2015) used cultures comprising only one or two taxa as inocula. The results of the present study, in addition to many others (e.g. Rifón-Lastra & Noguerol-Seoane 2001, Gaylarde & Gaylarde 2005, Rindi 2007, Macedo et al. 2009, Cutler et al. 2013), demonstrate that subaerial biofilms naturally grown on rocks are composed by microbial communities far more complex. It seems reasonable to assume that a more diverse culture would emulate more closely the natural colonization of stone, since this would allow the presence of competition/synergy processes between species. An artificially mixed culture can also be composed of a variety of organisms wide enough to resemble a natural biofilm, but from an experimental point of view, this is more easily achieved through the cultivation of natural biofilms and their characterization when the microbial communities are established. The reliability of the phototrophic multi-species cultures obtained in the present study to emulate natural colonization on granite should be confirmed in further experiments.

As an appraisal of the potential use of each of the five cultures obtained as inoculum for stone colonization experiments, culture C1 can be considered as a

cyanobacterial assemblage mainly formed by a mixture of coccoid and filamentous forms; however, this culture is very hard to handle due to its extremely mucilaginous aspect, leading to issues concerning the reproducibility of inoculations. Culture C2 was shown to consist of a unique dominant species, *Bracteacoccus minor*, which is indeed a common granitic rock colonizer (Rifón-Lastra & Noguerol-Seoane 2001). This could be useful when a mono-species culture is required, for example, as a control, but it should not be taken as a model to simulate natural biofilms. In contrast, C3, C4 and C5 seem to be potentially the most adequate cultures concerning the objectives of this study, since they are easy to handle and composed of a stable and diverse phototrophic microbial community that could simulate stone colonization in natural environments. All these three cultures had common and widespread subaerial biofilm taxa of Chlorophyta and Cyanobacteria, but differences are also noted, which can lead to special applications. For example, culture C3 had a greater cyanobacterial biomass, dominated by N2-fixing *Gloeocapsa* spp., which could be useful for studies involving, for example, nutrient limitation; on the other hand, the presence of bryophyte protonemata in C5 could lead to the application of this culture for the development of mosses under the appropriate conditions.

3.5 CONCLUSIONS

Pacific Biosciences sequencing of environmental DNA revealed complex microbial communities mainly composed of Chlorophyta and Ascomycota, and identified taxa previously reported to be associated with stone building surfaces. To the authors' knowledge, this is the first time that next-generation sequencing data have been analysed to characterize subaerial biofilms developed on granite surfaces. The estimates of species richness and diversity were higher for the fungal assemblages than for algae. Moreover, fungi showed a higher heterogeneity among samples. The results also underline the necessity of enhancing the production of high-quality molecular datasets and increasing the representation of subaerial biofilm-forming microorganisms in DNA sequence repositories.

One year was necessary for the establishment of stable microbial communities in the liquid BG11 cultures derived from natural biofilms. Morphological characterization revealed that most taxa found in these cultures, mainly members of the Chlorophyta and Cyanobacteria, were not part of the major biomass in the original biofilms, but can be

considered as common pioneer colonizers of building stone surfaces, including granite. Hence, stable characterized cultures that can be used to reliably reproduce an environmental-like colonization of granitic stone under laboratory conditions were obtained. Further work should focus on experiments directed to evaluating the applicability of these cultures as inocula on granitic stone and the assessment of their ability to form subaerial biofilms.

CHAPTER 4

RESPONSE SURFACE OPTIMIZATION OF A METHOD FOR EXTRACTING EXTRACELLULAR POLYMERIC SUBSTANCES (EPS) FROM SUBAERIAL BIOFILMS ON ROCKY SUBSTRATA[2]

4.1 INTRODUCTION

A biofilm is defined as 'a multicellular community composed of prokaryotic and/or eukaryotic cells embedded in a matrix composed, at least partially, of material synthesized by the sessile cells in the community' (Costerton 2007). The matrix holds the microorganisms together and also facilitates adhesion to surfaces, thus promoting aggregation of cells and growth of the biofilm. This matrix is formed by extracellular polymeric substances (EPS), which mainly comprise carbohydrates and proteins. Other constituents of EPS include humic substances, lipids, nucleic acids, uronic acids and some inorganic compounds. Differences in the production and composition of EPS in biofilms depend on the physiological state of the microbial community and the environmental conditions such as the substrate type or the nutrient/energy sources (Flemming & Wingender 2010). The EPS matrix is therefore considered key to understanding the biofilm mode of life.

Biofilms grow at solid-water and solid-air interfaces in virtually all natural environments as well as many man-made structures. Although subaquatic biofilms are permanently submerged, subaerial biofilms must be able to resist wetting-drying cycles, leading to different survival strategies. In subaerial biofilms, such as those developed on rock surfaces, the EPS matrix enables the microbes to withstand periods of desiccation.

[2]The content of this chapter has been published in:
Vázquez-Nion D, Echeverri M, Silva B, Prieto B. 2016. Response surface optimization of a method for extracting extracellular polymeric substances (EPS) from subaerial biofilms on rocky substrata. Analytical and Bioanalytical Chemistry (In press). doi: 10.1007/s00216-016-9752-0.

The EPS in subaerial biofilms protect cells from diffusion and also prevent enormous stresses by retaining water for long periods and facilitating access to water vapour in the atmosphere (Gorbushina 2007). The EPS matrix also protects cellular and enzyme function during dry periods, so that cells remain active and extracellular enzymes are stabilized at lower water potentials (Kemmling et al. 2004). Nutrient and energy resources may be limited in environments where subaerial biofilms grow. However, the adhesive properties of the EPS matrix facilitate the capture of particles and volatile matter from the atmosphere; this material accumulates on the biofilm surface and serves as a nutrient source for chemoorganotrophic microorganisms (Gorbushina 2007).

Subaerial biofilms on rock surfaces play an important role in geomorphology across a wide range of environments through processes of weathering, precipitation of minerals and protection of surfaces from erosion (Viles 2012). These processes occur on all rock surfaces where biofilms have developed, including stone-made buildings and monuments, in which case the term biodeterioration (or bioprotection for positive effects) is usually employed. The study of biodeterioration is of practical relevance for the conservation of cultural heritage. In addition to the anti-aesthetic impact that subaerial biofilms may have on stone buildings, biofilm-forming microorganisms are known to secrete metabolic acids that induce biodeterioration through biogeochemical processes such as acidolysis and complexation (Warscheid & Braams 2000). EPS play a central role in these processes, as the biofilm matrix (rather than the microorganisms themselves) is in direct contact with the surface of the substratum, acting as a reactive interface for the biogenic weathering of rocks (Hoppert et al. 2002).

The participation of EPS in stone biodeterioration is largely due to physical processes. Water absorption and desiccation cause swelling and shrinkage of the biofilm matrix, exerting mechanical stresses on the mineral structure and finally leading to cracks and fissures in the stone. This can alter the pore size distribution in the stone or even cause exfoliation of surface layers. The adhesive properties of the biofilm matrix also accelerate the accumulation of atmospheric particles, which then act as precursors to the formation of detrimental crusts on rock surfaces (Warscheid & Braams 2000). Some matrix-compounding polymers may also cause biogeochemical deterioration of stone materials, such as the polysaccharide alginic acid, which is suggested to increase the dissolution of calcite (Perry et al 2004). However, although EPS are known to be involved in several biogeochemical processes (Tourney & Ngwenya 2014), many

aspects of their potential to cause biodeterioration remain unclear, mainly due to the difficulty in studying these substances.

Several protocols for extracting EPS have been developed. These include physical methods (e.g. heating, sonication, centrifugation), chemical methods (e.g. acidic/alkaline treatment, EDTA, cationic exchange resin) and combinations of both. The physical methods are generally less effective than the chemical methods (Sheng et al. 2010). As it is not possible to develop a universal extraction method, different protocols must be developed and optimized by considering the characteristics of the type of biofilm and EPS concerned.

Most of the currently available extraction methods are designed for water-covered biofilms, such as subaquatic mats grown on sediments (Perkins et al. 2004, Takahashi et al. 2009) or biofilms used in biological wastewater treatment plants (Liu & Fang 2002, Zhu et al. 2015) and other engineered systems (Sheng et al 2005). Some authors have used solidified media (Jachlewski et al. 2015) or glass discs (Barranguet et al. 2004) as artificial substrata to promote growth of biofilms for subsequent development of extraction protocols. In these cases, the biofilms under study were weakly attached to the substrata and the extraction protocols usually included a step involving mechanical detachment of the biofilm. This is not possible when studying subaerial biofilms developed on rocky substrata, as the microorganisms are firmly adhered to the rock surface; as the biofilm cannot be completely removed by scraping, the EPS content would be underestimated. Redmile-Gordon et al. (2014) designed a method of extracting EPS from soil biofilms by use of a soil/extractant suspension with cationic exchange resin. However, this method cannot be used for rock biofilms without crushing the stone, which leads to a high risk of contamination and is labour-intensive and extremely time-consuming. To our knowledge, no specific protocol has yet been developed for extracting EPS from this type of biofilm directly on the stone surface.

The aim of the present study was to develop and optimize, by the response surface methodology, a protocol for extracting EPS from subaerial biofilms grown on rocky substrata. An efficient extraction procedure would enable analytical quantification and characterization of EPS components in this type of biofilm, thus substantially improving our understanding of the processes occurring during the microbial colonization of stone surfaces.

4.2 MATERIALS AND METHODS

4.2.1 Preparation of samples

Experiments were carried out using multi-species culture C3 (described in Chapter 3, Vázquez-Nion et al. 2016a) as the inoculum. This culture was obtained by scraping a naturally occurring subaerial biofilm from a granite wall in the Palace of San Xerome (Santiago de Compostela, NW Spain). The material thus obtained was incubated in liquid BG11 medium (Rippka et al. 1979), at 23 °C under a 12-h light/dark photoperiod, until establishment of a stable microbial community, mainly composed of Chlorophyta *Chlorella* sp. and *Stichococcus bacillaris* and Cyanobacteria *Aphanocapsa fuscolutea*, *Gloeocapsa aeruginosa*, *Gloeocapsa punctate* and *Isocystis* sp.

Biofilms were developed by inoculating 1 mL of culture C3 (equivalent to 0.89 mg dry weight biomass) in exponential growth phase onto the upper surface of each of 61 autoclaved 4×4×2 cm^3 granite blocks. The granite blocks were maintained permanently in contact with water by placing them in dishes periodically filled with sterilized water. The blocks were incubated in a climatic chamber under stationary conditions of 23 °C, 95 % relative humidity and a 12-h light/dark photoperiod (~20 µmol photon m^{-2} s^{-1}) for 2 months, within which time biofilm formation was clearly visible (Figure 4.1a).

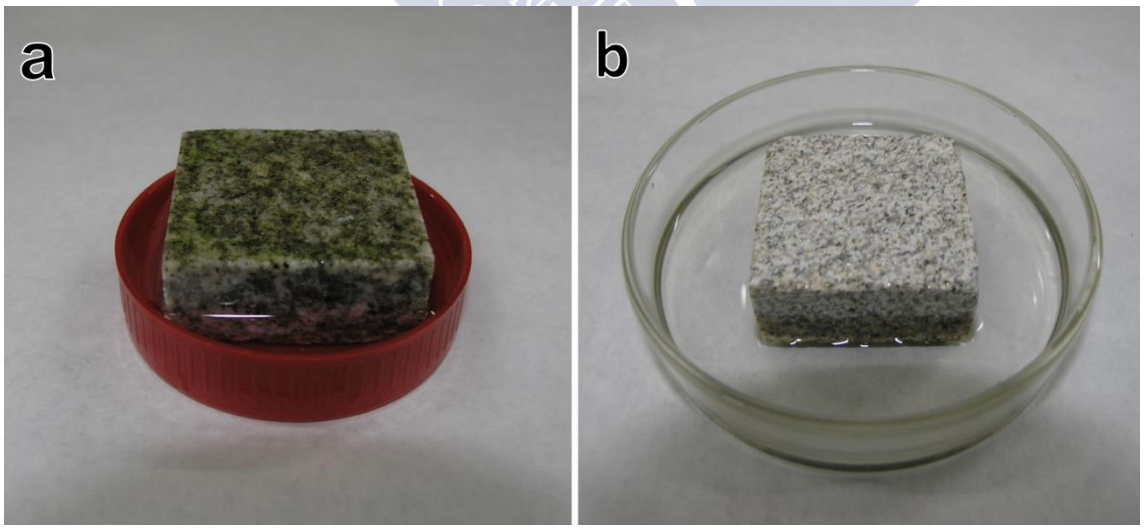

Figure 4.1 (a) Subaerial biofilm developed on a granite block after incubation for 60 days under laboratory conditions. (b) Block placed in a Petri dish with the colonized face turned down to ensure complete in contact with the extractant solution.

The biofilm biomass on each block was estimated before EPS extraction by quantification of the variation in the colour of the granite surface generated by the biofilm (Prieto et al. 2004, Sanmartín et al. 2012). Calibration was performed by measuring the colour change generated by inoculation of nine granite blocks with known quantities of culture C3 (from 0.32 to 8.05 mg dry weight biomass (DWB)). Colour measurements were carried out following the protocol described by Prieto et al. 2010. A close relationship between the biomass of culture C3 and variation in luminosity (ΔL^*; CIE 1986) of the inoculated surface was experimentally established as shown in Figure 4.2.

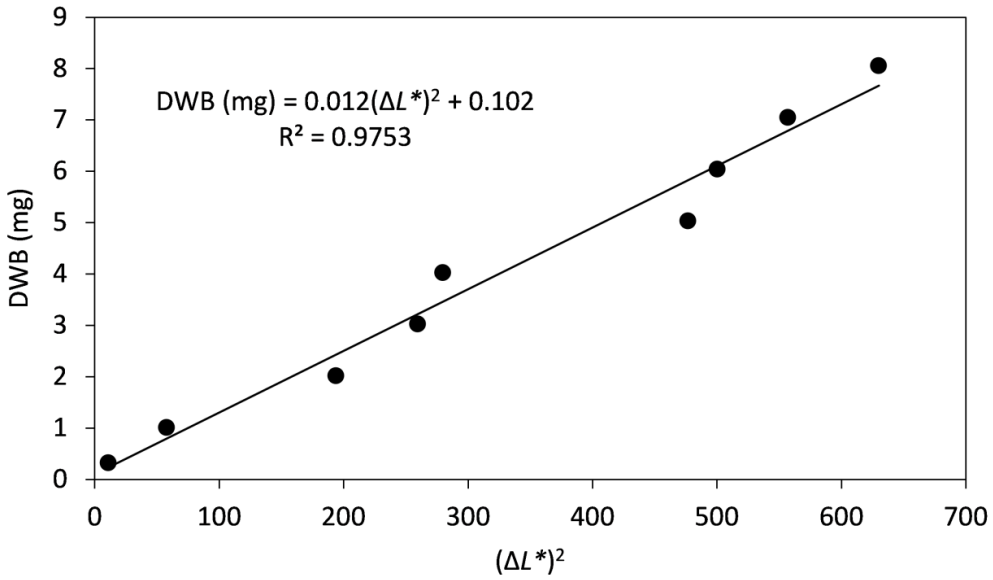

Figure 4.2 Calibration curve for estimating the dry weight biomass (DWB) of the biofilm from the variation in luminosity (ΔL^*) on the granite block surface.

4.2.2 Confocal laser scanning microscopy (CLSM)

Three inoculated blocks were observed by CLSM to evaluate biofilm formation after the 2-month incubation period. EPS was stained using the fluorescently labelled lectin concanavalin A, tetramethylrhodamine conjugate (ConATRITC, Molecular Probes) by applying 100 µL of a 0.5-g L^{-1} ConA-TRITC solution as a droplet to each biofilm. The blocks were incubated for 30 min at 25 °C and then carefully rinsed with sterile distilled water. Bacteria were stained with the fluorescent nucleic acid stain SYTO 9 (Molecular Probes) by applying 100 µL of a 1.67-µM SYTO 9 solution to each biofilm. The blocks were incubated for 30 min at 25 °C and then carefully rinsed with

sterile distilled water. Photosynthetic microorganisms (green algae and cyanobacteria) were visualized via chlorophyll auto-fluorescence.A Leica TCS-SP5 AOBS CLSM (Leica Microsystems) with a 63× (NA 1.4, glycerol) objective was used to capture images of the biofilms directly on the granite surface. Observations were made in five randomly selected areas of each biofilm by multi-channel detection: SYTO 9 (excitation, 488 nm; emission, 505-550 nm) targeting bacterial DNA was recorded in the blue channel; ConA-TRITC (excitation, 543 nm; emission, 560-615 nm) targeting EPS was recorded in the green channel; and chlorophyll auto-fluorescence (excitation, 633 nm; emission, 650-750 nm) was recorded in the red channel. Three-dimensional projections were generated from XY images recorded at 1.5-µm intervals in Z (depth) by using ImageJ v.1.50e software.

4.2.3 Experimental procedure for EPS extraction

In order to optimize the EPS extraction from the subaerial biofilms developed on the granite blocks, the extraction efficacy of H_2SO_4 and NaOH at different concentrations, temperature and extraction times were evaluated. Two experimental designs were used for each extractant: a Box-Behnken design, considering extractant concentration, time and temperature of extraction as independent variables, and a full factorial design, considering only extractant concentration and time of extraction as independent variables at a constant temperature of 4 °C, as heating might provoke EPS disruption and/or cell lysis (Comte et al. 2006). The experimental designs are illustrated in Figure 4.3.

For extraction of EPS from the biofilms, each block was placed in a Petri dish with the colonized face turned down, and 10 mL of distilled water was added. This volume ensured that the biofilm was completely in contact with the solution (Figure 4.1b); 60 µL of formaldehyde (37 % w/w, 6 µL mL^{-1} water) was also added in order to prevent cell lysis, as formaldehyde can bind to cells by reacting with amino, hydroxyl, carbonyl and sulfhydryl groups in proteins and nucleic acids in the cell membrane (Alcamo 1997). The Petri dishes were sealed and maintained for 30 min at 30 °C in the case of Box-Behnken designs and for 60 min at 4 °C in the full factorial designs. Two millilitres (0.2 mL mL^{-1} water) of extractant (NaOH or H_2SO_4) was then added to each Petri dish, and the corresponding extraction conditions were maintained (Tables 4.1 and 4.2). The extracts obtained were then centrifuged at 5000 rpm for 20 min and the

supernatant was filtered (0.20 μm). The filtrate was collected for further chemical analysis. In order to obtain control values for extracted EPS, an extraction procedure with distilled water as the extractant (incubation at 4 °C for 60 min) was applied to three inoculated blocks. The results thus obtained were considered as reference values for evaluating extraction yields and cell lysis.

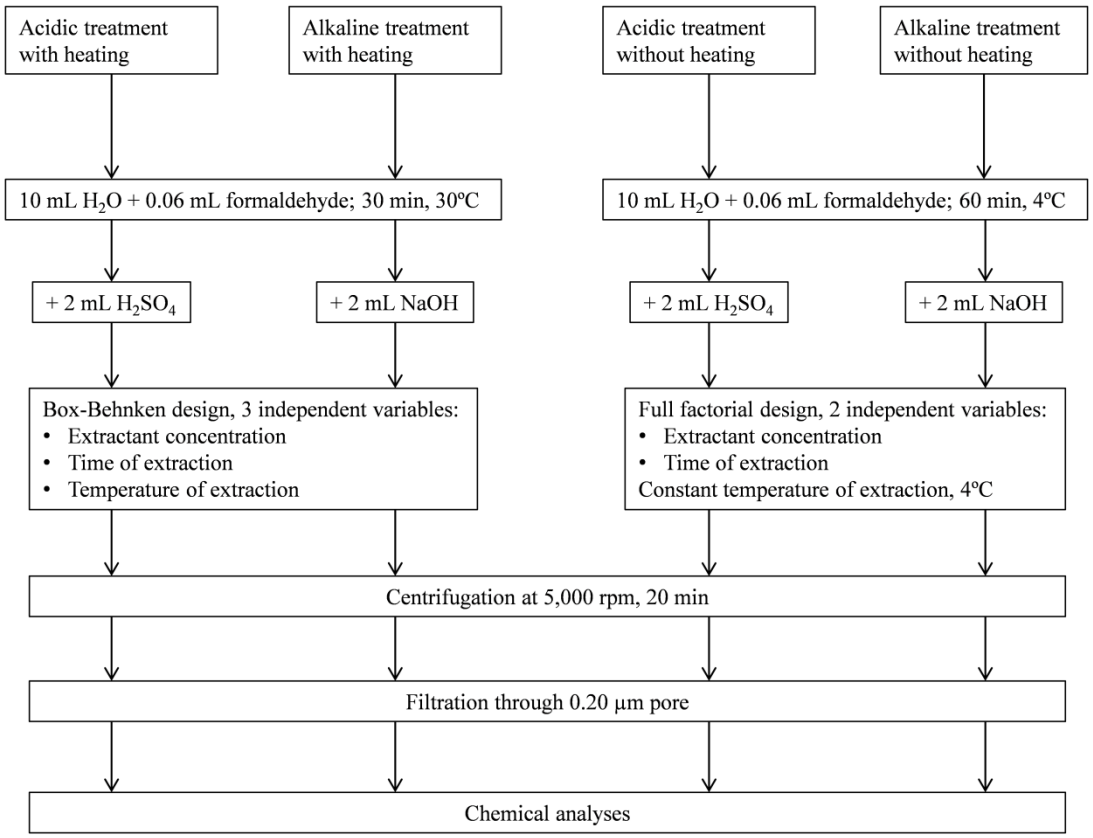

Figure 4.3 Flow chart of EPS extraction experiments carried out in the present study.

In order to study the influence of the experimental conditions on the extraction yield, for the treatments including heating, a Box-Behnken design with 3 independent variables (each with 3 levels), involving 13 experimental points plus additional experiments at the central point (3 central replicates), was used for each extractant. This design requires a total of 15 experiments, which is more economical and efficient than a 3^3 design (27 experiments) (Bezerra et al. 2008). For treatments without heating, only two independent variables at three levels each were considered, so that a full factorial 3^2 design with 9 experiments and 3 central replicates (a total of 11 experiments) was applied. The independent variables studied and their levels are listed in Tables 4.1 and

4.2. The levels of independent variables were coded, i.e. each real value studied was transformed into coordinates on a scale with dimensionless values (-1, 0, 1) proportional to its location in the experimental space. Such codification enables investigation of variables of different orders of magnitude without the variable of greater magnitude influencing evaluation of the variable of lesser magnitude (Bezerra et al. 2008). The dependent variables considered for quantifying extraction yields were the carbohydrate, protein and DNA contents of the extract.

4.2.4 Characterization of extracted EPS

Extracted EPS were characterized by quantifying carbohydrates and proteins present in the extract, as these are considered the main EPS components (Flemming & Wingender 2010). The DNA content was also determined, as the nucleic acid content in the extract can be used as an indicator to evaluate the extent of cell lysis during extraction (Wingender et al. 1999). The DNA contents of the control extracts (obtained using distilled water as extractant and incubation at 4 °C for 60 min) were considered reference values for evaluating cell lysis. The carbohydrate, protein and DNA contents were measured spectrophotometrically (Varian Cary 100) by, respectively, the phenol-sulphuric acid method (Dubois et al. 1956) with D(+)-glucose (Panreac) as standard, the Lowry method (Lowry et al. 1951) with bovine albumin serum (Sigma-Aldrich) as standard and the diphenylamine method (Burton 1956) with fish sperm (Sigma-Aldrich) as standard. The values obtained were expressed relative to the biomass on each block (expressed as mg g^{-1} DWB), estimated colorimetrically as described above.

4.2.5 Statistical analyses

To evaluate the importance of the independent factors considered in the EPS extraction, the experimental data obtained in each experimental design were subjected to analysis of variance (ANOVA). Tests on equality of the different factor levels were performed, and the main (linear and quadratic) and interaction (linear by linear) effects were estimated. Replicates at the centre point enable estimation of the pure error associated with repetitions. Thus, the sum of the square of residuals (SS_{res}) can be separated into the sum of squares due to pure error (SS_{pe}) and the sum of squares due to lack of fit (SS_{lof}): this allows evaluation of the suitability of the model through a lack-of-fit test (Bezerra et al. 2008).

The experimental data were analysed by the response surface methodology (Box & Wilson 1954), implemented using Statistica 10 (StatSoft, Inc.) software. This allowed development of empirical models describing the interrelationship between operational and experimental variables by use of equations including linear, quadratic and interaction terms. The equations were calculated from experimental data by multiple regressions applied using the least-squares method to enable prediction of the optimal experimental conditions for EPS extraction. Finally, the optimized extraction protocol thus developed was applied to three inoculated blocks in order to test the extraction efficiency.

4.3 RESULTS

CLSM images (Figure 4.4) showed almost complete colonization of the surface in each of the three granite blocks. Examination of the vertical profiles of the CLSM images indicated attenuation of the three fluorescence signals at depth, revealing a biofilm of thickness ranging between 10 and 30 μm. The biofilms were dominated by phototrophic microorganisms, with agglomerations of both coccoid and bacilli cells: heterotrophic bacteria were disperse and far less abundant. The fluorescent signal produced by ConA-TRITC was strong in all images taken, mainly around the phototrophic cells.

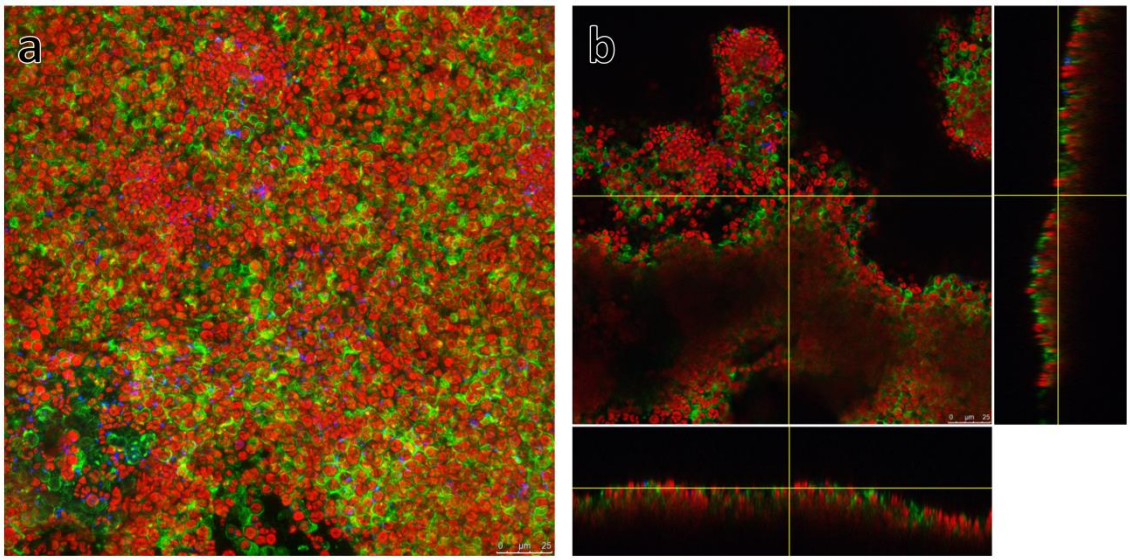

Figure 4.4 CLSM image from subaerial biofilm developed on one of the inoculated granite blocks (blue: bacterial DNA dyed with SYTO 9; green: EPS dyed with ConA-TRITC; red: chlorophyll auto-fluorescence). (a) Z projection of an area of 256x256 μm^2. (b) Orthogonal views at the central point of the area.

Tables 4.1 and 4.2 show the experimental conditions assayed in, respectively, the Box-Behnken (with heating) and full factorial (without heating) designs (independent variables expressed in terms of both coded and real values), as well as the experimental data obtained for carbohydrate, protein and DNA contents of the respective extracts.

Table 4.1 Operational conditions of the Box-Behnken designs (with heating) applied, and yields of carbohydrates, proteins and DNA in the experimental extraction protocols tested.

Extractant	Exp.	Independent variables			Dependent variables		
		Conc.* (mol L^{-1})	Temp. (°C)	Time (min)	Carbohydrates (mg g^{-1} DWB)	Proteins (mg g^{-1} DWB)	DNA (mg g^{-1} DWB)
NaOH	1	2 (0)	90 (1)	30 (-1)	316.52	77.27	35.72
	2	2 (0)	30 (-1)	30 (-1)	299.48	94.53	21.80
	3	2 (0)	90 (1)	90 (1)	520.24	311.12	9.62
	4	2 (0)	30 (-1)	90 (1)	377.62	120.10	38.47
	5	1 (-1)	90 (1)	60 (0)	405.09	221.79	152.44
	6	1 (-1)	30 (-1)	60 (0)	417.85	52.10	15.48
	7	3 (1)	90 (1)	60 (0)	340.39	124.00	52.47
	8	3 (1)	30 (-1)	60 (0)	318.52	52.10	0.80
	9	1 (-1)	60 (0)	30 (-1)	216.91	56.93	56.97
	10	1 (-1)	60 (0)	90 (1)	257.63	116.20	42.87
	11	3 (1)	60 (0)	30 (-1)	332.62	19.14	18.36
	12	3 (1)	60 (0)	90 (1)	433.81	101.54	48.72
	13	2 (0)	60 (0)	60 (0)	441.18	109.62	43.41
	14	2 (0)	60 (0)	60 (0)	358.75	88.98	65.38
	15	2 (0)	60 (0)	60 (0)	300.18	81.93	42.22
H_2SO_4	1	2 (0)	90 (1)	30 (-1)	714.02	83.02	334.70
	2	2 (0)	30 (-1)	30 (-1)	647.69	21.85	298.20
	3	2 (0)	90 (1)	90 (1)	567.19	137.57	221.62
	4	2 (0)	30 (-1)	90 (1)	572.74	54.64	369.49
	5	1 (-1)	90 (1)	60 (0)	814.99	119.75	385.84
	6	1 (-1)	30 (-1)	60 (0)	636.35	46.85	222.26
	7	3 (1)	90 (1)	60 (0)	617.72	105.60	266.63
	8	3 (1)	30 (-1)	60 (0)	716.73	5.71	321.14
	9	1 (-1)	60 (0)	30 (-1)	445.07	36.73	356.18
	10	1 (-1)	60 (0)	90 (1)	355.83	117.02	259.10
	11	3 (1)	60 (0)	30 (-1)	320.73	29.33	296.54
	12	3 (1)	60 (0)	90 (1)	874.10	159.17	607.11
	13	2 (0)	60 (0)	60 (0)	545.66	124.45	466.27
	14	2 (0)	60 (0)	60 (0)	669.41	76.50	486.45
	15	2 (0)	60 (0)	60 (0)	553.09	59.89	273.39

*Extractant concentration in the 2 mL of solution added to the Petri dish.
Coded dimensionless levels for independent variables are indicated in brackets.

Table 4.2 Operational conditions of full factorial designs (without heating) considered and yields of carbohydrates, proteins and DNA in the experimental extraction protocols tested.

Extractant	Exp.	Independent variables		Dependent variables		
		Conc.* (mol L^{-1})	Time (min)	Carbohydrates (mg g^{-1} DWB)	Proteins (mg g^{-1} DWB)	DNA (mg g^{-1} DWB)
NaOH	1	1 (-1)	60 (-1)	292.39	60.51	83.38
	2	1 (-1)	120 (0)	271.77	52.71	51.99
	3	1 (-1)	180 (1)	242.68	56.97	38.44
	4	2 (0)	60 (-1)	328.08	64.58	31.20
	5	2 (0)	180 (1)	288.38	62.82	8.48
	6	3 (1)	60 (-1)	286.74	57.54	4.57
	7	3 (1)	120 (0)	341.78	55.15	21.49
	8	3 (1)	180 (1)	343.72	84.61	26.02
	9	2 (0)	120 (0)	328.44	48.97	7.70
	10	2 (0)	120 (0)	345.93	43.12	10.15
	11	2 (0)	120 (0)	332.89	48.00	8.35
H_2SO_4	1	1 (-1)	60 (-1)	495.75	57.41	352.99
	2	1 (-1)	120 (0)	361.85	44.47	403.29
	3	1 (-1)	180 (1)	425.99	52.19	411.81
	4	2 (0)	60 (-1)	547.99	49.66	438.68
	5	2 (0)	180 (1)	732.76	45.39	509.87
	6	3 (1)	60 (-1)	408.56	15.85	405.79
	7	3 (1)	120 (0)	449.07	12.23	432.24
	8	3 (1)	180 (1)	717.37	4.16	340.70
	9	2 (0)	120 (0)	549.59	36.47	342.85
	10	2 (0)	120 (0)	664.65	47.73	458.78
	11	2 (0)	120 (0)	581.45	31.54	453.77

*Extractant concentration in the 2 mL of solution added to the Petri dish.
Coded dimensionless levels for independent variables are indicated in brackets.

Experiments 1-13 in the Box-Behnken designs and 1-9 in the complete factorial design evaluated the effect of factors on extraction yield. Experiments 13-15 and 9-11 were replications at the central point of the design used to estimate the influence of experimental error (pure error). The EPS concentrations obtained in control extractions were as follows: carbohydrates, 7.13 ± 4.47 mg g^{-1} DWB; proteins, 6.25 ± 5.41 mg g^{-1} DWB; and DNA, 15.14 ± 7.58 mg g^{-1} DWB (expressed as mean value ± standard deviation of three replicates).

Table 4.3 Results of ANOVA, lack-of-fit tests and determination coefficients for DNA extraction in the Box-Behnken and full factorial designs with NaOH as extractant.

Factor	*SS*	*df*	*MS*	F	*P*-value
Box-Behnken design					
[NaOH] (mol L^{-1})	2716.44	1	2716.44	15.9739	0.0573
$[NaOH]^2$ (mol^2 L^{-2})	379.83	1	379.83	2.2336	0.2736
Temp (ºC)	3772.49	1	3772.49	22.1840	0.0422
$Temp^2$ (ºC^2)	99.20	1	99.20	0.5834	0.5248
Time (min)	5.83	1	5.83	0.0343	0.8702
$Time^2$ (min^2)	1298.41	1	1298.41	7.6353	0.1098
[NaOH]·Temp (mol L^{-1} ºC)	1818.53	1	1818.53	10.6938	0.0822
[NaOH]·Time (mol L^{-1} min)	494.25	1	494.25	2.9064	0.2303
Temp·Time (ºC min)	457.25	1	457.25	2.6888	0.2427
Lack of fit	6100.59	3	2033.53	11.9581	0.0782
Pure error	340.11	2	170.06		
Total SS	17580.32	14			
					R^2 = 0.6336
					Adjusted R^2 = 0.0000
Full factorial design					
[NaOH] (mol L^{-1})	2469.43	1	2469.43	878.7844	0.0215
$[NaOH]^2$ (mol^2 L^{-2})	1168.48	1	1168.48	415.8222	0.0312
Time (min)	355.91	1	355.91	126.6572	0.0564
$Time^2$ (min^2)	70.07	1	70.07	24.9359	0.1258
[NaOH]·Time (mol L^{-1} min)	1101.93	1	1101.93	392.1391	0.0321
Lack of fit	168.98	3	56.33	20.0441	0.1624
Pure error	2.81	2	2.81		
Total SS	5471.12	10			
					R^2 = 0.9686
					Adjusted R^2 = 0.9294

SS sum of squares, *df* degrees of freedom, *MS* mean square, R^2 coefficient of determination.

The amounts of EPS extracted varied widely both between extractants and designs. Much larger quantities of carbohydrates and proteins were extracted than in the controls. However, the large amounts of DNA extracted in many of the experiments, relative to those obtained in the controls, indicated cell lysis as a critical problem for developing an efficient extraction protocol, as the extracts could be contaminated by intracellular material. The use of H_2SO_4 as extractant yielded excess DNA (221.62 mg g^{-1} DWB in the Box-Behnken design and 340.70 mg g^{-1} DWB in the full factorial design; Tables 4.1 and 4.2, respectively). EPS extraction with NaOH yielded DNA values below those considered representative of cell lysis (15.14 ± 7.58 mg g^{-1} DWB

obtained in control extractions) in some experiments with both designs. This finding suggests that cell lysis could be minimized by controlling the extraction conditions. Thus, the experimental results of the NaOH-mediated DNA extraction were used to construct second-order models with linear, quadratic and interaction effects, in order to predict the amount of DNA in the extracts (dependent variable) as a function of the NaOH concentration, temperature and time of extraction (independent variables). The sum of squares (SS) of residuals and F-tests associated with the combined linear and quadratic effects and their interactions are shown in Table 4.3. The mean of squares due to pure error (MS_{pe}) and the mean of squares due to lack of fit (MS_{lof}) were also calculated. Taking into account the MS_{lof}/MS_{pe} ratios, the lack of fit was satisfactory for both designs; however, the values of the coefficients R^2 and adjusted R^2 obtained in the Box-Behnken design were low, and the model fit was only satisfactory for the full factorial design, with values of R^2 and adjusted R^2 higher than 0.90. Thus, in order to develop the EPS extraction protocol in biofilms growing on rocks, only the results obtained from the NaOH full factorial design (Table 4.2) were taken into account for optimization.

Table 4.4 Estimates of main and interaction effects of studied factors (as coded variables) for models of NaOH-mediated extraction of carbohydrates, proteins and DNA derived from the full factorial design.

Factor	Carbohydrates (mg g^{-1} DWB)		Proteins (mg g^{-1} DWB)		DNA (mg g^{-1} DWB)	
	Effect	*P*-value	Effect	*P*-value	Effect	*P*-value
Mean/Intercept	304.06	0.0083*	59.90	0.0139*	30.19	0.0114*
[NaOH] (mol L^{-1})	55.13	0.1153	9.04	0.2240	-40.57	0.0215*
$[NaOH]^2$ (mol^2 L^{-2})	22.66	0.2184	-4.05	0.3700	-22.38	0.0312*
Time (min)	-10.81	0.4783	7.26	0.2731	-15.40	0.0564
$Time^2$ (min^2)	21.21	0.2321	-13.82	0.1211	-5.48	0.1258
[NaOH]·Time (mol L^{-1} min)	53.34	0.1450	15.30	0.1653	33.20	0.0321*
MS pure error	152.82		16.52		2.81	
Lack of fit *P*-value	0.4738		0.4356		0.1624	
R^2	0.9073		0.8784		0.9686	
Adjusted R^2	0.7915		0.7265		0.9294	

*Statistically significant effect at a 95% confidence level.

The amounts of the different components in the EPS extracts obtained from the NaOH-full factorial design ranged from 242.68 to 343.72 mg g^{-1} DWB for carbohydrates, from 43.12 to 84.61 mg g^{-1} DWB for proteins and from 4.57 to

83.38 mg g^{-1} DWB for DNA. In theory, optimization of EPS extraction should focus on maximizing the extraction yields of carbohydrates and proteins, as the main components of EPS. However, as some experiments (1-4 and 8, Table 4.2) yielded DNA values indicating cell lysis, experimental variables (NaOH concentration and extraction time) were optimized to minimize this effect. Table 4.4 presents estimates of the main (linear and quadratic) and interactive effects of these factors on the extraction yield of the EPS components under study. Student tests (t-tests) and their associated probabilities (*P*-values) were used to confirm the significance of the factors studied.

None of the EPS components showed a significant lack of fit ($p > 0.05$); however, it is not possible to assign any significant effect of the factors studied on the extraction yield of carbohydrates and proteins, probably because of the high pure error associated with the central replicates. The DNA extraction yield proved to be significantly affected by NaOH concentration (mean linear and quadratic effects) and the interaction between NaOH concentration and extraction time, resulting in high R^2 and adjusted R^2 values (0.9686 and 0.9294, respectively). Thus, the multiple regression model for estimating the amount of DNA extracted as a function of the extraction conditions (expressed for uncoded values) was calculated as follows:

$$DNA\ (mg\ g^{-1}\ DWB) = 245.42 - 143.00[NaOH] + 22.38[NaOH]^2 - 1.05t + 0.0015t^2 + 0.28[NaOH]t$$

where *[NaOH]* is the concentration of NaOH in moles per litre and *t* is the extraction time in minutes.

The response surface for the DNA extraction is depicted in Figure 4.5. Within the range of conditions considered, there is a critical point corresponding to a minimum value of extracted DNA, which can be resolved from the model. The solution to this minimum is a value of 7.02 mg g^{-1} DWB of extracted DNA, estimated for 2.44 mol L^{-1} NaOH and 122 min extraction time. These extraction conditions can thus be considered as optimal, as the presence of DNA in the extracts (indicative of cell lysis) was decreased to acceptable levels in comparison with those obtained in the controls. Hence, the conditions considered optimal for the extraction of EPS from subaerial biofilms was 2.50 mol L^{-1} NaOH and 120 min of extraction to yield 7.07 ± 12.02 mg g^{-1} DWB of DNA (expressed as estimated value ± 95 % confidence interval).

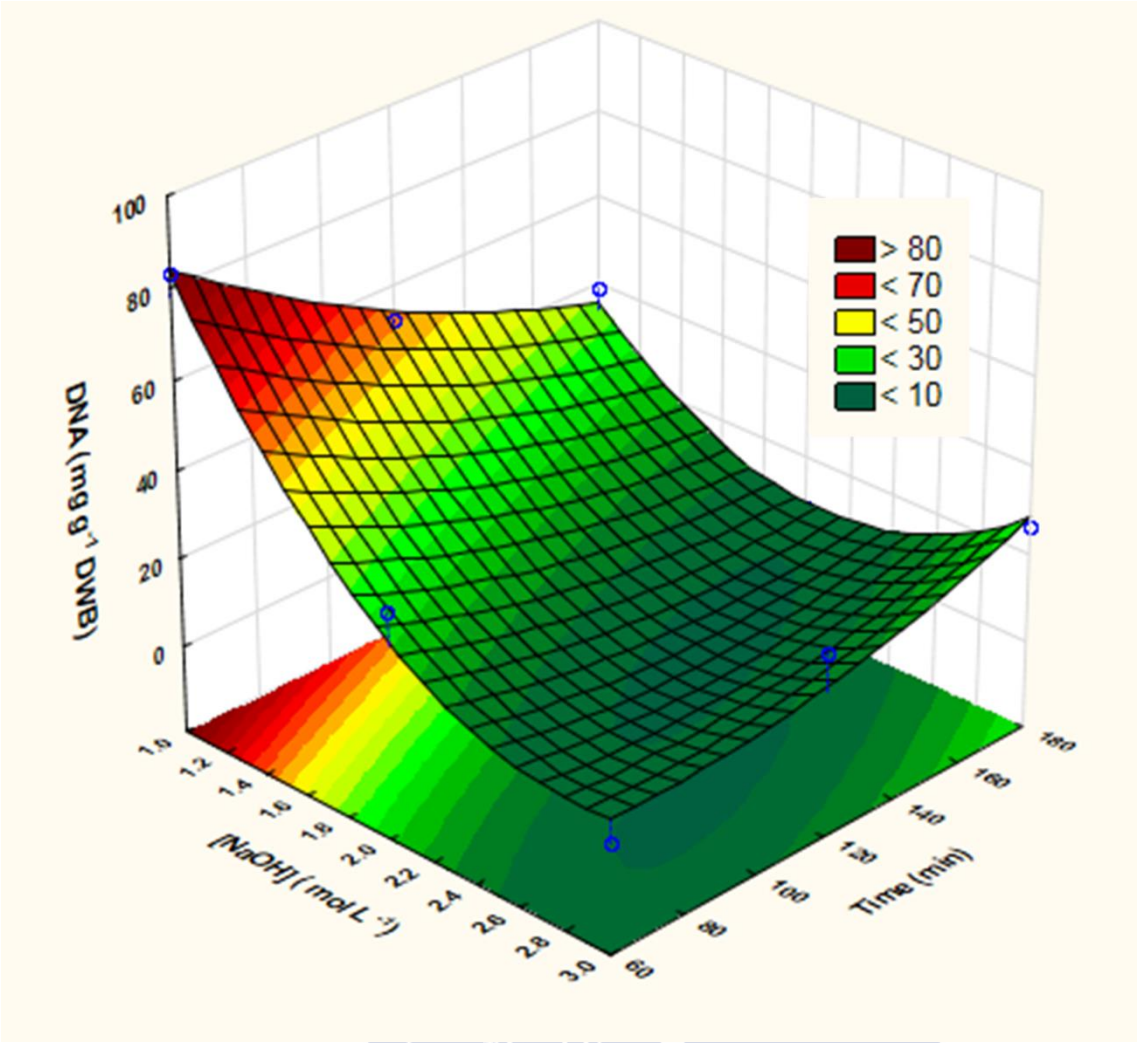

Figure 4.5 Response surface of DNA extraction yield as a function of NaOH concentration and time of extraction.

To test the suitability of this optimization procedure, EPS were extracted from three additional inoculated blocks following the protocol described in the 'Materials and methods' under the experimental conditions established above (Table 4.5). The concentrations of DNA in the extracts were within the 95 % confidence interval predicted in all cases, which confirms the effectiveness of the model. Thus, these concentrations were not significantly different (t test, $p < 0.05$) from those obtained from controls, so that we can assume that no significant cell lysis occurred.

Table 4.5 Quantification of EPS by application of optimized extraction conditions (2.5 mol L^{-1} NaOH and 120 min) to laboratory-grown subaerial biofilms.

Replicate	DNA (mg g^{-1} DWB)	Carbohydrates (mg g^{-1} DWB)	Proteins (mg g^{-1} DWB)
1	15.01	312.92	23.79
2	11.56	353.27	46.73
3	12.55	447.47	42.69
Mean ± SD	13.04 ± 1.78	371.22 ± 69.05	37.74 ± 12.25

4.4 DISCUSSION

Incubation of inoculated granite blocks for 2 months under laboratory conditions allowed the development of subaerial biofilms, as confirmed by CLSM observations (Figure 4.4). The EPS content of laboratory-grown biofilms was thus considered sufficiently high to enable development of an extraction protocol. In view of the results obtained (Tables 4.1 and 4.2), cell lysis was the main analytical obstacle to efficient extraction. Hence, in order to select the most suitable design, the following criteria were taken into account: (i) minimum DNA content in the extracts, as a significantly higher amount than extracted from controls can be considered an indicator of excessive cell lysis, which would invalidate the extraction protocol; (ii) the *P*-value of the lack-of-fit test for DNA extraction; and (iii) the coefficient of determination (R^2) for each DNA extraction design, as these parameters indicate the goodness of fit of the model, which would minimize cell lysis through appropriate modification of independent factors according to the surface response methodology.

Considering the minimum allowable DNA content in the extracts, H_2SO_4 proved unsuitable as an extractant (Tables 4.1 and 4.2). Acidic treatment improves the repulsive force and disrupts the interaction between EPS and cells, causing the EPS to fall away from the cell surface (Sheng et al. 2010). Although this extractant was successfully used with other types of biofilms (Barranguet et al. 2004), it caused excessive cell lysis in the present trial and was thus disregarded. However, extraction conditions for NaOH could be optimized in order to minimize cell lysis, the main analytical obstacle to efficient extraction. NaOH was successfully used to extract EPS from other types of biofilms (Liu & Fang 2002, Comte et al. 2006, Adav & Lee 2008, Zhu et al. 2015), as it causes the acidic groups, such as carboxylic acids, to be ionized, resulting in a strong repulsion

between the EPS and the cells and thus enabling dissolution of the EPS in water (Sheng et al. 2010).

Taking into account the lack-of-fit tests and R^2 values of the NaOH-mediated DNA extractions (Table 4.3), the model fit was only satisfactory for the full factorial design, which was taken into account for optimization. The absence of significant effects of the factors studied on the extraction yield of carbohydrates and proteins (Table 4.4) caused a decrease in the adjusted R^2 values relative to those of R^2 for both variables, as inclusion of the factors studied did not provide any useful information for the response model fit (Montgomery 1997). These results preclude development of a robust model for controlling the extraction of carbohydrates and proteins from biofilms. This does not mean that carbohydrates and proteins are not effectively extracted. Moreover, although it was not possible to obtain a robust model for optimizing the yields of carbohydrates and proteins, the optimization procedure will always be limited by the presence of DNA in the extract. Considering the DNA content, the effect of NaOH concentration proved to be more important than the extraction time (Table 4.4). These effects represent the difference in performance of the process caused by a change from low (−1) to high (+1) levels of the corresponding factor (Haaland 1989). A model for estimating the amount of extracted DNA as a function of the extraction conditions was developed. This model predicted optimal conditions for the extraction as a concentration of NaOH of 2.5 mol L^{-1} and an extraction time of 120 min.

The procedure was applied to additional inoculated blocks in order to assess its efficacy (Table 4.5). DNA contents yielded by the extractions proved suitable, as they matched the values predicted by the model, which we considered acceptable in terms of cell lysis (these values were not significantly different from those obtained in the control extractions). Regarding the extraction yields of the main EPS components, we obtained mean values of 371.22 mg g^{-1} DWB for carbohydrates and 37.74 mg g^{-1} DWB for proteins, representing, respectively, ∼52 and ∼6 times more than obtained in the controls. Although these values demonstrate an improvement of the extraction yields relative to the control extractions, caution is required in interpreting the results. The lack of commercially available reference materials of this type of sample, as well as the experimental difficulties in quantifying the recovery rate of the analytical procedure, precludes interpretation of the results in absolute terms. These limitations imply that the amounts of EPS extracted must be considered as relative values. Thus, the extraction

protocol enables comparison of EPS produced by different biofilms; however, the values obtained should not be interpreted as the actual EPS contents of the biofilms.

The EPS obtained using the optimised extraction protocol imply a protein/polysaccharide ratio (PN/PS) of ~0.10 (Table 4.5). Considering the PN/PS ratios in the initial NaOH-mediated extractions (Tables 4.1 and 4.2), values ranging between 0.06 and 0.60 were observed. These data suggest that the efficiency of extraction of polysaccharides and proteins will differ depending on the extraction conditions applied. Therefore, the range 0.06-0.60 should be considered an estimate of the actual PN/PS ratio present in the biofilms studied. To our knowledge, these values represent the first quantitative data of EPS extracted from subaerial biofilms developed on rocky substrata. The PN/PS ratio estimated is far lower than reported for other types of biofilm, in which the amounts of protein exceeded the carbohydrate content (e.g. Liu & Fang 2002, Comte et al. 2006, Adav & Lee 2008). However, the difference is small in comparison with results obtained for more similar biofilms, such as soil biofilms, for which Redmile-Gordon et al. (2014) obtained values ranging from 0.2 to 0.4. Subaerial biofilms may produce larger amounts of polysaccharides to enhance water retention, thus enabling them to tolerate desiccation in dry environments (Flemming & Wingender 2010). Use of the extraction protocol developed here to quantify and characterize the EPS in subaerial biofilms grown on stone, in combination with currently available microscopy techniques, could help us to clarify this and other questions regarding the role of the biofilm matrix, thus leading to a better understanding of subaerial biofilms. The extraction protocol can be applied to a broad range of research, such as ecological studies, estimation of potential biodeteriorative effects or possible biotechnological applications. For example, a comparison can be made of EPS produced by biofilms composed of different microbial communities, subjected to different environmental conditions and/or grown on different lithotypes. Although the extraction protocol was developed using biofilms grown under laboratory conditions, it could be also applied to subaerial biofilms grown naturally on rocks or even other types of substrata (e.g. biofilms grown on glass, ceramic or metallic surfaces). However, the suitability of the extraction protocol should be evaluated before being applied in each new case. For this purpose, assessment of the DNA content in the extracts to confirm the absence of significant cell lysis is highly recommended.

4.5 CONCLUSIONS

Multi-species subaerial biofilms were successfully grown on granite blocks under laboratory conditions and an efficient method for extracting EPS from rocks was developed. H_2SO_4 proved unsuitable as an extractant as it gave rise to an excessive cell lysis. However, response surface optimization of NaOH-mediated extraction enabled cell lysis to be minimized. Confirmation experiments were performed under the optimal conditions established and a protocol for extracting EPS is proposed, yielding the first quantitative data on EPS extracted from subaerial biofilms developed on rocky substrata.

The extraction protocol developed can be summarized as follows. The granite block with biofilm is placed in a Petri dish with the colonized face turned down. Sufficient distilled water is added to ensure complete contact between the biofilm and the solution, and 6 μL mL^{-1} solution of formaldehyde (37 % w/w) is added. The Petri dish is sealed and maintained at 4 °C for 60 min, and 0.2 mL mL^{-1} of a solution of NaOH 2.5 mol L^{-1} is added. The Petri dish is then incubated at 4 °C for 120 min. The extract obtained is centrifuged at 5000 rpm for 20 min and the supernatant passed through a 0.20-μm filter. Finally, the filtrate with extracted EPS is collected for further chemical analyses.

USC
UNIVERSIDADE
DE SANTIAGO
DE COMPOSTELA

CHAPTER 5

LABORATORY GROWN SUBAERIAL BIOFILMS ON GRANITE: APPLICATION TO THE STUDY OF BIORECEPTIVITY

5.1 INTRODUCTION

Subaerial biofilms are complex microbial communities that grow on almost all terrestrial surfaces exposed to the atmosphere. These biofilms are composed of a variety of microorganisms, including phototrophic green algae and cyanobacteria and also heterotrophic fungi and bacteria. The biofilms occur widely on rock surfaces, where they actively participate in weathering (Viles 2012). In urban habitats, colonization of stone-made buildings and monuments by biofilm-forming microorganisms may cause biodeterioration that can be costly to repair (Warscheid & Braams 2000, Prieto & Sanmartín 2016, Villa et al. 2016).

As natural subaerial biofilms are often difficult to investigate *in situ*, several studies have been carried out to investigate the growth of biofilms under laboratory conditions. Most studies emulating microbial colonization and biofilm formation on rock surfaces have used individual species (Tiano et al. 1995, Shirakawa et al. 2003) or artificially mixed cultures (Guillite & Dreesen 1995, Prieto & Silva 2005, Seiffert et al. 2014, Villa et al. 2015) as inocula. These simplified laboratory models are useful in many studies owing to their genetic tractability and high degree of experimental control. However, they do not enable the complex processes involving an environmental community structure to be taken into account. This is sometimes necessary, as in the case of laboratory experiments designed to study the bioreceptivity of rocks.

The term bioreceptivity, defined by Guillitte (1995) as the aptitude of a material to be colonized by one or several groups of living organisms, refers solely to the properties of the material. Hence, if a culture formed by only one or two species is used to evaluate the potential bioreceptivity of a rock, there is a risk that what is actually being studied is the capacity of the specific microorganisms to colonize the rock rather than the capacity of the rock to be colonized. The use of multi-species cultures derived from natural biofilms grown on the specific type of rock therefore seems a more suitable approach. The complex community structure formed by microorganisms that actual colonize rocks allows competition and/or synergy between species. The colonization process resembles environmental colonization and the bioreceptivity of the rock can thus be more accurately evaluated. Moreover, it seems reasonable to assume that the multi-species culture should comprise pioneering colonizers. Although the establishment of a heterotrophic microflora on rocks is possible even without the pioneering participation of phototrophic organisms, the presence of organic substrates is necessary. Such substrates are usually derived from deposits introduced by dust and rain or particulate and gaseous organic compounds from air pollution (Warscheid & Braams 2000). As these conditions depend on external factors, the correct term for describing the ability of a rock to be colonized is extrinsic bioreceptivity (Guillitte 1995). However, the capacity of phototrophic organisms to colonize a rock will ultimately depend on the inherent properties of the rock (intrinsic bioreceptivity; Guillitte 1995), although it is also influenced by environmental parameters such as temperature, light and moisture (Ortega-Calvo et al. 1995). When the pioneering colonizers become established and conditions are favourable, biological succession of heterotrophic microorganisms will occur.

Miller et al. (2009a, 2010a, 2010b) used a phototrophic multi-species culture as an inoculum to study the bioreceptivity of various types of limestone in southern Europe. The culture, derived from a natural biofilm grown on a Portuguese limestone, was able to grow both epilithically and endolithically, depending on the physical characteristics of the rock under study. The adaptation to the substratum, which resembled the complexity of natural colonization, enabled proper evaluation of the bioreceptivity of the lithotypes under study and highlighted the benefits of the use of this type of culture for such studies.

As seen in Chapter 3 (Vázquez-Nion et al. 2016a), we obtained stable phototrophic multi-species cultures derived from natural subaerial biofilms grown on historical granite buildings in a World Heritage Site (Santiago de Compostela, NW Spain). The cultures were taxonomically characterized and found to be complex microbial communities composed by common pioneering colonizers of the surfaces of building stone, including granite.

The aims of the present study were (i) to induce environmental-like colonization of granitic stone under laboratory conditions by using phototrophic multi-species cultures, and (ii) to evaluate the potential suitability of the different cultures as inocula for investigating the bioreceptivity of granite. For this purpose, we designed an experimental set-up to enhance biofilm growth on granite blocks, and we monitored the colonization ability of each culture during a three-month period by colour measurement, quantification of photosynthetic pigments and extracellular polymeric substances (EPS), and confocal laser scanning microscopy (CLSM) observations.

5.2 MATERIALS AND METHODS

5.2.1 Procedure for biofilm formation

The phototrophic multi-species cultures tested are described in detail in Chapter 3 (Vázquez-Nion et al. 2016a). Briefly, five cultures (C1, C2, C3, C4 and C5) were obtained by incubating natural subaerial biofilm samples, obtained from granite surfaces, in BG11 liquid medium (Rippka et al. 1979) until establishment of stable microbial communities. Of these cultures, C1 proved very difficult to handle as it was extremely mucilaginous, which could lead to difficulty in successfully reproducing the inoculations. This culture was therefore not included in the present study. The other four cultures, taxonomically characterized as summarized in Table 5.1, were used as inocula for biofilm formation under laboratory conditions.

Table 5.1 Major phototrophic taxa present in the four cultures used as inocula for producing subaerial biofilms on granite blocks. Data from Chapter 3 (Vázquez-Nion et al. 2016a).

Culture			
C2	**C3**	**C4**	**C5**
Chlorophyta	**Chlorophyta**	**Chlorophyta**	**Bryophyta**
Bracteacoccus minor	*Chlorella* sp.	*Bracteacoccus* sp.	*Syntrichia ruralis*
	Stichococcus bacillaris	**Cyanobacteria**	**Charophyta**
	Cyanobacteria	*Chroococcus* sp.	*Klebsormidium* sp.
	Aphanocapsa fuscolutea	*Isocystis* sp.	**Chlorophyta**
	Gloeocapsa aeruginosa		*Bracteacoccus* sp.
	Gloeocapsa punctata		*Chlamydomonas* sp.
	Isocystis sp.		*Chlorella* sp.
			Stichococcus bacillaris
			Cyanobacteria
			Aphanocapsa sp.
			Leptolyngbya cebennensis

A volume equivalent to 0.85 mg dry weight biomass of each of the four cultures (C2, C3, C4, C5), in exponential growth phase, was inoculated onto the upper surface of each of 12 previously autoclaved 4×4×2 cm^3 granite blocks (48 blocks in total). The inoculated granite blocks were subjected to favourable conditions of temperature, light and moisture to promote biofilm formation. Thus, the blocks were placed in dishes periodically filled with sterilized distilled water (so that the blocks were constantly damp) and were incubated in a climatic chamber (SCLAB PGA-1228/2 HR) under stationary conditions of 23°C, 95% relative humidity and a 12h light/dark photoperiod (~20 µmol photon m^{-2} s^{-1}) for three months (Figure 5.1). Lightning was provided by fluorescent lamps (OSRAM L 36W/765). The position of each block was periodically changed in a semi-random way to avoid influence from possible micro-climatic variations in the chamber.

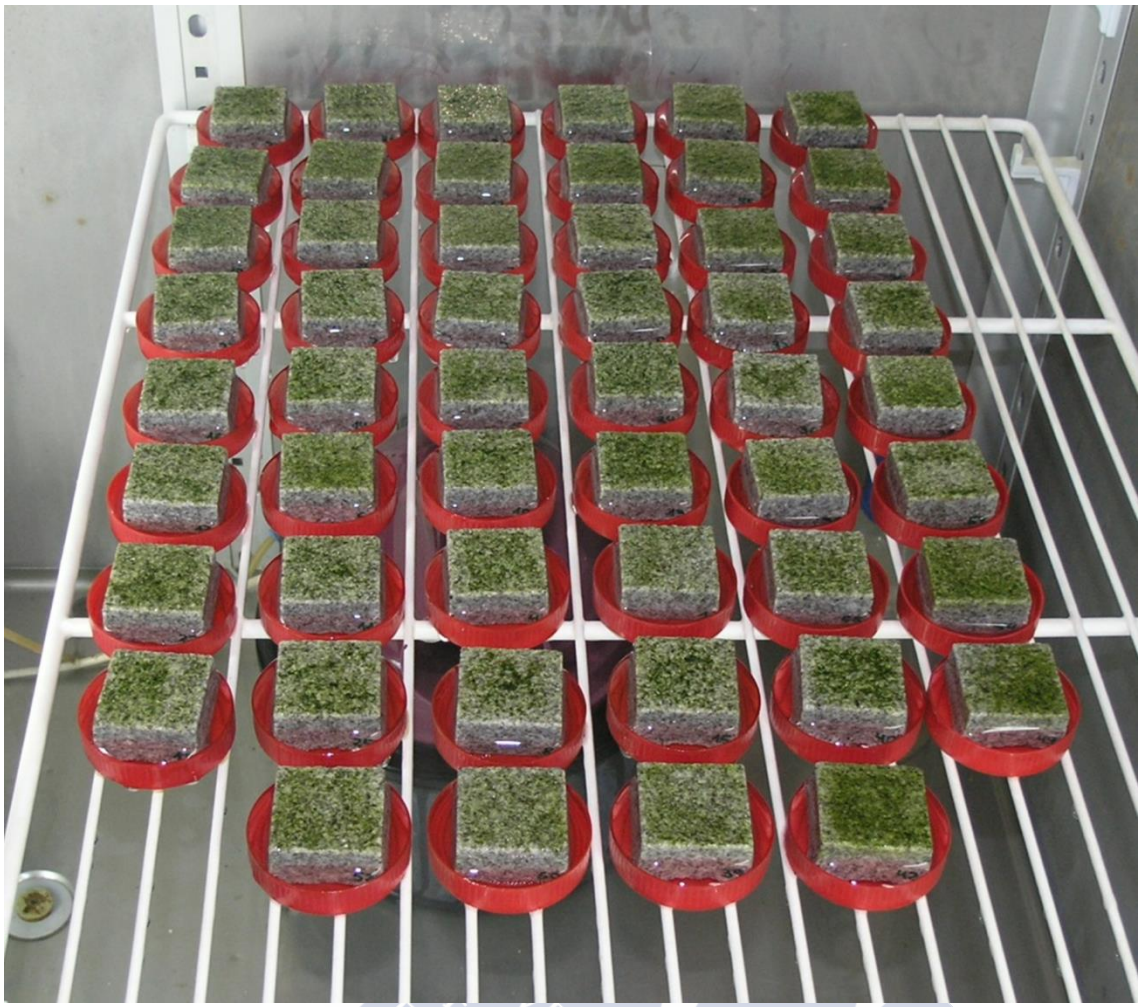

Figure 5.1 Subaerial biofilms developed on the granite blocks after incubation for three months in the climatic chamber.

5.2.2 Assessment of biofilm growth by colour measurement

Colour measurement has been demonstrated to be a reliable non-destructive method for monitoring biofilm growth on stone surfaces (Prieto et al. 2004, Sanmartín et al. 2012). Colour was measured with a portable spectrophotometer (Konica Minolta CM-700d) directly on the surface of the humid blocks, following protocol developed by Prieto et al. (2010). Measurements consisted of a total of 9 readings taken at different zones on each block under the following conditions: illuminant D65, observer 2º and a 10 mm diameter target area. The colour was measured on three replicate blocks for each culture, before inoculation and then once a week during the three-month incubation period.

Colour measurements were analysed using the CIELAB colour system (CIE 1986), which represents each colour by means of three scalar parameters or Cartesian coordinates: *L**, lightness or luminosity of colour; *a**, associated with changes in redness-greenness; and *b**, associated with changes in yellowness-blueness. Alternatively, each colour is represented by means of three angular parameters or cylindrical coordinates, most closely related to the psychophysical perception of the colour: *L**, lightness or luminosity of colour, also defined in both scalar and angular colour sets; C^*_{ab}, chroma or saturation, related to the intensity of colour; and h_{ab}, hue angle or tone of colour, which refers to the dominant wavelength and indicates redness, yellowness, greenness, or blueness on a circular scale. To evaluate biofilm growth, colour data were processed as colour differences between a colonized block and the block before inoculation. This enables quantification of the colour change due to biofilm growth. Thus, colour differences were calculated as follows:

$$\Delta L^* = L^*_x - L^*_0$$

$$\Delta a^* = a^*_x - a^*_0$$

$$\Delta b^* = b^*_x - b^*_0$$

$$\Delta H^*_{ab} = 2(C^*_{ab:\,x} \cdot C^*_{ab:\,0})^{1/2} \cdot \sin[(h_{ab:x} - h_{ab:0})/2]$$

$$\Delta E^*_{ab} = [(\Delta L^*)^2 + (\Delta a^*)^2 + (\Delta b^*)^2]^{1/2}$$

where the subscript *x* denotes the colour parameter of an inoculated block after *x* days of incubation, and the subscript *0* denotes the colour parameter of the block before inoculation.

5.2.3 Quantification of photosynthetic pigments and EPS

For determination of chlorophyll *a* (chl *a*), chlorophyll *b* (chl *b*) and total carotenoids, three replicates of three-month-old biofilms from each culture were subjected to the extraction protocol developed by Fernández-Silva et al. (2011). Colonized blocks were placed in Petri dishes containing 7 mL of dimethylsulfoxide (DMSO) and sonicated by inserting the narrow tip of an ultrasonic generator (Vibra-Cell, Sonics & Materials, Inc.) into the extractant. Sonication was carried out for 5 x 30

s (0.5 duty cycle, 60% amplitude), with breaks of 30 s to prevent overheating. Extracts were heated at 63ºC for 40 min, filtered and measured in a UV-Visible Spectrophotometer (Varian Cary 100), using the equations developed by Wellburn (1994) to calculate the contents of chl *a*, chl *b* and carotenoids.

For EPS quantification, three replicates of three-month-old biofilms derived from each culture were subjected to the extraction protocol developed in Chapter 4 (Vázquez-Nion et al. 2016b). Colonized blocks were placed in Petri dishes containing 10 mL of distilled water and 60 µL of formaldehyde (37% w/w) and maintained at 4°C for 60 minutes. Two mL aliquots of NaOH (2.5 mol L^{-1}) were then added to the Petri dishes, which were maintained at 4°C for 120 minutes. The extracts were centrifuged at 5000 rpm for 20 min and the supernatant was filtered. The carbohydrate fraction of the EPS was quantified spectrophotometrically (Varian Cary 100) by the phenol-sulphuric acid method (Dubois et al. 1956), with D(+)-glucose (Panreac) as standard.

5.2.4 Confocal laser scanning microscopy (CLSM)

Three inoculated blocks from each culture were observed by CLSM after the three-month incubation period to establish any possible differences in the spatial organization, architecture and depth profiles of the biofilms. EPS were stained using the fluorescently labelled lectin Concavalanin A, tetramethylrhodamine conjugate (ConA-TRITC, Molecular Probes): 100 µL of a 0.5 g L^{-1} ConA-TRITC solution was applied as a droplet to the biofilms, which were then incubated for 30 min at 25ºC and subsequently carefully rinsed with sterile distilled water. Bacteria were stained with the fluorescent nucleic acid stain SYTO 9 (Molecular Probes): 100 µL of a 1.67 µM SYTO 9 solution was applied to the biofilms, which were incubated for 30 min at 25ºC and subsequently carefully rinsed with sterile distilled water. Photosynthetic microorganisms were visualized by chlorophyll auto-fluorescence.

A Leica TCS SP5 X CLSM (Leica Microsystems) equipped with a white light laser and a 63X objective (NA 1.4, glycerol) was used to obtain images of the biofilms directly on the block surface. Observations were made in three randomized areas of each biofilm by multi-channel detection: SYTO 9 (excitation, 488 nm; emission, 505-550 nm) targeting bacterial DNA was recorded in the blue channel; ConA-TRITC (excitation, 543 nm; emission, 560-615 nm) targeting EPS was recorded in the green

channel; chlorophyll auto-fluorescence (excitation, 633 nm; emission, 650-750 nm) was recorded in the red channel. Three-dimensional projections were generated from XY images recorded at 1.5 µm intervals in Z (depth) by using ImageJ v.1.50e software.

5.2.5 Statistical analysis

Data on colour differences obtained during the three months of biofilm growth were analysed by two-way repeated measures analysis of variance (ANOVA) to test for differences between the cultures used as inocula (between-subjects factor) over time (within-subjects factor). Within-subjects effects (time and interactions) were corrected for sphericity by applying Greenhouse-Geisser correction.

Considering colour differences as indirect estimators of biofilm biomass (Prieto et al. 2002), data from the whole colonization period were fitted to sigmoidal curves to characterize and compare growth patterns between cultures. The colour data from each inoculum were fitted to the following sigmoidal growth model by using SigmaPlot 12.0 (Systat Software, Inc.):

$$y = y_0 + \frac{y_{st} - y_0}{1 + e^{k(x_0 - x)}}$$

where y_0 is the initial value, y_{st} is the value approached at the stationary phase, k is a rate constant and x_0 is the time when maximal growth rate is achieved.

Data derived from colour measurements, photosynthetic pigments and EPS at the end of the experiment were subjected to one-way ANOVA and post hoc Tukey HSD tests to compare cultures. Statistical analyses were implemented using SPSS Statistics v19.0 (IBM) software, and differences were considered statistically significant at $p < 0.05$.

5.3 RESULTS

5.3.1 Colour measurements during biofilm formation

The experimental conditions proved suitable for biofilm development as growth of green biofilms was visible on all inoculated blocks (Figure 5.1). The extent of colonization achieved by each of four inocula under study was assessed by the variation in colour undergone by blocks throughout the three-month colonization period. Results obtained for the five colour difference parameters calculated are shown in Figure 5.2.

For all cultures and CIELAB parameters studied, the absolute colour differences increased significantly between the initial inoculation and the end of the experiment, despite an initial decrease in the colour difference in some cases. Considering colour differences as indirect estimators of biofilm biomass, sigmoidal shapes typical of microbial growth curves were observed (Figure 5.2). These shapes were more clearly observed for colour parameters Δa^*, Δb^* and ΔH^*_{ab}. The increase in ΔL^* was almost linear (in absolute terms), with little difference between cultures. The shape of ΔE^*_{ab}, calculated from parameters ΔL^*, Δa^* and Δb^*, was intermediate. The different cultures under study also revealed variable patterns of development. According to the colour data, the biomass of biofilms developed from inocula C2 and C3 appeared to decrease in the two first weeks of incubation, although the subsequent exponential growth phase for C3 was more pronounced than for C2. Biofilms derived from cultures C4 and C5 did not seem to suffer any initial loss of biomass. Growth of C4 was slower than for the other three cultures and the stationary phase did not appear to have been reached. Development of biofilm from C5 appeared to fit to a sigmoidal growth curve from the beginning to the end of the experiment, with a shorter lag phase than with the other three inocula. From around the fourth week of incubation, biofilms derived from cultures C3 and C5 showed very similar growth patterns, as indicated by colour measurements.

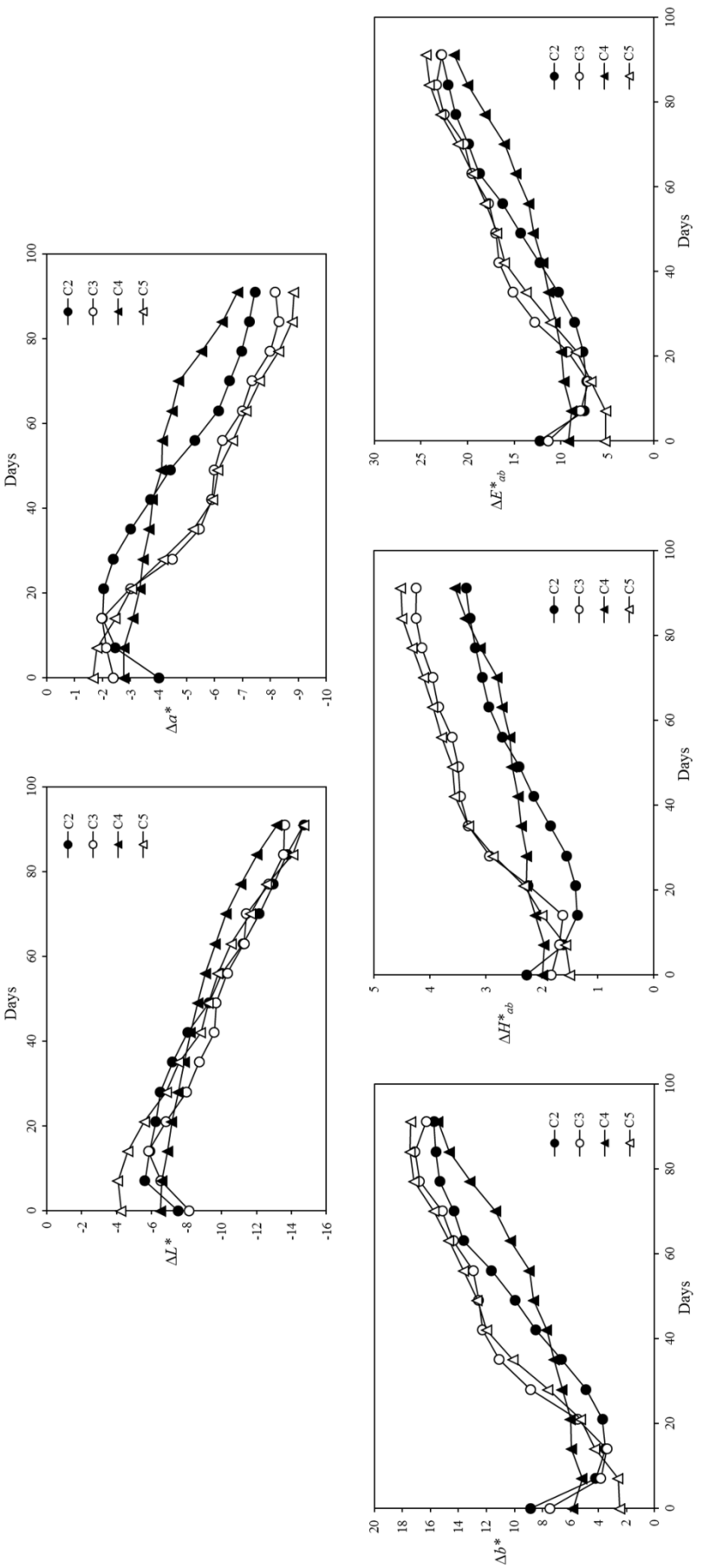

Figure 5.2 CIELAB colour parameters (ΔL^*, Δa^*, Δb^*, ΔH^*_{ab} and ΔE^*_{ab}) measured on biofilms during the three-month incubation period for the four cultures used as inocula (C2, C3, C4 and C5), represented as mean values of three replicates.

Results of the ANOVA analyses for colour-time data are shown in Table 5.2. The time and the interaction between time and culture used as inoculum significantly affected all of the colour difference parameters. However, regarding the main effects produced by the culture used, only Δa^* and ΔH^*_{ab} were significantly affected.

Table 5.2 Results of two-way repeated measures ANOVA for each colour parameter studied, considering time of incubation as the within-subjects factor and culture used as inoculum as the between-subjects factor. *P*-values < 0.05 are indicated in bold type.

Source of variation	ΔL^*	Δa^*	Δb^*	ΔH^*_{ab}	ΔE^*_{ab}
Time	**< 0.001**	**< 0.001**	**< 0.001**	**< 0.001**	**< 0.001**
	F = 165.0	F = 329.0	F = 457.6	F = 260.0	F = 416.9
Culture	0.725	**0.028**	0.123	**0.007**	0.273
	F = 0.4	F = 5.2	F = 2.6	F = 8.5	F = 1.6
Time x Culture	**0.017**	**< 0.001**	**< 0.001**	**< 0.001**	**< 0.001**
	F = 3.4	F = 13.8	F = 13.8	F = 14.4	F = 10.8

The colour parameter most significantly affected by the factors considered, ΔH^*_{ab}, was used to estimate biofilm growth for fitting sigmoidal growth curves (Figure 5.3). Growth of biofilms derived from cultures C2 and C4 did not satisfactorily fit the sigmoidal model, probably because C2 showed a substantial initial biomass loss and C4 did not reach the stationary growth phase. However, growth of the biofilms derived from cultures C3 and C5 did fit the sigmoidal model. Maximal growth rate of C3 occurred on the 28th day of colonization and that of C5, on day 16. Moreover, the values of ΔH^*_{ab} at the stationary phase, as estimated by the sigmoidal model, were 4.15 and 4.67 for cultures C3 and C5, respectively. These values are not statistically different from those experimentally measured at the end of the experiment (4.24 ± 0.13 for C3 and 4.52 ± 0.28 for C5, expressed as mean ± standard deviations of three replicates; t-test, $p < 0.05$), and we therefore conclude that the three-month colonization period was long enough for the stationary growth phase to be reached in biofilms developed from these cultures.

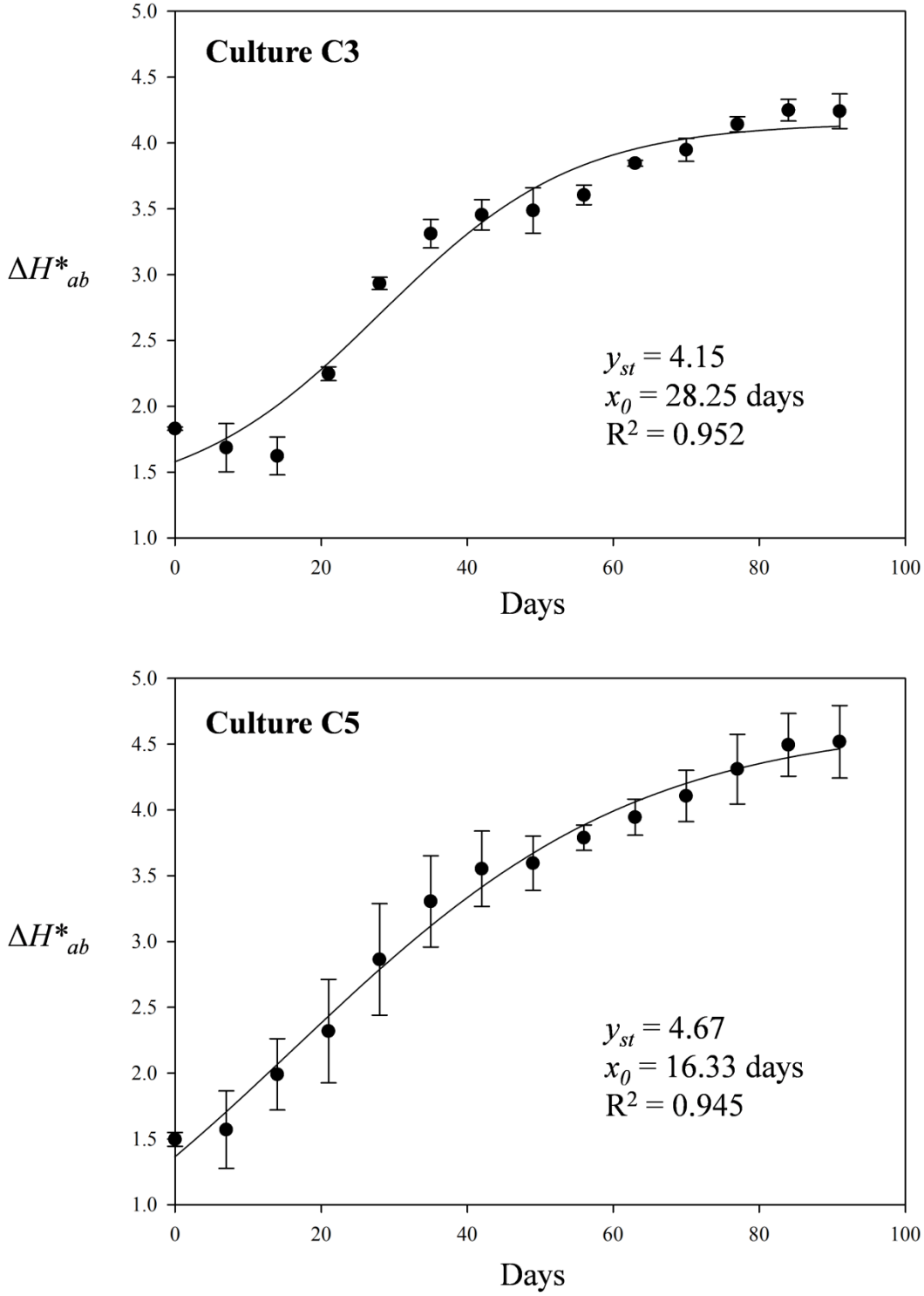

Figure 5.3 Graphical representation of ΔH^*_{ab} over time, as an indirect estimator of biomass, for biofilms derived from cultures C3 and C5. Values of ΔH^*_{ab}, represented as mean values with standard error of three replicates, were fitted to a sigmoidal model.

5.3.2 Biofilm characterization

Data derived from colour measurements and quantification of photosynthetic pigments and EPS at the end of the colonization period are shown in Table 5.3. These data were examined by ANOVA to compare the different cultures used as inocula. As reported above for the results of the repeated measures ANOVA, the colour parameters Δa^* and ΔH^*_{ab} (as indirect estimators of biofilm biomass) were significantly affected by the use of different cultures at the end of the experiment. Culture C5 accounted for the larger colour differences, and it was significantly different from C4 in terms of Δa^* and from C2 and C4 in terms of ΔH^*_{ab}. The colour data are consistent with the amounts of photosynthetic pigments extracted from the biofilms. Significant differences were observed for chl *a* and total carotenoids, with the highest values observed in biofilms derived from culture C5. The biofilms derived from culture C4 contained the largest amount of EPS (quantified as the carbohydrate fraction), significantly more than the C2 biofilms.

Table 5.3 Results of one-way ANOVA for colour parameters, photosynthetic pigments and EPS measured at the end of the colonization period (three months). Results are expressed as mean values ± standard deviation of three replicates. Different upper case letters indicate significantly differences between cultures. *P*-values < 0.05 are indicated in bold type.

	Culture				
	C2	C3	C4	C5	ANOVA
ΔL^*	-14.7 ± 3.4	-13.6 ± 0.4	-13.2 ± 1.0	-14.7 ± 1.5	0.706 F = 0.478
Δa^*	-7.4 ± 1.1^{ab}	-8.2 ± 0.4^{ab}	-6.8 ± 0.2^{a}	-8.8 ± 0.7^{b}	**0.035** F = 4.737
Δb^*	15.8 ± 1.3	16.3 ± 0.9	15.5 ± 1.2	17.4 ± 0.7	0.206 F = 1.913
ΔH^*_{ab}	3.4 ± 0.5^{a}	4.2 ± 0.1^{bc}	3.6 ± 0.3^{ab}	4.5 ± 0.3^{c}	**0.004** F = 10.127
ΔE^*_{ab}	22.8 ± 3.5	22.8 ± 1.0	21.4 ± 1.5	24.4 ± 1.6	0.435 F = 1.016
Chl *a* (μg cm^{-2})	6.07 ± 1.13^{ab}	6.40 ± 0.92^{ab}	4.15 ± 0.25^{a}	6.86 ± 1.20^{b}	**0.035** F = 4.727
Chl *b* (μg cm^{-2})	5.09 ± 1.58	4.87 ± 0.74	2.77 ± 0.61	4.76 ± 1.09	0.082 F = 3.231
Carotenoids (μg cm^{-2})	1.21 ± 0.28^{a}	1.34 ± 0.15^{ab}	0.87 ± 0.05^{a}	1.70 ± 0.19^{b}	**0.004** F = 10.295
EPS (μg carbohydrate cm^{-2})	47.7 ± 8.3^{a}	65.5 ± 9.2^{ab}	73.4 ± 10.6^{b}	69.8 ± 12.0^{ab}	**0.028** F = 5.188

CLSM images showed differences in biofilm thickness and structural profiles, as well as in the microbial composition of the cultures used as inocula (Figure 5.4). Biofilms derived from C2 were the thinnest, never exceeding 25 µm, and with many non-colonized areas. Phototrophic cells appeared as small agglomerations, and the signal from EPS was sparse. However, bacteria were more abundant in the C2 biofilms than in the other biofilms. Culture C3 yielded a biofilm of thickness up to ~50 µm, and almost all of the block surface was colonized by phototrophs. The signal from bacteria was weak and EPS were clearly observed surrounding most of the cells. The maximum thickness of biofilms derived from C4 was ~40 µm and the biofilms were dominated by EPS, in accordance with the results of the chemical analysis. The EPS were usually observed surrounding dead cells or with weak signal from chlorophyll autofluorescence. Biofilms derived from culture C5 (similar to C3 biofilms) were homogeneously distributed, dominated by phototrophic microorganisms and were up to ~50 µm thick. Bryophyta protonemata were also detected in CLSM images of these biofilms (Figure 5.4-4a).

5.4 DISCUSSION

Subaerial biofilms were successfully obtained by inoculating granite block with relatively small amounts of phototrophic microorganisms. These pioneering colonizers were able to adapt to the substratum and proliferate. The temperature (23ºC), light (~20 µmol photon m^{-2} s^{-1}, 12h light/dark photoperiod) and moisture (95% relative humidity and permanent access to water by capillarity) conditions chosen for biofilm incubation were similar to those used by other authors in similar experiments (Guillite & Dreesen 1995, Prieto & Silva 2005, Miller et al. 2006, Escadeillas et al. 2007) and proved optimal for the development of microorganisms on granitic substrata, as required for a correct approach to the study of the bioreceptivity of a material (Guillitte 1995).

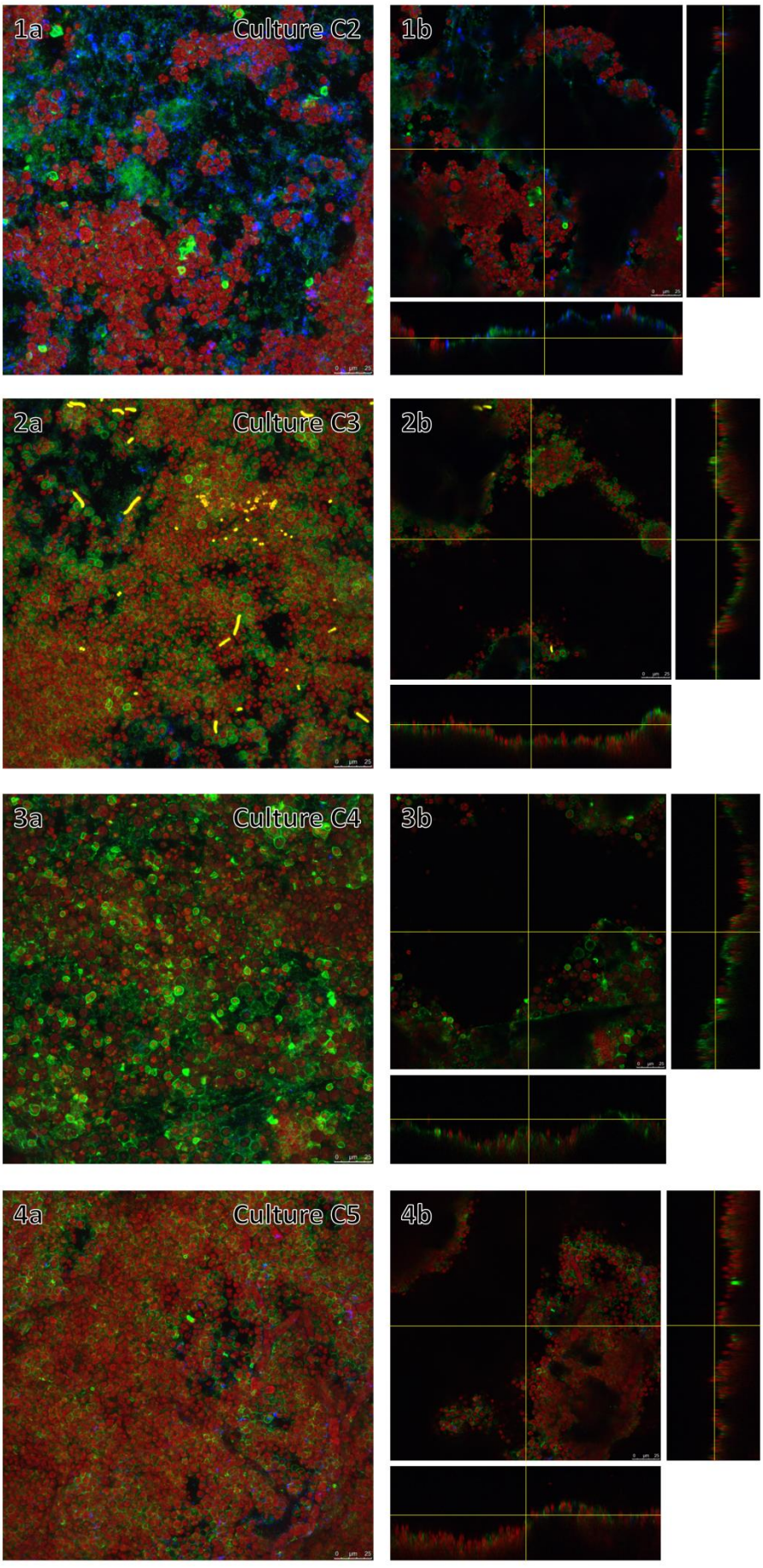
1a
Culture C2
1b
2a
Culture C3
2b
3a
Culture C4
3b
4a
Culture C5
4b

← **Figure 5.4** CLSM images of biofilms developed from the four cultures at the end of the three-month colonization period. (1a, 2a, 3a, 4a): Maximum fluorescence Z projections. (1b, 2b, 3b, 4b): Orthogonal views at the central point of those projections. Blue: bacterial DNA dyed with SYTO 9; green: EPS dyed with ConA-TRITC; red: chlorophyll auto-fluorescence.

Colour measurements provided a reliable assessment of the colonization process throughout the whole incubation period (Figure 2.2). The non-destructive nature of this technique, which is widely used for monitoring biofilm-forming microorganisms (Urzi & Realini 1998, Sanmartín et al. 2012, Vázquez-Nion et al. 2013 Prieto et al. 2014, Marques et al. 2015), enabled growth curves to be produced for the biofilms under study. Fitting the curves to a model provided valuable information concerning the growth patterns of different biofilms (Figure 5.3). At the end of the experiment, destructive methods were used to extract the photosynthetic pigments, which were then quantified, thus enabling comparison of the cultures (Table 5.3). However, the use of non-destructive methods to quantify these pigments on subaerial biofilms could improve the monitoring of biofilms growth, resulting in a more comprehensive evaluation of bioreceptivity.

Data obtained from EPS extraction, which together with the results of Chapter 4 (Vázquez-Nion et al. 2016b), represent the first quantitative data on EPS from subaerial biofilms grown on rocky substrata, yielded interesting information. Biofilms derived from culture C2, dominated by only one algal species (Table 5.1), produced the lowest amounts of EPS. However, biofilms derived from inoculum C4, which contained even lower quantities of photosynthetic pigments than those derived from C2, yielded significantly higher EPS production. The bioprotective role of EPS (Flemming & Wingender 2010) may explain this behaviour, which also suggests a higher capacity of multi-species cultures to produce EPS; however, more data concerning the matrix of this type of biofilms is needed in order to clarify this point.

The CLSM provided information about the structure of the biofilms and enabled identification of different components (phototrophic organisms, bacteria and EPS; Figure 5.4). Although quantification of these components by CLSM may be possible by means of image analysis (Lawrence et al. 1998), the biofilm thickness may limit use of this technique due to attenuation of fluorescence with depth (Barranguet et al. 2004). However, the qualitative results obtained from CLSM were consistent with quantitative

data obtained for both chlorophyll and EPS (Table 5.3) and reliably described the spatial organization and structural changes in biofilms from the different cultures.

Although all cultures used as inocula were obtained from natural subaerial biofilms composed by phototrophic multi-species communities adapted to granite substrata, the microbial composition of each of the cultures was different (Table 5.1; Chapter 3, Vázquez-Nion et al. 2016a). The particular characteristics of each culture led to differences in the biofilms formed, in relation to the colour change on the substratum, the growth rate and the extent of colonization. Hence, to evaluate the potential suitability of these cultures for use as inocula for bioreceptivity experiments aimed at studying granitic rocks, and based on suggestions proposed by Guillitte (1995), the results were analysed and compared by considering the following criteria: a) The culture should comprise a complex microbial community capable of adapting to the granite substratum, thus resembling natural colonization; b) The time needed for the biofilm to reach a stationary growth phase should be reasonably short. Early achievement of this phase, thus enabling comparisons between samples in bioreceptivity studies is desirable; c) The colonization should be as extensive as possible. A culture capable of forming a densely populated biofilm would improve the sensitivity of bioreceptivity studies, thus enabling differences between i.e. biofilms grown on distinct types of granitic rocks to be clearly established.

In this context, culture C2, dominated by a single phototrophic taxa (the green algae *Bracteacoccus minor*), failed to meet the first requirement. The initial biomass loss suffered by biofilms derived from this inoculum, as revealed by colour measurements (Figure 5.2), indicates the lack of adaptability to the substratum of a mono-species culture, although it can be considered as a 'control' for comparative purposes. Thus, biofilms derived from culture C4 showed the lowest colonization capacity at the end of the experiment, as revealed by the content of photosynthetic pigments, which was even lower than in the biofilms derived from C2 (Table 5.3). Colour measurements also indicated much slower biofilm growth than with the other three cultures, and the stationary phase was not reached within the study period. These results justify rejection of C4 for use as an inoculum for bioreceptivity experiments.

However, C3 and C5 seemed to be suitable for this purpose. Both are multi-species cultures dominated by several phototrophic taxa; the growth curves fitted a sigmoidal

model in which the stationary phase was reached within three months; and at the end of the incubation period the colonization was extensive, as revealed by colour measurements, photosynthetic pigment quantification and CLSM images. Regarding the advantages of the use of one culture over the other, C5 was microbially richer than that of C3 (Table 5.1). Species of Chlorophyta present in C3 (*Chlorella* sp. and *Stichococcus bacillaris*) were also present in C5, in addition to others. This could lead to a better adaptation to different substrata. Indeed, the maximum growth rate of biofilms derived from C5 was reached on day 16 of incubation, whereas in biofilms derived from C3, the maximum growth rate was reached on day 28, with a longer lag phase (Figure 5.3). Moreover, although the differences were not significant, by the end of the experiment the values of all colour parameters studied, chl *a*, total carotenoids and EPS were higher in the biofilms derived from C5 than in those derived from C3.

These findings indicate that C5 is the most suitable culture for use as an inoculum in experiments aimed at studying the bioreceptivity of granitic rocks. In a similar study, Miller et al. (2010) inoculated limestone blocks with a phototrophic culture derived from a natural biofilm grown on the same type of stone. Biofilms incubated for three months under laboratory conditions similar to those used in the present work yielded up to 2.40 µg chl *a* cm^{-2}. The corresponding value for the biofilms derived from culture C5 was 6.86 µg chl *a* cm^{-2}. As granite is expected to be less bioreceptive than limestone (Miller et al. 2006), the growth results for culture C5 can be considered satisfactory.

5.5 CONCLUSIONS

The experimental set-up evaluated in the present study proved appropriate for producing environmental-like colonization of granite in the laboratory. The temperature (23ºC), light (~20 µmol photon m^{-2} s^{-1}, 12h light/dark photoperiod) and moisture (95% relative humidity and permanent access to water by capillarity) conditions contributed to successful growth of subaerial biofilms after inoculation of multi-species phototrophic cultures on granite blocks. Colour measurements, quantification of photosynthetic pigments and EPS, and CLSM observations enabled proper assessment of biofilm formation and comparison of the four cultures under study.

Growth data indicated that C3 and C5 are appropriate for use as inocula in experiments aimed at studying the bioreceptivity of granitic rocks. Culture C5,

comprising several taxa (including Bryophyta, Charophyta, Chlorophyta and Cyanobacteria), proved particularly suitable for this purpose, mainly due to its microbial richness, rapid adaptability to the substratum and high capacity for colonization. Use of this culture as an inoculum, together with the experimental set-up described here for the development of subaerial biofilms under laboratory conditions, will contribute to standardization of the method and hence, to more objective assessment of the bioreceptivity of granite.

USC
UNIVERSIDADE
DE SANTIAGO
DE COMPOSTELA

CHAPTER 6

PRIMARY BIORECEPTIVITY OF GRANITIC ROCKS TO PHOTOTROPHIC BIOFILMS: DEVELOPMENT OF A BIORECEPTIVITY INDEX

6.1 INTRODUCTION

The term 'bioreceptivity', introduced by Guillitte (1995) as an alternative to the term 'susceptibility' for use in building ecology studies, is defined as the aptitude of a material to be colonised by living organisms. This concept focuses on the characteristics of the material that allow colonisation to take place rather than on the effects that the organisms have on the colonised materials (biodeterioration). Guillitte (1995) also established differences between 'primary bioreceptivity' (the initial bioreceptivity of a material which has not yet been exposed to colonisation), 'secondary bioreceptivity' (the potential of colonisation when the properties of a material have undergone a change due to the action of the colonising organisms or other factors) and 'tertiary bioreceptivity' (the bioreceptivity of a material after undergoing treatments such as consolidation, coating, etc.). The bioreceptivity can also be investigated by applying specific microorganisms or groups of microorganisms to the material in question and incubating the samples under optimal conditions for growth of the microorganisms. On the basis of these principles, the study of the bioreceptivity of building stone aimed at preventing biofilm formation should focus on the primary bioreceptivity of the material to pioneer colonizers, as the accumulation of photosynthetic biomass on the stone surface provides an organic nutrient base for heterotrophic microflora and the biodeterioration they cause (Warscheid & Braams 2000).

As outlined in Chapter 1 (General Introduction), several studies have been carried out to investigate the primary bioreceptivity of stone materials under laboratory conditions. Most of these experiments used individual species of microorganisms (e.g. Tiano et al. 1995, Shirakawa et al. 2003, De Muynck et al. 2009b) or artificially mixed cultures (e.g. Guillite & Dreesen 1995, Giannantonio et al. 2009, Marques et al. 2015), usually comprising cyanobacteria, green algae and/or fungi, to induce biofilm formation. Use of these types of cultures as inocula is simple and affords a high degree of experimental control; however, the complex processes involved in natural colonization may not be well represented. Miller et al. (2009a, 2010a, 2010b) used a multi-species phototrophic culture derived from a natural biofilm to inoculate various limestones. These authors highlighted the benefits of the use of this type of culture, which resembles a complex environmental community and thus enables better assessment of the bioreceptivity. Prieto et al. (2005, 2006a) also produced a multi-species liquid culture composed of organisms adapted to the conditions of quartz-rich substrata, mainly cyanobacteria, bacteria and bryophytes. These researchers then used the culture as an inoculum to induce biofilm formation on open rock faces in a quartz quarry, with the aim of reducing the visual impact generated by quartz mining and thus demonstrating the value of these types of culture for field applications.

The types of rock most commonly studied are limestone and marble (Guillite & Dreesen 1995, Tomaselli et al. 2000, Favero-Longo et al. 2009, Miller et al. 2009a, 2010b). The potential colonisation of artificial stone material (e.g. bricks and concrete) is also quite well documented (Guillite & Dreesen 1995, Shirakawa et al. 2003, De Muynck et al. 2009b, Giannantonio et al. 2009, D'Orazio et al. 2014). Some researchers have even designed cementitious materials with physico-chemical properties specifically aimed at enhancing the bioreceptivity (Manso et al. 2014a, 2014b), as the biological colonisation of facades can also be considered beneficial in modern constructions, from an ecological point of view. However, the bioreceptivity of granitic stones has been less well investigated (Tiano et al. 1995, Prieto & Silva 2005, Miller et al. 2006, Prieto et al. 2014, Marques et al. 2015). In general, the potential bioreceptivity of stone materials has not been clearly correlated with the physical or chemical characteristics, although some properties such as the surface roughness, open porosity and mineralogical nature of the stones are considered key factors (Guillite & Dreesen 1995, Silva et al. 1997, Shirakawa et al. 2003, Prieto & Silva 2005, Miller et al. 2006,

2009a, Wiktor et al. 2009). Moreover, the standardization of laboratory protocols and the use of appropriate inocula to induce natural biofilm formation may enable the development of a bioreceptivity index, as suggested by Guillitte (1995). The definition of such an index, which has not yet been established for any stone material, would help in the selection of appropriate lithotypes for building and/or ornamental purposes.

In Chapter 3 (Vázquez-Nion et al. 2016a), we described how we produced stable multi-species phototrophic cultures derived from natural subaerial biofilms grown on historical granite buildings in Santiago de Compostela (NW Spain). These cultures were taxonomically characterized and proved to be complex microbial communities composed by common pioneer colonizers of building stone surfaces, including granite. In Chapter 5, we described the development of a standardised laboratory protocol in which multi-species phototrophic cultures are used to induce environmental-like colonization of granitic stone. We also evaluated the potential use of these cultures as inocula in experiments aimed at studying the bioreceptivity of granitic rocks. One of these cultures, comprising several taxa including Bryophyta, Charophyta, Chlorophyta and Cyanobacteria, was particularly suitable for this purpose due to its microbial richness, rapid adaptability to the substratum and high capacity for colonization. The aims of the present study were to use the inoculum and experimental protocol described herein a) to assess the influence of the physical and chemical properties of several types of granite, commonly used as building material and/or ornamental stone, on their primary bioreceptivity to phototrophic biofilms, and b) to develop a bioreceptivity index capable of describing the potential susceptibility of different types of granite to colonization. The proposed index is of potential use as a decision-making tool in stone cultural heritage and civil engineering studies.

6.2 MATERIALS AND METHODS

Eleven varieties of stone, commonly used as construction material and ornamental stone, and commercially available under the denomination ‘granite’, were selected for study (Table 6.1). Freshly cut quarry samples of the eleven varieties were used in all experimental procedures. The surface finish of all stone samples was the same (honed) so that comparisons could be made between the types of rock, independently of the surface roughness. In addition, different surface finishes (polished, honed, sawn and sanded) were applied to samples of one of the lithotypes to enable the influence of the

roughness on the bioreceptivity to be assessed independently of the inherent physical and chemical properties of the stone.

6.2.1 Characterization of lithotypes studied

The rock samples were characterized by observation of thin sections under petrographic microscope (Nikon Eclipse 50i Pol equipped with a camera Nikon Unit DS-U2), with special attention given to the mineralogy, texture and grain size, as well as to possible mineral weathering patterns. The mineral composition (modal analysis) of each sample was determined by the point counting method, using a counting grid (mesh size 0.5-1.0 mm: ca. 750-1300 points per thin section). The grain size was determined by measuring the area of the crystal sections for the major minerals.

The chemical composition of the different lithotypes was determined after complete acid digestion of the samples. For each sample, 4 mL of HF 48%, 4 mL of HNO_3 60% and 2 mL of H_2SO_4 96% were added to 0.25 g of rock powder (< 50 µm) in a Teflon vessel and the mixture was digested in a microwave oven (CEM Mars Xpress) at 180ºC (ramp 10 min, hold 15 min). Thirty mL of saturated boric acid (60 g L^{-1}) was then added to the vessel and the mixture was digested at 160ºC (ramp 10 min, hold 10 min). The major elements in the resulting extracts were then analysed by flame atomic absorption/emission spectroscopy (FAAS/FAES) (Varian SpectrAA 220FS). Certified reference materials (IPT-72, BCS-CRM 376/1, ECRM 776-1) were subjected to the same procedure and used as standards.

As an indicator of the intrinsic propensity of each variety of rock to provide nutrients for the colonising organisms, the abrasion pH was measured after grinding the rock in distilled water (20g 40 mL^{-1}) for 2.25 min and allowing the mixture to settle for another 2 min. Fifteen mL of the supernatant was then centrifuged and the solubilized cations Mg^{2+}, Ca^{2+} and K^{+} (potential nutritional requirements) were determined by FAAS/FAES (Grant 1969).

The rock samples were also physically characterized by determining the bulk density and open porosity, according to EN 1936:1999. As water can be a limiting factor in biological colonisation, the maximum amount of water absorbed by capillary suction (capillary water content) was determined according to EN 1925:1999.

In order to study the effect of the surface roughness on the bioreceptivity of the stones without varying the other physico-chemical properties, four different surface finishes (polished, honed, sawn and sanded) were applied to samples of one of the lithotypes (granite SIN). The surface roughness of each finish was measured, in sample areas of 1 cm^2, by White Light Optical Interferometry (WLOI) (Wyko NT1100) in Vertical Scanning Interferometry (VSI) mode. WLOI is a non-contact optical profiling system that provides high resolution of 3D surface measurement, and the VSI mode enables examination of rough surfaces up to several millimetres high. The results are reported as *Sa*, representing the mean roughness of the surface, and *Sz*, representing the maximum height achieved.

The colour of the different types of granite was measured with a portable spectrophotometer (Konica Minolta CM-700d). Measurements were made directly on the surface of the humid blocks, following protocol developed by Prieto et al. (2010). Measurements consisted of a total of 9 readings taken from different areas of each block under the following conditions: illuminant D65, observer 2º and a 10 mm diameter target area. The colour was measured using the CIELAB colour system (CIE 1986), which represents each colour by means of three scalar parameters or Cartesian coordinates: L^*, lightness or luminosity of colour; a^*, associated with changes in greenness-redness; and b^*, associated with changes in blueness-yellowness. Alternatively, each colour is represented by three angular parameters or cylindrical coordinates, most closely related to the psychophysical perception of the colour: L^*, lightness or luminosity of colour, also defined in both scalar and angular colour sets; C^*_{ab}, chroma or saturation, related to the intensity of colour; and h_{ab}, hue angle or tone of colour, which refers to the dominant wavelength and indicates redness, yellowness, greenness, or blueness on a circular scale.

6.2.2 Procedure for the development of subaerial biofilms

A multi-species phototrophic culture was used as an inoculum for inducing biofilms on stone samples in the laboratory. The culture was derived from a natural biofilm grown on granite and comprised several taxa, including Bryophyta (*Syntrichia ruralis* protonemata), Charophyta (*Klebsormidium* sp.), Chlorophyta (*Bracteacoccus* sp., *Chlamydomonas* sp., *Chlorella* sp. and *Stichococcus bacillaris*) and Cyanobacteria

(*Aphanocapsa* sp. and *Leptolyngbya cebennensis*). This culture is described in detail in Chapters 3 (Vázquez-Nion et al. 2016a) and 5.

For each of the eleven lithotypes studied, a culture volume equivalent to 1.51 mg dry weight biomass (1 mL), in exponential growth phase, was inoculated on the upper surface of each of 12 previously autoclaved 4×4×2 cm^3 blocks, all with a honed surface finish. The same procedure was also carried out with 12 blocks of granite SIN for each of the four surface finishes (polished, honed, sawn and sanded) in order to study the effect of surface roughness on bioreceptivity. A total of 168 blocks were inoculated for the primary bioreceptivity study. The inoculated blocks were incubated under conditions favourable to biofilm formation, as described in Chapter 5. The blocks were placed in dishes that were periodically filled with sterilized distilled water to provide permanent access to water by capillarity. The blocks were then incubated in a climatic chamber (SCLAB PGA-1228/2 HR) under stationary conditions of 23°C, 95% relative humidity and a 12h light/dark photoperiod (~20 µmol photon m^{-2} s^{-1}) for three months. Lightning was provided by fluorescent lamps (OSRAM L 36W/765). The position of each block was periodically changed in a semi-random way to avoid any possible effects of micro-climatic variations in the chamber.

6.2.3 Assessment of biofilm growth by PAM fluorometry

Pulse Amplitude Modulated (PAM) fluorometry was used to assess biofilm growth on the stones during the three-month incubation period. Measurements were carried out one week after inoculation and every 15 days until the end of the experiment. Fluorescence signals were measured using a Phyto-PAM system (Heinz Walz GmbH) equipped with a Phyto-EDF fibre optics emitter-detector unit, which allows measurement on surfaces through a 50 mm long and 4 mm diameter perspex rod (Schrieber et al. 2002). The inoculated granite blocks were kept in darkness for 20 min prior to the measurements, carried out with the tip of the rod directly in contact with the block/biofilm surface. The fluorescence parameters recorded were F_0, the minimal fluorescence signal of dark-adapted cells, and F_m, the maximal fluorescence signal after a saturating light pulse in dark-adapted cells. These parameters enable the maximum quantum yield (Y) to be calculated using the equation $Y = (F_m - F_0)/F_m$. This gives a measure of the maximum photochemical efficiency of photosystem II (PSII) and can be used as an indicator of the general level of fitness of the photosynthetic organisms. A

total of 9 readings were taken from different zones on each block and averaged to produce the final value. No background signal was detected for any of eleven lithotypes studied.

The Phyto-PAM system measures (non-destructively) *in vivo* fluorescence at four wavelength signals (470 nm, 520 nm, 645 nm and 665 nm) and it can therefore indicate the contribution of various types of photosynthetic pigments. Because the F_0 values produced by Phyto-PAM are relative units, calibration was carried out using the actual chl *a* content as a biofilm biomass estimator for the culture used as inoculum. For this purpose, 40 additional granite blocks were inoculated with different amounts of culture C5 (0.1 to 2.0 mL) and incubated under the previously described growth conditions for one month. The F_0 values for the biofilms formed were then measured at 665 nm (signal related to chl *a* content) and blocks were subsequently subjected to the chl *a* extraction and quantification protocol developed by Fernández-Silva et al. (2011). The experimentally determined chl *a* contents were plotted against F_0 (665 nm), and regression analysis was applied to the data. As the signals obtained at different wavelengths depend on pigment composition, they also can be used to detect changes in the algal community structure. The signal at 470 nm is related to chl *b* and the signal at 645 nm to allophycocyanin. The $F_{0,470nm}$ / $F_{0,645nm}$ ratio was therefore used as an indicator of the dominance of green algae (high values) or cyanobacteria (low values) in the biofilms.

6.2.4 Assessment of biofilm growth by colour measurements

The colour of the inoculated blocks was monitored under the same measurement conditions as those described previously for characterizing the colour of granites before inoculation. Measurements were carried out one week after inoculation and every 15 days until the end of the three-month incubation period. To evaluate the change in the colour of the blocks produced by biofilm growth, colour data were processed as colour differences between a colonized block and the block before inoculation. For this purpose, we used the difference colour parameters ΔL^*, Δa^*, Δb^*, ΔH^*_{ab} and ΔE^*_{ab} (CIE 1986), described in detail in Chapter 5.

6.2.5 Quantification of EPS produced by biofilms

Blocks with each lithotype/surface finish were subjected to the EPS extraction protocol developed in Chapter 4 (Vázquez-Nion et al. 2016b), after incubation for one, two and three months. Colonised blocks were placed in Petri dishes containing 10 mL of distilled water and 60 µL of formaldehyde (37% w/w) and maintained at 4°C for 60 minutes. Two mL of NaOH 2.5 mol L^{-1} was added to the Petri dishes, which were then held at 4°C for 120 minutes. Extracts were centrifuged at 5000 rpm for 20 min and the supernatant was filtered. The carbohydrate fraction of the EPS was spectrophotometrically quantified (Varian Cary 100) by the phenol-sulphuric acid method (Dubois et al. 1956) with D(+)-glucose (Panreac) as standard.

6.2.6 Statistical analyses

The data on the physical and chemical properties of the rocks studied and the parameters used to quantify biofilm growth at the end of the three-month incubation period were subjected to one-way analysis of variance (ANOVA) and post-hoc Tukey HSD tests for comparison between the different lithotypes and surface finishes. The Phyto-PAM and colour measurement data were analysed by two-way repeated measures ANOVA in order to test for differences between lithotypes/surface finishes (between-subjects factor) over time (within-subjects factor). The EPS data were analysed by two-way ANOVA to test for differences between lithotypes/surface finishes over time.

The data on both the different lithotypes studied (i.e. physical properties, chemical and mineralogical composition, and initial colour of the rocks) and the biological colonisation at the end of the three-month incubation period (i.e. data derived from Phyto-PAM, colour measurements and EPS) were analysed together by hierarchical clustering of the variables. A dendrogram was constructed using between-groups average linkage based on Pearson's correlations of the standardised (*Z* scores) variables, for graphical visualisation of the relationships between the different factors. Principal component analysis (PCA) with orthogonal rotation was also carried out, to identify homogeneous groups of variables and thus simplify the bioreceptivity study.

All statistical analyses were performed with SPSS Statistics v19.0 (IBM) software, and differences were considered statistically significant at $p < 0.05$.

6.3 RESULTS

6.3.1 Characterization of lithotypes studied

The petrographic characteristics of the different lithotypes studied are shown in Table 6.1. Nine of the eleven lithotypes studied were classified as granitic rocks, according to Le Maitre (2002), while two (LCL and NSA) were found to be other types of plutonic rocks (monzonite and gabbro, respectively). However, these varieties were included in the study because they are commonly used as construction material and ornamental stone and they are commercially available under the denomination 'granite', possibly because of the similar grain patterns. Hereafter the eleven lithotypes studied will be referred to as 'granites' for practical purposes. The petrographic analysis also revealed that all the lithotypes can be considered as sound rocks, with the exception of SAM, SIN and SRI, in which mineral weathering processes were detected. In these three granites, the plagioclases appeared turbid, especially in their core, where clay minerals were formed, biotites were chloritized and fissures were filled by segregated iron oxyhydroxides, giving the rock a brownish colour (Figure 6.1).

Table 6.1 Petrographic description of the lithotypes used in this study.

Lithotype	Abbreviation	Classification*	Texture
Blanco Castilla	**BCA**	Monzogranite	Allotriomorphic, heterogranular, medium to coarse-grained
Blanco Cristal	**BCR**	Monzogranite	Allotriomorphic, heterogranular, medium-grained
Grissal**	**GRI**	Syenogranite	Hypidiomorphic, porphydic tendency, coarse to very coarse-grained
Labrador Claro	**LCL**	Monzonite	Allotriomorphic, porphydic, coarse to very coarse-grained
Mondariz**	**MON**	Syenogranite	Hypidiomorphic, porphydic tendency, coarse to very coarse-grained
Negro Sudáfrica	**NSA**	Gabbro	Hypidiomorphic, fine to medium-grained
Rosa Porriño**	**RPO**	Syenogranite	Allotriomorphic, heterogranular, coarse-grained
Rosavel	**RSV**	Monzogranite	Hypidiomorphic, porphydic with megacrystals, coarse-grained
Silvestre AM	**SAM**	Monzogranite	Allotriomorphic, medium-grained
Silvestre Ingemar	**SIN**	Monzogranite	Allotriomorphic, fine-grained
Silvestre Ribadavia	**SRI**	Monzogranite-granodiorite	Allotriomorphic, heterogranular, medium to coarse-grained

*According to Le Maitre (2002).
**Data from Sánchez-Delgado et al. (2014).

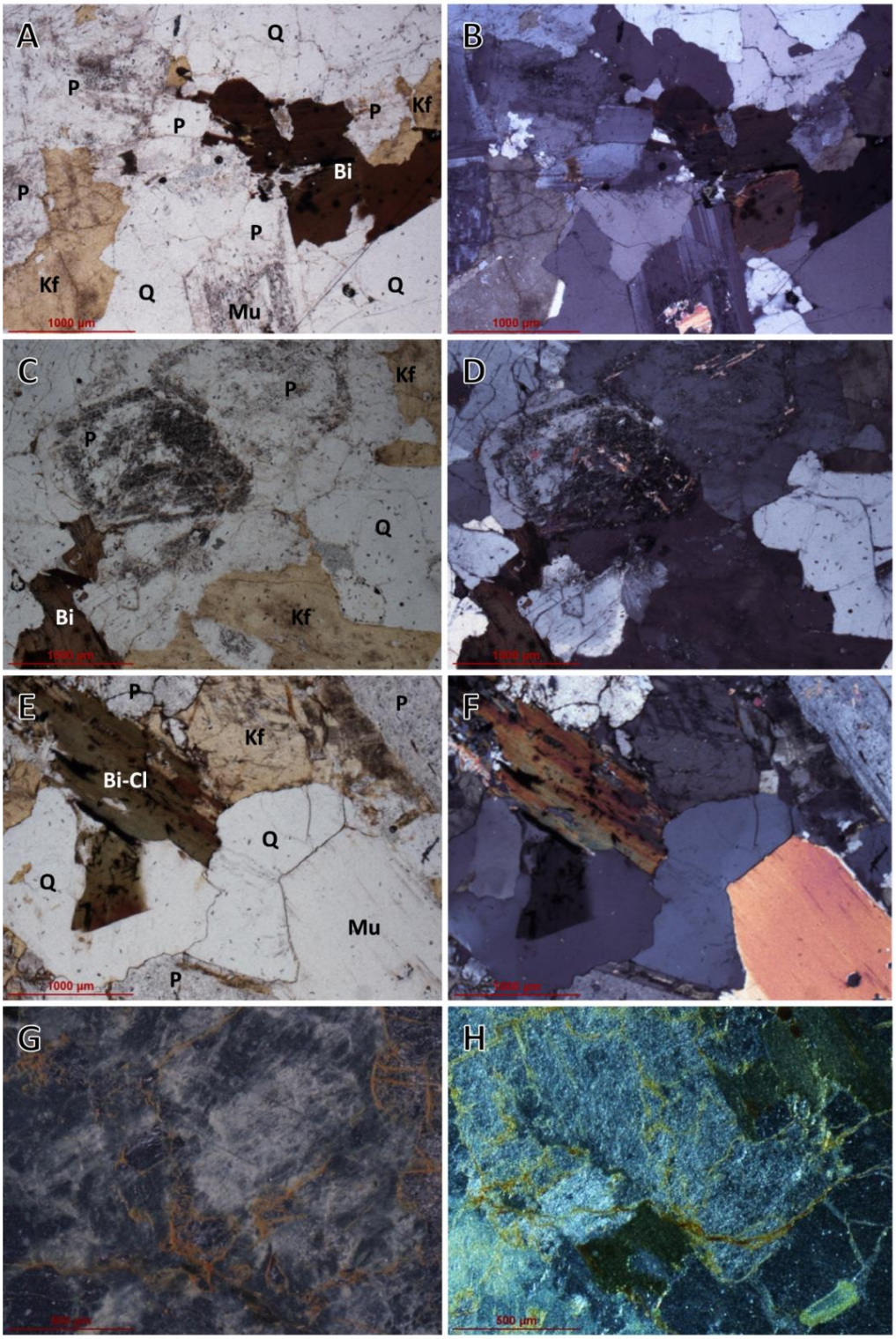

Figure 6.1 Microphotographs of granite samples examined under a petrographic microscope (left: parallel nicols, right: crossed nicols): A,B,C,D) plagioclases (P) with turbid appearance in their cores due to alteration to clay minerals, biotite (Bi) with zircon inclusions, K feldspar (Kf), quartz (Q) and muscovite (Mu) in granite SRI; E,F) chloritized biotite (Bi-Cl) with needles of rutile, K feldspar with holes filled by ferrous materials, quartz and muscovite in granite SAM; G,H) Reflected light microphotographs of granite SAM with iron oxyhydroxides filling fissures and grain boundaries.

Modal analysis revealed the mineralogical composition of the granites (Figure 6.2), with quartz contents ranging between 26% (RSV) and 39% (SRI), except in LCL and NSA, in which no quartz was detected (demonstrating their basic nature). Volumes of K feldspar ranged from 17% (SRI) to 44% (RPO), and no K feldspar was found in NSA. Plagioclases were present in all the lithotypes studied in proportions ranging between 16% (RPO) and 58% (NSA). The biotite content of all granites except NSA was lower than 10%, and muscovite was only present in SRI (2%), SAM (8%) and SIN (12%). Lithotypes SRI, SAM and SIN are therefore two-mica granites, while BCA, BCR, GRI, MON, RPO and RSV are biotite granites. The presence of olivine in LCL (5%) and pyroxenes in NSA (42%), common minerals in basic rocks, was also noted. As mentioned previously, these two lithotypes are not classified as granites (Table 6.1), but they were included in this study because they are commonly referred to as granites in the ornamental stone industry.

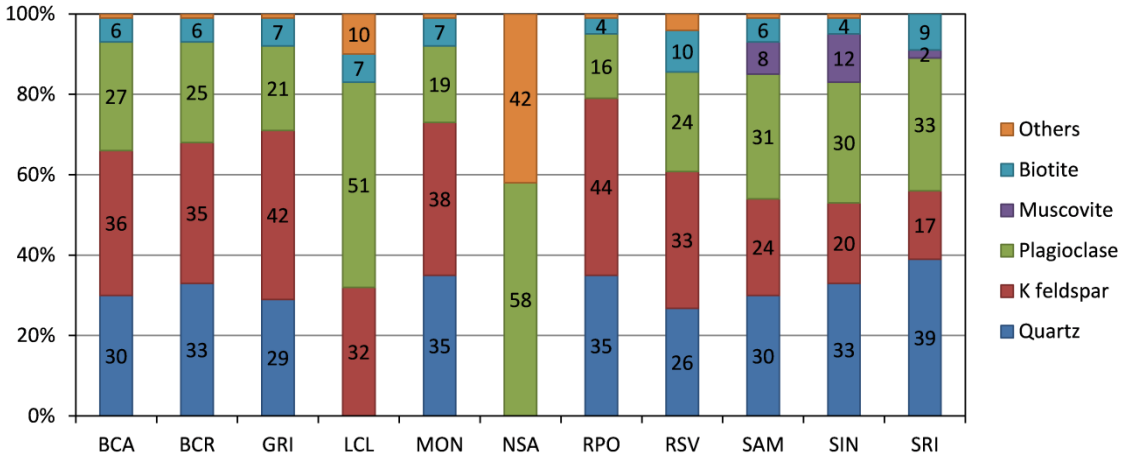

Figure 6.2 Mineralogical composition (% volume) of the different lithotypes studied.

The chemical composition of the stones is directly related to their mineralogy. The major elemental components of the lithotypes studied, expressed as oxides, are presented in Table 6.2. The siliceous nature of the lithotypes was revealed by SiO_2 as the main component, in proportions ranging between 51.38 % (NSA) and 77.59 % (SRI), followed by Al_2O_3, ranging between 13.55 % (BCR) and 21.15 % (LCL). The Fe_2O_3 contents were particularly high in NSA and LCL (8.47 % and 5.01 %, respectively) but varied from 0.65 % (SIN) to 2.84 % (MON) in the other granites. The amounts of the basic elements in NSA and LCL, classified respectively as gabbro and

monzonite, were quite different from those observed in the other rocks, classified as granites. NSA contained the largest amounts of MgO (8.90 %) and CaO (10.80 %), and the lowest amounts of Na_2O (2.53 %) and K_2O (0.23). LCL contained the highest amount of Na_2O (6.49 %) and relatively high amounts of MgO (1.32 %) and CaO (4.78 %). In the other granites, the MgO content ranged from 0.12 % (BCR) to 0.55 % (MON), the CaO content ranged from 0.85 % (SAM) to 2.72 % (BCA), the Na_2O content ranged from 3.11 % (BCA) to 3.95 % (SIN), and the K_2O content from 3.64 % (GRI) to 6.27 % (RSV). These data are consistent with the previously described mineralogical composition. NSA and, to a lesser degree, LCL, showed the typical chemical compositions of basic rocks, with relatively low contents of SiO_2 and high contents of Fe_2O_3, MgO and CaO. The other stones contained more Na_2O than CaO, indicating a predominance of sodium plagioclases, as commonly observed in acidic rocks.

Table 6.2 Major elements (% of oxides) in the different lithotypes, expressed as mean value ± standard deviation of three replicates. Different upper case letters indicate significant differences between lithotypes ($p < 0.05$).

Lithotype	SiO_2	Al_2O_3	Fe_2O_3	MgO	CaO	Na_2O	K_2O
BCA	66.82 ± 2.88^{c}	14.88 ± 0.09^{abc}	1.67 ± 0.03^{c}	0.45 ± 0.00^{a}	2.72 ± 0.02^{c}	3.11 ± 0.01^{b}	4.39 ± 0.32^{ef}
BCR	76.48 ± 0.88^{f}	13.55 ± 0.30^{a}	0.80 ± 0.03^{a}	0.12 ± 0.00^{a}	1.26 ± 0.06^{ab}	3.55 ± 0.04^{e}	3.70 ± 0.16^{bcd}
GRI	71.90 ± 1.89^{de}	15.55 ± 0.09^{bc}	2.37 ± 0.06^{d}	0.38 ± 0.00^{a}	2.38 ± 0.05^{c}	3.68 ± 0.09^{ef}	3.64 ± 0.14^{bc}
LCL	60.57 ± 1.34^{b}	21.15 ± 0.58^{g}	5.01 ± 0.09^{f}	1.32 ± 0.04^{b}	4.78 ± 0.29^{d}	6.49 ±0.01^{h}	3.20 ± 0.08^{b}
MON	69.81 ± 2.79^{d}	15.93 ± 0.40^{cd}	2.84 ± 0.15^{e}	0.55 ± 0.02^{a}	2.67 ± 0.07^{c}	3.87 ± 0.15^{fg}	4.76 ± 0.16^{f}
NSA	51.38 ± 0.35^{a}	18.78 ± 1.34^{f}	8.47 ± 0.18^{g}	8.90 ± 0.58^{c}	10.80 ± 0.61^{e}	2.53 ± 0.10^{a}	0.23 ± 0.01^{a}
RPO	76.44 ± 1.04^{f}	14.07 ± 0.13^{ab}	1.77 ± 0.08^{c}	0.22 ± 0.00^{a}	1.30 ± 0.02^{ab}	3.33 ± 0.02^{cd}	4.28 ± 0.14^{def}
RSV	67.91 ± 0.97^{cd}	18.26 ± 0.50^{ef}	1.27 ± 0.08^{b}	0.22 ± 0.01^{a}	1.41 ± 0.01^{ab}	3.51 ± 0.01^{de}	6.27 ± 0.39^{g}
SAM	71.75 ± 0.85^{de}	16.29 ± 0.11^{cd}	1.23 ± 0.06^{b}	0.37 ± 0.01^{a}	0.85 ± 0.02^{a}	3.21 ± 0.07^{bc}	4.74 ± 0.25^{f}
SIN	74.89 ± 0.76^{ef}	17.08 ± 0.14^{de}	0.65 ± 0.08^{a}	0.27 ± 0.00^{a}	1.36 ± 0.01^{ab}	3.95 ± 0.03^{g}	4.07 ± 0.14^{cde}
SRI	77.59 ± 0.44^{f}	15.03 ± 0.10^{abc}	1.64 ± 0.03^{c}	0.27 ± 0.01^{a}	1.63 ± 0.02^{b}	3.84 ± 0.06^{fg}	3.89 ± 0.07^{cde}

Data on abrasion pH and the solubilized cations analysed are shown in Table 3. The lowest values of abrasion pH (7.76 to 7.96) were obtained for granites SAM, SIN and SRI. The other eight types of granite showed significantly higher values, ranging from 9.11 (RPO) to 9.58 (MON). These values are consistent with the mineral weathering processes observed in SAM, SIN and SRI, as the abrasion pH is directly related to the amount of basic cations that the rock can supply to solutions that come in contact with it. This parameter thus expresses the degree of weathering of the rock. By analysing the amounts of three basic cations (Mg^{2+}, Ca^{2+} and K^{+}) solubilised in the abrasion pH solutions, as possible nutrient sources for the biofilms, different proportions were observed for the different lithotypes (Table 6.3). Granites with the lowest abrasion pH (SAM, SIN and SRI) also solubilised small amounts of Mg^{2+} and Ca^{2+}, but relatively high amounts of K^{+}. NSA contained the highest amount of MgO and the lowest of K_2O, which was clearly reflected in the respective solubilised cations. The solubilised fraction of Ca^{2+} in BCA, GRI, LCL, MON, RPO and RSV was not significantly different from that observed in NSA, although the amount of CaO in NSA was much higher. These differences may be explained by factors such as the mineralogical composition of the stone, which ultimately determines the cation lability.

Table 6.3 Abrasion pH and solubilised cations for the different lithotypes, expressed as mean value ± standard deviation of three replicates. Different upper case letters indicate significant differences between lithotypes ($p < 0.05$).

		Solubilised cations (mg kg^{-1})		
Lithotype	Abrasion pH	Mg^{2+}	Ca^{2+}	K^{+}
BCA	9.38 ± 0.13^{bc}	0.30 ± 0.06^{ab}	4.25 ± 0.82^{bc}	7.42 ± 1.48^{abc}
BCR	9.23 ± 0.04^{bc}	0.22 ± 0.04^{ab}	2.29 ± 0.57^{ab}	10.00 ± 0.98^{bc}
GRI	9.29 ± 0.13^{bc}	0.70 ± 0.12^{d}	8.47 ± 1.17^{d}	10.65 ± 1.92^{bc}
LCL	9.55 ± 0.12^{c}	0.58 ± 0.11^{cd}	6.48 ± 0.77^{cd}	7.10 ± 3.55^{abc}
MON	9.58 ± 0.09^{c}	0.32 ± 0.08^{ab}	8.05 ± 1.10^{d}	9.03 ± 1.58^{bc}
NSA	9.50 ± 0.05^{bc}	1.38 ± 0.10^{e}	6.15 ± 0.58^{cd}	2.93 ± 0.31^{a}
RPO	9.11 ± 0.11^{b}	0.71 ± 0.04^{d}	4.18 ± 0.39^{bc}	7.52 ± 1.11^{abc}
RSV	9.41 ± 0.04^{bc}	0.39 ± 0.03^{bc}	6.69 ± 0.28^{cd}	11.81 ± 2.11^{c}
SAM	7.76 ± 0.21^{a}	0.11 ± 0.05^{a}	1.66 ± 0.96^{ab}	9.10 ± 0.50^{bc}
SIN	7.76 ± 0.24^{a}	0.20 ± 0.03^{ab}	1.18 ± 1.42^{a}	9.26 ± 2.03^{bc}
SRI	7.96 ± 0.11^{a}	0.20 ± 0.08^{ab}	2.79 ± 1.08^{ab}	4.82 ± 1.74^{ab}

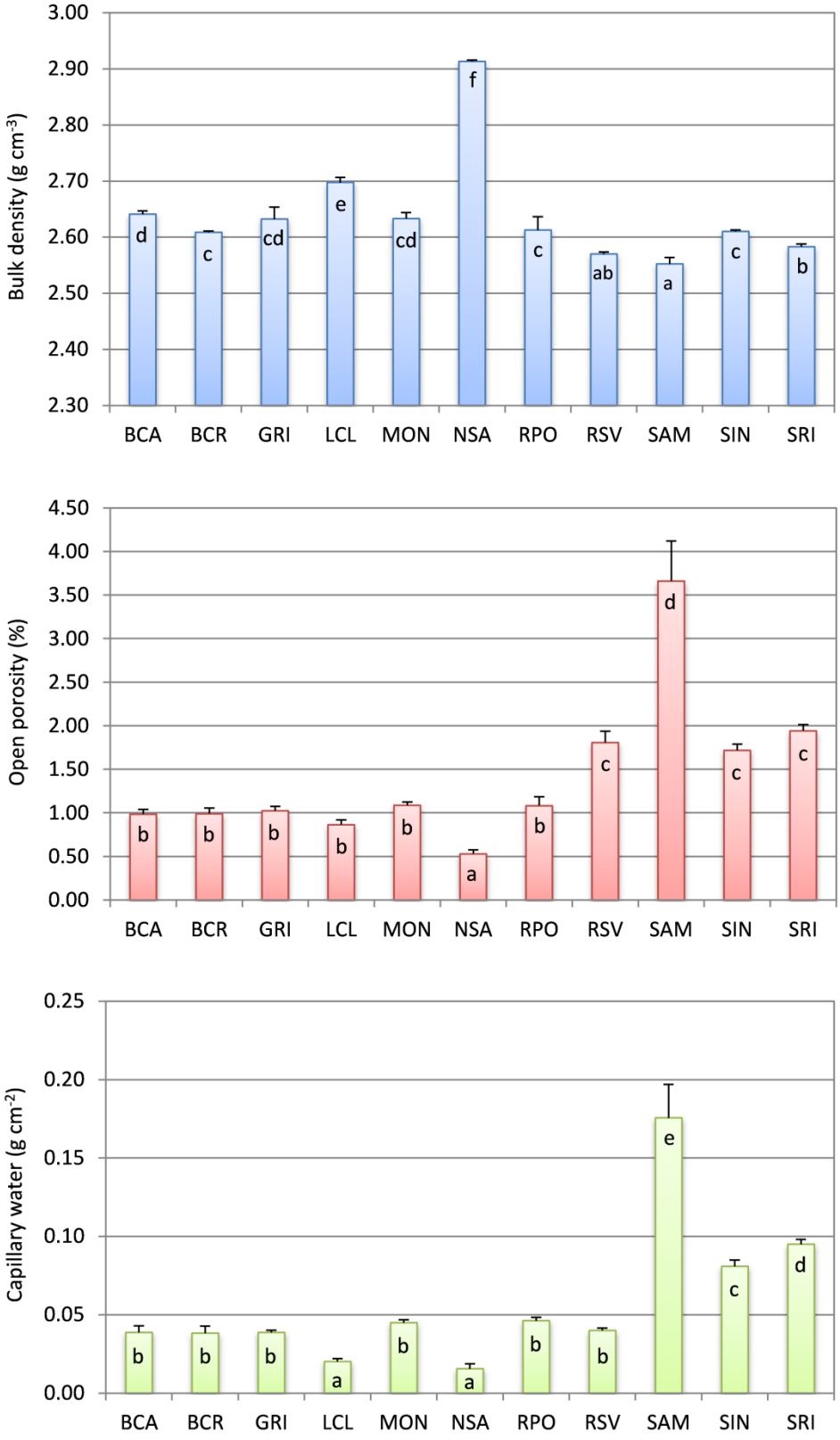

Figure 6.3 Bulk density, open porosity and content of capillary water for the different lithotypes studied, expressed as mean values of six replicates (error bars indicate standard deviations). Different letters in the bars indicate significantly differences among lithotypes ($p < 0.05$).

Figure 6.3 shows the physical parameters measured in each lithotype. As expected, the data clearly showed a relationship between the three parameters studied. High bulk density is associated with low open porosity and vice versa. As open porosity reflects the volume of empty spaces connected with each other and the exterior, it is related to the movement and storage of water in the rock, and consequently to the capillary water content. Hence, the bulk density was highest (2.91 g cm^{-3}) and open porosity (0.53 %) and capillary water (0.016 g cm^{-2}) were lowest in NSA, while bulk density (2.55 g cm^{-3}) was lowest and the open porosity (3.66 %) and capillary water (0.176 g cm^{-2}) were highest in SAM.

The roughness parameters measured for the different surface finishes applied to granite SIN are presented in Table 6.4. Examples areas of analysed surfaces are shown in Figure 6.4. The different finishes applied to the surface of the blocks produced significant differences in roughness parameters *Sa* and *Sz*. Thus, surface roughness increased as follows: polished < honed < sawn < sanded. The difference in roughness between the smoothest (polished) and the roughest (sanded) finish varied considerably, with *Sa* ranging from 2.05 to 115.70 µm and *Sz* from 115.06 to 973.87 µm.

Table 6.4 Roughness (*Sa* and *Sz*) of the different surface finishes studied, expressed as mean value ± standard deviation of two replicates (areas of 1 cm^2). Different upper case letters indicate significant differences between surface finishes ($p < 0.05$).

Surface finish	*Sa* (µm)	*Sz* (µm)
Polished	2.05 ± 0.14^{a}	115.06 ± 13.79^{a}
Honed	15.62 ± 1.25^{b}	219.43 ± 10.05^{ab}
Sawn	50.96 ± 0.56^{c}	422.75 ± 10.00^{c}
Sanded	115.70 ± 0.64^{d}	973.87 ± 135.96^{d}

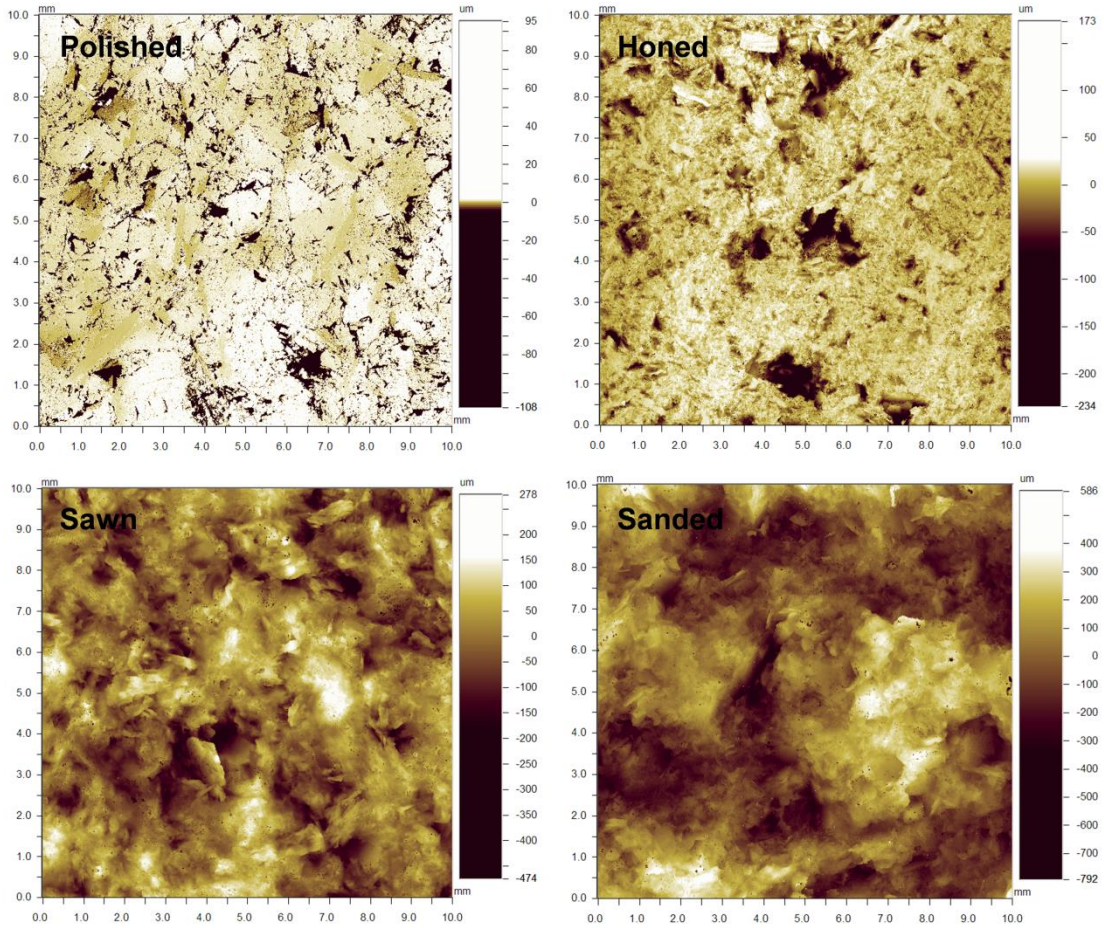

Figure 6.4 Images of the surface of granite SIN blocks with different surface finishes (polished, honed, sawn and sanded), derived from WLOI. Colour scale indicates the variation on surface roughness.

The initial colours of the lithotypes studied are shown in Table 6.5. Significant differences between the different granites and surface finishes were found for all CIELAB colour parameters. Regarding the lightness parameter (L^*), NSA was the darkest lithotype, followed by LCL and SIN, while BCR, BCA and RSV were the lightest lithotypes. The values of parameter a^*, associated with changes in greenness-redness, were close to zero for all lithotypes, except RSV, RPO (pinkish granites) and SAM (orangey). Greater variability was observed in parameter b^*, associated with blueness-yellowness, with values ranging from -1.00 (LCL, bluish) to 13.80 (SAM). Chroma (C^*_{ab}) values were very similar to those of b*, revealing it as the dominant colour parameter in the granites studied. The tones of the colours, which are defined by the hue angle (h_{ab}), varied from 74.16 (RPO) to 217.95 (LCL). These data reveal a great variety in the colour gamut of the granites studied, as can be appreciated in Figure 6.5. The different surface finishes applied to granite SIN seemed to have mainly affected L*,

and the lightness increased with roughness. The other parameters also varied significantly with the surface finish, but these were not directly related to the roughness.

Table 6.5 Initial colour of the different lithotypes studied and surface finishes applied to granite SIN, represented by CIELAB colour parameters. Results are expressed as mean value ± standard deviation of three replicates. Different upper case letters indicate significant differences between lithotypes/surface finishes. *P*-values < 0.05 are indicated in bold type.

Lithotype	L^*	a^*	b^*	C^*_{ab}	h_{ab}
BCA	57.79 ± 2.10^{cd}	-0.38 ± 0.21^{a}	2.50 ± 0.27^{bc}	2.61 ± 0.26^{abc}	105.16 ± 4.30^{cd}
BCR	62.33 ± 2.07^{d}	-0.71 ± 0.28^{a}	6.29 ± 1.19^{de}	6.34 ± 1.21^{de}	96.31 ± 1.27^{abc}
GRI	51.90 ± 1.49^{c}	-0.99 ± 0.08^{a}	0.99 ± 0.07^{ab}	1.50 ± 0.14^{ab}	142.81 ± 2.44^{e}
LCL	43.78 ± 3.32^{b}	-0.58 ± 0.06^{a}	-1.00 ± 0.42^{a}	1.49 ± 0.46^{ab}	217.95 ± 22.50^{f}
MON	51.23 ± 1.45^{c}	-0.03 ± 0.45^{a}	5.03 ± 1.58^{cd}	5.21 ± 1.50^{cd}	100.93 ± 12.33^{bcd}
NSA	33.31 ± 0.69^{a}	-0.50 ± 0.07^{a}	0.88 ± 0.08^{ab}	1.03 ± 0.07^{a}	121.62 ± 6.28^{de}
RPO	53.85 ± 0.29^{cd}	3.50 ± 0.43^{b}	11.42 ± 0.56^{fg}	12.00 ± 0.64^{gh}	74.16 ± 1.63^{a}
RSV	57.60 ± 2.32^{de}	2.30 ± 1.15^{b}	9.35 ± 1.83^{f}	9.71 ± 2.01^{fg}	79.92 ± 5.05^{ab}
SAM	53.78 ± 0.74^{cd}	3.70 ± 0.69^{b}	13.80 ± 0.95^{g}	14.32 ± 1.06^{h}	75.19 ± 2.19^{a}
SIN	44.48 ± 0.68^{b}	0.14 ± 0.09^{a}	4.23 ± 1.09^{cd}	4.24 ± 1.08^{bcd}	87.73 ± 2.02^{abc}
SRI	55.24 ± 1.80^{cd}	0.27 ± 0.47^{a}	8.98 ± 0.60^{ef}	9.01 ± 0.61^{ef}	88.84 ± 3.20^{abc}
ANOVA	**< 0.001** *F* = 63.7	**< 0.001** *F* = 38.4	**< 0.001** *F* = 72.5	**< 0.001** *F* = 61.5	**< 0.001** *F* = 74.8
SIN polished	44.41 ± 0.29^{a}	1.00 ± 0.08^{b}	10.62 ± 0.23^{c}	10.67 ± 0.23^{c}	84.60 ± 0.32^{a}
SIN honed	44.48 ± 0.68^{a}	0.14 ± 0.09^{a}	4.23 ± 1.09^{a}	4.24 ± 1.08^{a}	87.73 ± 2.02^{ab}
SIN sawn	49.06 ± 1.40^{b}	0.01 ± 0.16^{a}	6.53 ± 0.24^{b}	6.54 ± 0.24^{b}	90.07 ± 1.37^{b}
SIN sanded	52.66 ± 0.62^{c}	1.09 ± 0.19^{b}	12.42 ± 0.29^{d}	12.47 ± 0.31^{d}	84.96 ± 0.79^{a}
ANOVA	**< 0.001** *F* = 65.7	**< 0.001** *F* = 50.2	**< 0.001** *F* = 121.5	**< 0.001** *F* = 123.0	**0.003** *F* = 11.8

6.3.2 Assessment of biofilm formation on the different lithotypes studied

The experimental conditions proved suitable for biofilm development, as growth of green biofilms during the three-month incubation period was macroscopically visible on all inoculated blocks (Figure 6.5). The extent of colonization on each of the granites was periodically assessed by PAM fluorometry and colour measurements.

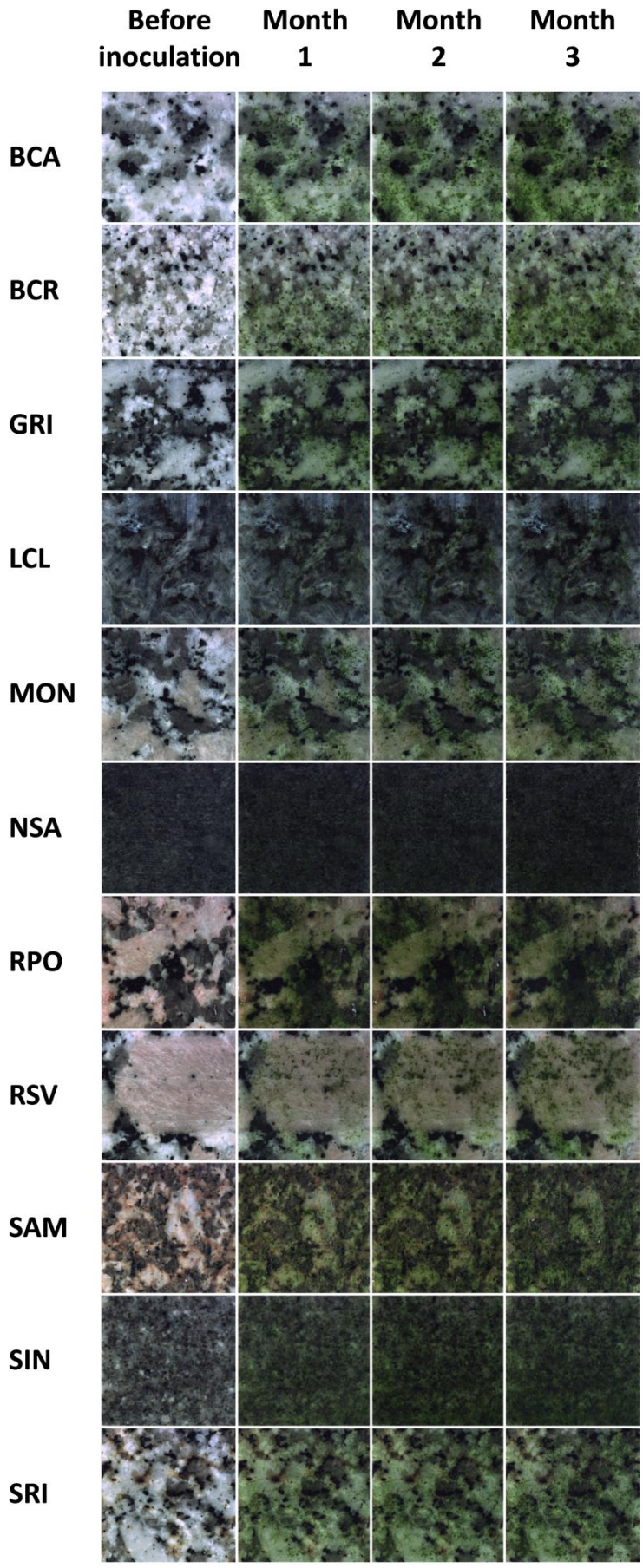
Before inoculation
Month 1
Month 2
Month 3
BCA
BCR
GRI
LCL
MON
NSA
RPO
RSV
SAM
SIN
SRI

← **Figure 6.5** Macroscopic appearance of the lithotypes studied before inoculation and during the three-month colonisation period.

The results of the calibration carried out for the estimation of the chl *a* content in biofilms from the F_0 signal at 665 nm, derived from Phyto-PAM measurements, are summarised in Figure 6.6. The fit of the data to a quadratic model yielded a $R^2 = 0.9293$ ($p < 0.001$), which enables estimation of the amounts of chl *a* on colonised blocks (as a biofilm biomass estimator) from the fluorescence measurements. The F_0 values measured at 665 nm were therefore converted to the chl *a* content (µg cm^{-2}) by using the equation obtained.

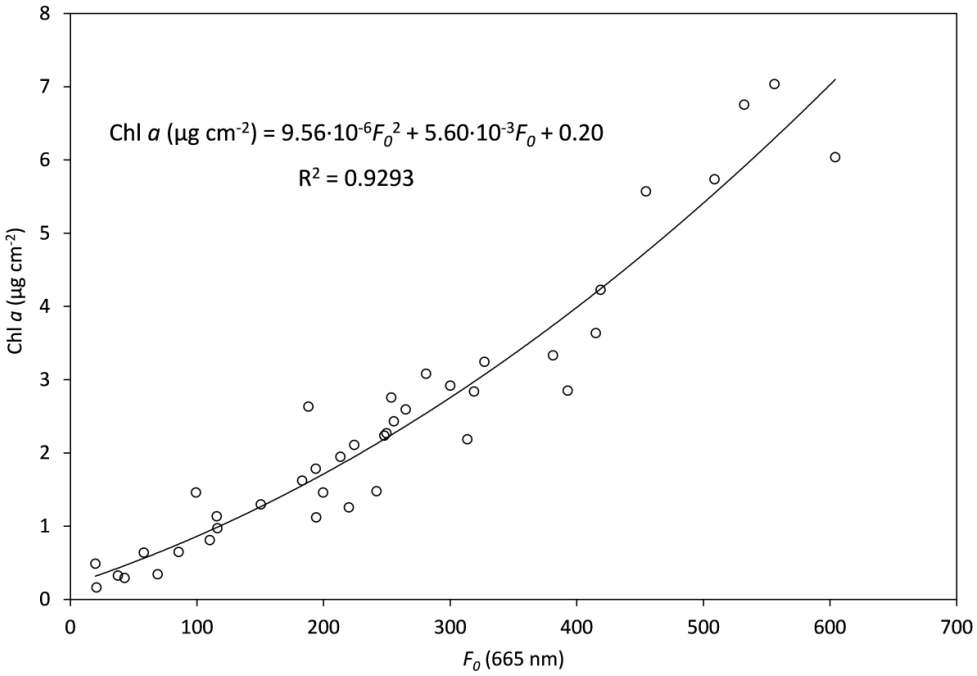

Figure 6.6 Quadratic model of the chl *a* content (µg cm^{-2}) as a function of the fluorescence F_0 at 665 nm for the biofilms derived from the multi-species phototrophic culture used as inoculum (n = 40).

The data derived from the Phyto-PAM parameters (i.e. chl *a* derived from $F_{0,665nm}$, maximum quantum yield and ratio $F_{0,470nm}$ / $F_{0,645nm}$) measured on the biofilms grown on the different lithotypes studied over time are shown in Figure 6.7. Growth of the biofilms on the different lithotypes varied widely throughout the incubation period. SAM was the only granite for which a sigmoidal growth curve was obtained, as for most of the granites the chl *a* content of biofilms decreased in the first week after the initial inoculation. The maximum quantum yield data were more homogeneous, with an initial rise and a subsequent decrease until a final value around 0.60 for most of the lithotypes. Regarding the $F_{0,470nm}$ / $F_{0,645nm}$ ratios, a decrease from the initial value was

observed for LCL and NSA (and BCR in the first half of the experiment), indicating an increased proportion of cyanobacteria. The values of this parameter increased in the other granites, revealing better adaptation of green algae. The results of the two-way repeated measures ANOVA of these data are presented in Table 6.6. Chl *a* values and $F_{0,470nm}$ / $F_{0,645nm}$ ratios were significantly affected by incubation time, lithotype and the interaction of both factors, whereas the maximum quantum yield of the biofilm-forming microorganisms was only affected by incubation time. Table 6.7 shows the Phyto-PAM parameters measured at the end of the three-month incubation period for all the lithotypes studied.

Table 6.6 Results of two-way repeated measures ANOVA of Phyto-PAM measurements for the different lithotypes studied, considering time of incubation as the within-subjects factor and lithotype as the between-subjects factor. *P*-values < 0.05 are indicated in bold type.

Source of variation	Chl *a* (µg cm^{-2})	Yield	$F_{0,470nm}$ / $F_{0,645nm}$
Time	**< 0.001**	**< 0.001**	**< 0.001**
	F = 8.2	*F* = 15.6	*F* = 9.3
Lithotype	**< 0.001**	0.762	**< 0.001**
	F = 18.5	*F* = 0.6	*F* = 11.5
Time x Lithotype	**< 0.001**	0.266	**0.043**
	F = 5.7	*F* = 1.2	*F* = 1.6

Table 6.7 Results of one-way ANOVA of Phyto-PAM measurements for the different lithotypes at the end of the colonization period studied (three months). Results are expressed as mean value ± standard deviation of three replicates. Different upper case letters indicate significant differences between lithotypes. *P*-values < 0.05 are indicated in bold type.

Lithotype	Chl *a* (µg cm^{-2})	Yield	$F_{0,470nm}$ / $F_{0,645nm}$
BCA	1.09 ± 0.49^{abc}	0.56 ± 0.02	0.48 ± 0.01^{c}
BCR	0.82 ± 0.20^{ab}	0.62 ± 0.07	0.46 ± 0.02^{bc}
GRI	0.71 ± 0.21^{ab}	0.60 ± 0.04	0.44 ± 0.02^{abc}
LCL	0.37 ± 0.09^{a}	0.66 ± 0.03	0.39 ± 0.06^{ab}
MON	1.13 ± 0.32^{abcd}	0.61 ± 0.01	0.46 ± 0.04^{bc}
NSA	0.39 ± 0.07^{a}	0.66 ± 0.01	0.37 ± 0.03^{a}
RPO	1.56 ± 0.23^{bcd}	0.59 ± 0.02	0.45 ± 0.00^{bc}
RSV	0.88 ± 0.31^{ab}	0.58 ± 0.08	0.45 ± 0.01^{bc}
SAM	3.61 ± 0.73^{e}	0.64 ± 0.02	0.45 ± 0.01^{bc}
SIN	2.11 ± 0.38^{d}	0.61 ± 0.01	0.47 ± 0.01^{c}
SRI	2.10 ± 0.28^{cd}	0.58 ± 0.04	0.46 ± 0.00^{bc}
ANOVA	**< 0.001** *F* = 22.5	0.057 *F* = 2.2	**< 0.001** *F* = 5.5

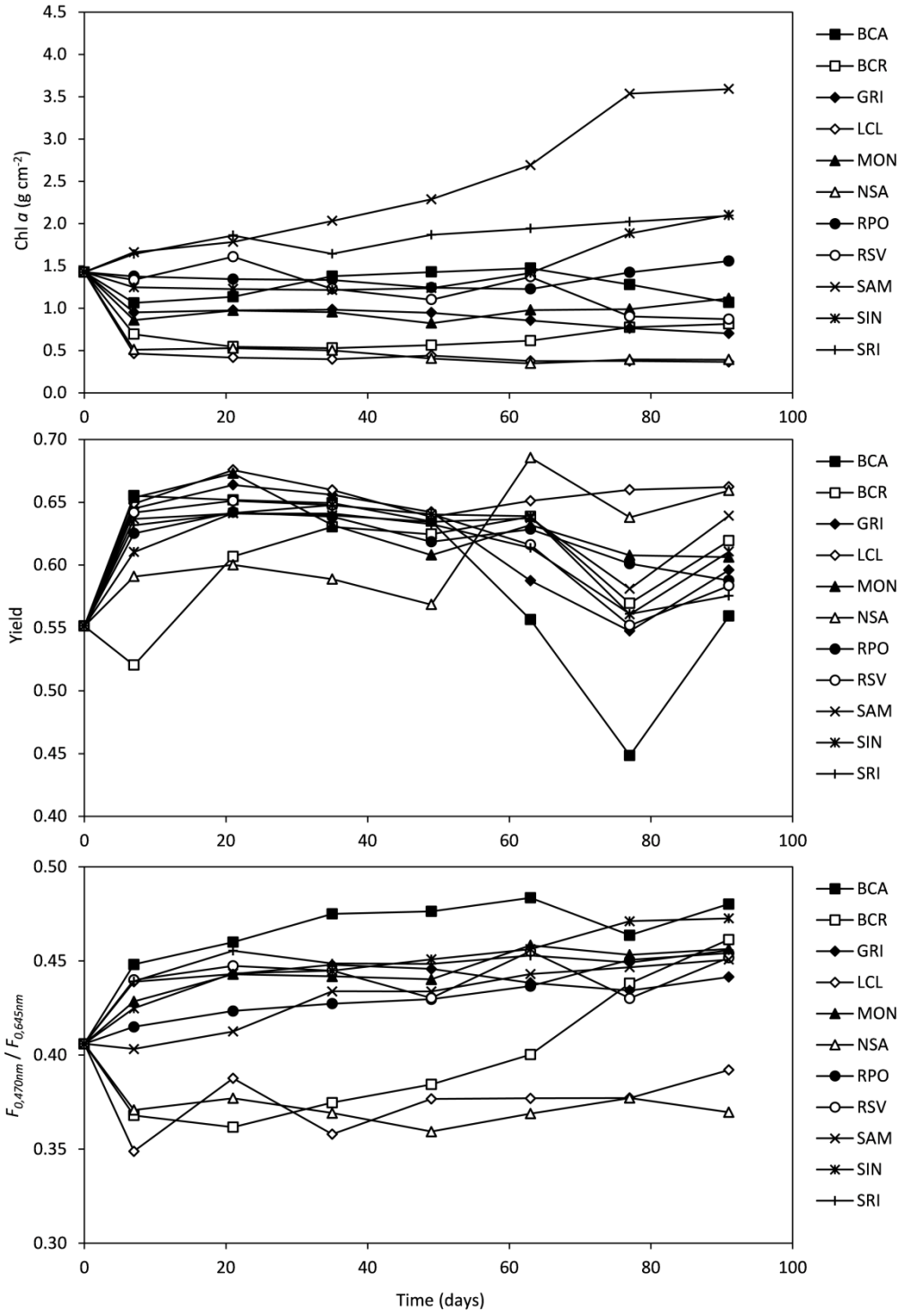

Figure 6.7 Phyto-PAM parameters (chl *a* derived from $F_{0,665nm}$, maximum quantum yield and $F_{0,470nm}$ / $F_{0,645nm}$ ratio) measured on biofilms grown on the different lithotypes studied during the three-month incubation period. Data are represented as mean values of three replicates.

The effects of incubation time and lithotype on the colour differences produced by biofilm growth during the three-month incubation period are shown in Table 6.8. Parameters ΔL^* and ΔH^*_{ab} were significantly affected by incubation time, lithotype and the interaction of both factors. ΔE^*_{ab} was influenced by incubation time and lithotype, whereas incubation time was the only factor that caused significant changes in parameters Δa^* and Δb^*. When only the colour data at the end of the experiment were taken into account (Table 6.9), significant differences between lithotypes were observed for all colour parameters studied.

Table 6.8 Results of two-way repeated measures ANOVA of colour measurements for the different lithotypes studied, considering time of incubation as the within-subjects factor and lithotype as the between-subjects factor. *P*-values < 0.05 are indicated in bold type.

Source of variation	ΔL^*	Δa^*	Δb^*	ΔH^*_{ab}	ΔE^*_{ab}
Time	**< 0.001**	**< 0.001**	**< 0.001**	**< 0.001**	**< 0.001**
	F = 110.6	F = 62.8	F = 30.0	F = 27.6	F = 74.2
Lithotype	**< 0.001**	0.055	0.088	**< 0.001**	**0.019**
	F = 6.3	F = 2.2	F = 2.0	F = 26.8	F = 2.9
Time x Lithotype	**0.009**	0.080	0.642	**< 0.001**	0.291
	F = 2.3	F = 1.6	F = 0.8	F = 4.5	F = 1.2

Table 6.9 Results of one-way ANOVA of colour measurements for the different lithotypes at the end of the colonization period studied (three months). Results are expressed as mean value ± standard deviation of three replicates. Different upper case letters indicate significant differences between lithotypes. *P*-values < 0.05 are indicated in bold type.

Lithotype	ΔL^*	Δa^*	Δb^*	ΔH^*_{ab}	ΔE^*_{ab}
BCA	-13.10 ± 0.94^{bc}	-7.50 ± 1.33^{ab}	16.84 ± 1.75^{c}	0.89 ± 0.56^{bcd}	22.62 ± 2.24^{bc}
BCR	-17.74 ± 6.75^{c}	-7.58 ± 2.18^{ab}	14.65 ± 3.59^{bc}	3.10 ± 0.57^{cde}	24.25 ± 7.78^{c}
GRI	-9.81 ± 1.25^{abc}	-4.83 ± 0.77^{ab}	10.94 ± 1.56^{abc}	-2.06 ± 0.45^{ab}	15.47 ± 2.09^{abc}
LCL	-6.31 ± 1.56^{ab}	-4.25 ± 1.51^{ab}	9.58 ± 3.31^{ab}	-5.66 ± 2.57^{a}	12.24 ± 3.91^{ab}
MON	-12.97 ± 0.86^{bc}	-6.85 ± 1.16^{ab}	12.92 ± 1.86^{abc}	2.14 ± 1.93^{cd}	19.58 ± 2.01^{bc}
NSA	-3.90 ± 0.47^{a}	-3.28 ± 0.35^{a}	6.18 ± 0.78^{a}	-0.18 ± 0.37^{bc}	8.03 ± 0.68^{a}
RPO	-14.79 ± 3.60^{c}	-7.68 ± 2.67^{ab}	8.37 ± 2.62^{ab}	7.56 ± 2.56^{fg}	18.66 ± 5.11^{abc}
RSV	-14.82 ± 0.60^{c}	-7.64 ± 1.10^{ab}	12.21 ± 1.15^{abc}	6.18 ± 1.07^{efg}	20.68 ± 1.41^{bc}
SAM	-13.73 ± 1.63^{bc}	-8.69 ± 0.57^{b}	8.73 ± 1.52^{ab}	8.57 ± 0.75^{g}	18.53 ± 0.72^{abc}
SIN	-9.66 ± 2.58^{abc}	-6.35 ± 1.66^{ab}	10.64 ± 1.78^{abc}	3.52 ± 0.86^{cde}	15.73 ± 3.40^{abc}
SRI	-12.24 ± 3.81^{bc}	-6.95 ± 1.79^{ab}	11.96 ± 3.46^{abc}	4.50 ± 0.66^{def}	18.50 ± 5.29^{abc}
ANOVA	**< 0.001** F = 6.0	**0.005** F = 3.7	**0.001** F = 5.1	**< 0.001** F = 28.4	**0.002** F = 4.5

The results of EPS quantification in biofilms developed on the different granites studied are shown in Figure 6.8. ANOVA (Table 6.10) revealed that neither incubation time nor lithotype significantly affected EPS production in biofilms.

Table 6.10 Results of two-way ANOVA of EPS quantification in biofilms for the different lithotypes studied, considering time of incubation and lithotype as factors. *P*-values < 0.05 are indicated in bold type.

Source of variation	EPS (µg cm^{-2})
Time	0.178
	F = 1.7
Lithotype	0.072
	F = 1.8
Time x Lithotype	0.119
	F = 1.5

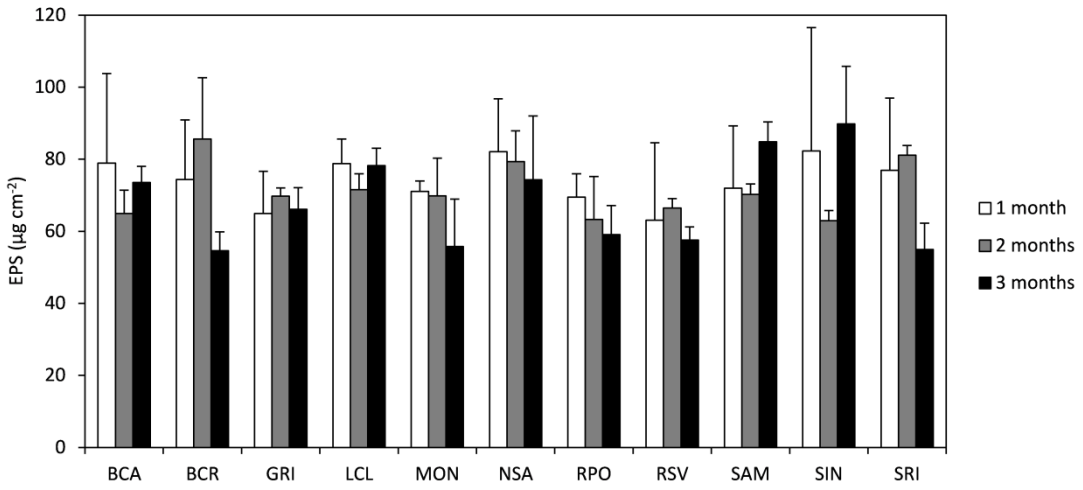

Figure 6.8 EPS, as the carbohydrate fraction, extracted in biofilms of the different lithotypes studied during the three-month incubation period, expressed as mean values of three replicates (error bars indicate standard deviations).

6.3.3 Effect of surface finish on biofilm growth

Unlike the other physico-chemical properties of rocks, surface roughness can be modified by the application of different surface finishes (Table 6.4), and the influence of this factor on biofilm growth was therefore studied separately. The Phyto-PAM measurements of the biofilms grown on the different surface finishes applied to granite SIN throughout the incubation period are shown in Figure 6.9. The results of the two-way repeated measures ANOVA of these data are shown in Table 6.11. The chl *a* values and $F_{0,470nm}$ / $F_{0,645nm}$ ratios were significantly affected by incubation time and surface finish, and the interaction of both factors was also significant for chl *a* contents. However, the maximum quantum yield was only affected by incubation time. Growth patterns of biofilms (as chl *a* content) on the different surface finishes were similar throughout the incubation period, although the differences in surface roughness led to differences in the extent of colonization. Maximum quantum yield varied very homogeneously for all surface finishes and, as with the different lithotypes, they initially increased and then decreased, showing values of around 0.60 at the end of the experiment. The $F_{0,470nm}$ / $F_{0,645nm}$ ratios also varied constantly, showing a slight increase throughout the incubation time, reflecting better adaptation of chlorophyta than of cyanobacteria. The Phyto-PAM parameters measured at the end of the three-month incubation period are shown in Table 6.12. The chl *a* content was the only parameter significantly affected by the surface finish, and the values increased with surface roughness.

Table 6.11 Results of two-way repeated measures ANOVA of Phyto-PAM measurements for the different surface finishes studied for granite SIN, considering time of incubation as within-subjects factor and surface finish as between-subjects factor. *P*-values < 0.05 are indicated in bold type.

Source of variation	Chl *a* (µg cm^{-2})	Yield	$F_{0,470nm}$ / $F_{0,645nm}$
Time	**< 0.001**	**< 0.001**	**< 0.001**
	F = 19.8	*F* = 14.7	*F* = 16.4
Surface finish	**0.003**	0.858	**0.040**
	F = 11.2	*F* = 0.3	*F* = 4.5
Time x Surface finish	**0.001**	0.651	0.551
	F = 5.1	*F* = 0.7	*F* = 0.9

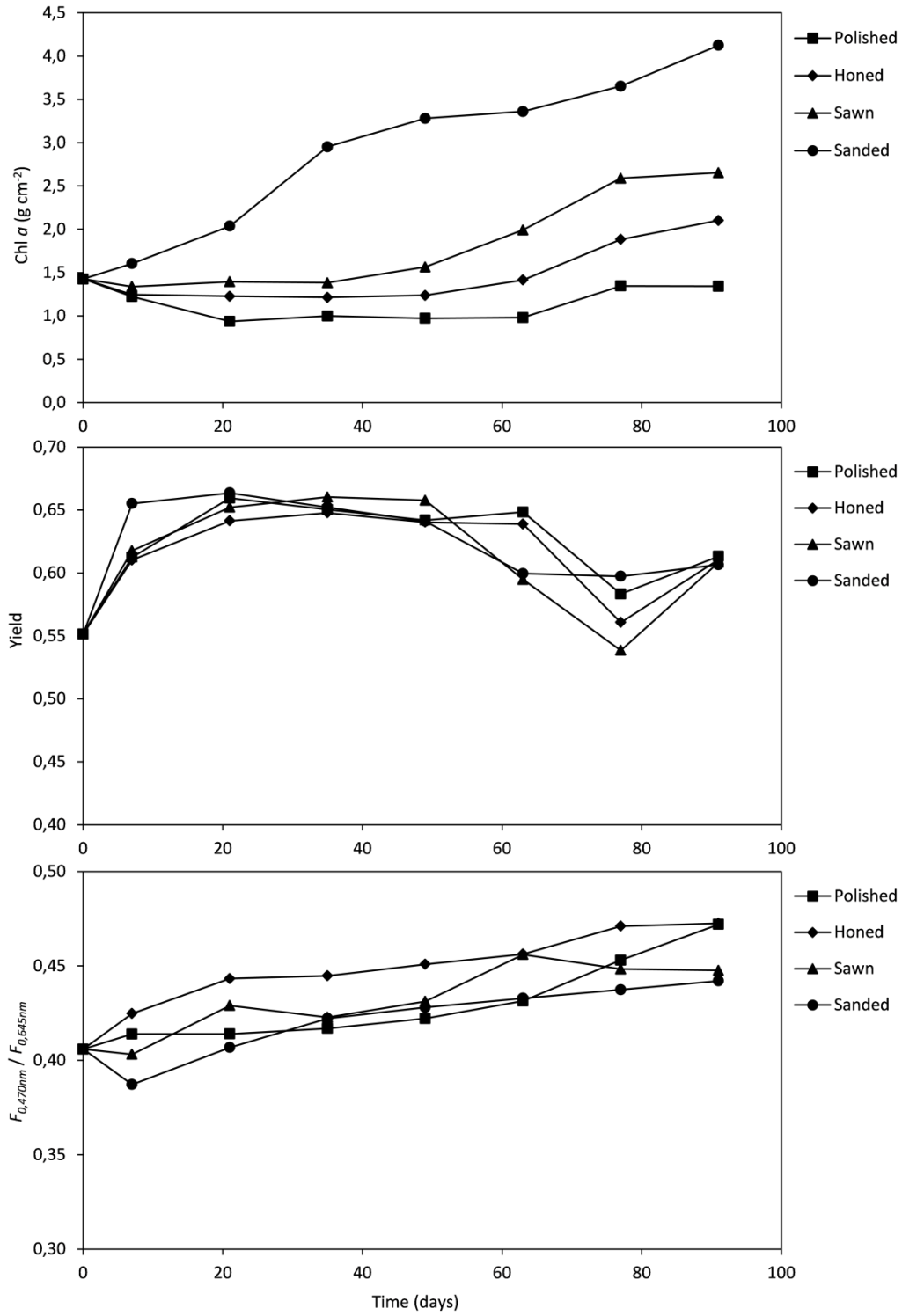

Figure 6.9 Phyto-PAM parameters (chl *a* derived from $F_{0,665nm}$, maximum quantum yield and $F_{0,470nm}$ / $F_{0,645nm}$ ratio) measured on biofilms grown on the different surface finishes studied during the three-month incubation period. Data are represented as mean values of three replicates.

Table 6.12 Results of one-way ANOVA of Phyto-PAM measurements for the different surface finishes studied for granite SIN at the end of the colonization period studied (three months). Results are expressed as mean value ± standard deviation of three replicates. Different upper case letters indicate significant differences between surface finishes. *P*-values < 0.05 are indicated in bold type.

Surface finish	Chl *a* (μg cm^{-2})	Yield	$F_{0,470nm}$ / $F_{0,645nm}$
Polished	1.35 ± 0.23^{a}	0.61 ± 0.04	0.47 ± 0.02
Honed	2.11 ± 0.38^{ab}	0.61 ± 0.01	0.47 ± 0.01
Sawn	2.66 ± 0.37^{b}	0.61 ± 0.04	0.45 ± 0.02
Sanded	4.14 ± 0.58^{c}	0.61 ± 0.02	0.44 ± 0.02
ANOVA	**< 0.001** *F* = 25.1	0.998 *F* < 0.1	0.071 *F* = 3.5

The effects of incubation time and surface finish on the colour differences produced by biofilm growth during the three-month incubation period are shown in Table 6.13. The parameters ΔL^*, Δb^* and ΔH^*_{ab} were significantly affected by incubation time and surface finish, whereas Δa^* and ΔE^*_{ab} were only influenced by incubation time. The colour data at the end of the colonization period studied are shown in Table 6.14.

Table 6.13 Results of two-way repeated measures ANOVA of colour measurements for the different surface finishes studied for granite SIN, considering time of incubation as within-subjects factor and surface finish as between-subjects factor. *P*-values < 0.05 are indicated in bold type.

Source of variation	ΔL^*	Δa^*	Δb^*	ΔH^*_{ab}	ΔE^*_{ab}
Time	**< 0.001**	**< 0.001**	**0.001**	**< 0.001**	**< 0.001**
	F = 53.7	*F* = 34.9	*F* = 10.8	*F* = 31.3	*F* = 35.4
Surface finish	**0.025**	0.108	**0.044**	**0.010**	0.077
	F = 5.4	*F* = 2.8	*F* = 4.3	*F* = 7.7	*F* = 3.3
Time x Surface finish	0.060	0.492	0.622	0.184	0.328
	F = 2.9	*F* = 0.9	*F* = 0.7	*F* = 1.7	*F* = 1.3

Table 6.14 Results of one-way ANOVA of colour measurements for the different surface finishes studied for granite SIN at the end of the colonization period studied (three months). Results are expressed as mean value ± standard deviation of three replicates. Different upper case letters indicate significant differences between surface finishes. *P*-values < 0.05 are indicated in bold type.

Surface finish	ΔL^*	Δa^*	Δb^*	ΔH^*_{ab}	ΔE^*_{ab}
Polished	-8.27 ± 2.73^{a}	-5.13 ± 2.16	6.40 ± 3.13	4.36 ± 1.65^{ab}	11.68 ± 4.55
Honed	-9.66 ± 2.58^{ab}	-6.35 ± 1.66	10.64 ± 1.78	3.52 ± 0.86^{a}	15.73 ± 3.40
Sawn	-12.86 ± 3.18^{ab}	-6.92 ± 0.71	11.18 ± 0.83	4.10 ± 0.23^{ab}	18.45 ± 2.83
Sanded	-15.05 ± 1.24^{b}	-7.75 ± 0.56	7.67 ± 0.53	6.60 ± 0.45^{b}	18.59 ± 1.41
ANOVA	**0.042** *F* = 4.4	0.223 *F* = 1.8	**0.038** *F* = 4.6	**0.020** *F* = 5.9	0.097 *F* = 3.0

The results of EPS quantification in biofilms developed on the different surface finishes studied for granite SIN are shown in Figure 6.10. As in the study of the different lithotypes, ANOVA (Table 6.15) revealed that neither incubation time nor surface finish significantly affected EPS production by biofilms.

Table 6.15 Results of two-way ANOVA of EPS quantification in biofilms for the different surface finishes studied for granite SIN, considering time of incubation and surface finish as factors. *P*-values < 0.05 are indicated in bold type.

Source of variation	EPS (μg cm^{-2})
Time	0.678
	F = 0.4
Surface finish	0.618
	F = 0.6
Time x Surface finish	0.801
	F = 0.5

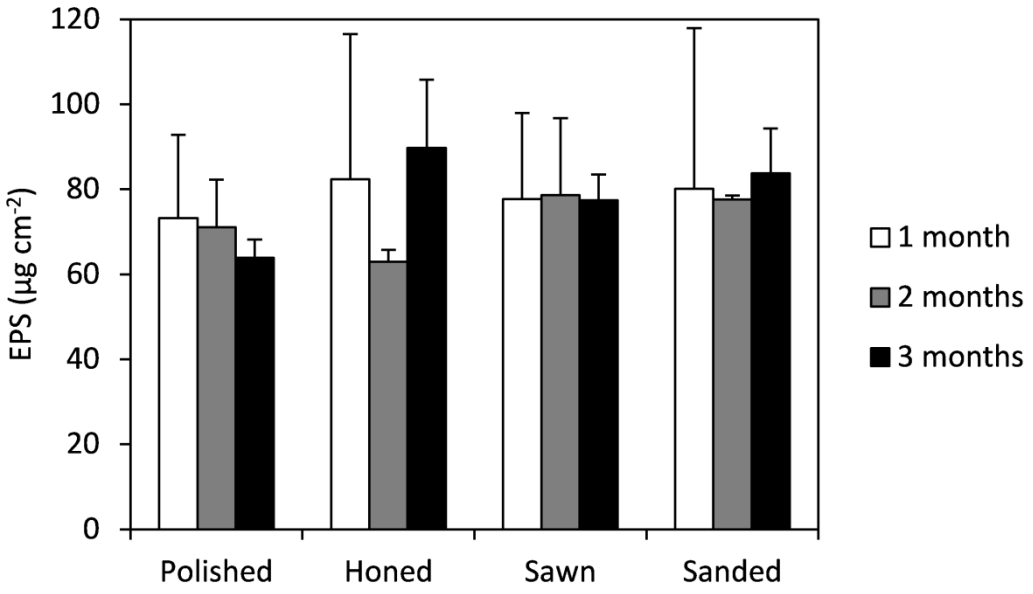

Figure 6.10 EPS, as the carbohydrate fraction, extracted in biofilms of the different surface finishes studied during the three-month incubation period, expressed as mean values of three replicates (error bars indicate standard deviations).

6.3.4 Relationships between stone properties and biofilm growth

A dendrogram derived from the hierarchical clustering of the variables relative to both stone properties and biofilm growth is shown in Figure 6.11. This graphical representation of the correlations between the different variables studied revealed interesting associations, and two large clusters were identified. The first included variables associated with the growth of biofilms such as the chl *a* content - the main biofilm biomass estimator in this study - and with several colour parameters and physico-chemical properties of the rocks. The second large cluster therefore includes variables that were probably not correlated with biofilm growth. The inclusion of variables such as the abrasion pH, which was grouped with the solubilised Ca^{2+}, and the bulk density, which was mainly correlated with the chemical composition of the stone, should be noted. This may be expected as the bulk density was highest in the basic rocks (NSA and LCL) containing large amounts of calcium plagioclase and ferromagnesian minerals. Although these factors were not grouped with chl *a*, the Pearson´s correlations (r) between chl *a* content and both abrasion pH (r = -0.804, p < 0.001) and bulk density (r = 0.545, p = 0.001) were relatively high. Neither Yield nor EPS were closely grouped with any other variable.

Focusing again on the first large cluster, some observations can be highlighted. The stone properties most closely correlated to the chl *a* content were the open porosity (r = 0.868, p < 0.001) and the capillary water content (r = 0.929, p < 0.001). Muscovite, only present in granites SAM, SIN and SRI, were grouped close to these variables. The colour difference parameter most closely correlated with chl *a* content was ΔH^*_{ab}, which was also grouped with the initial colour of the stone (a^*, b^* and C^*_{ab}). Other clusters confirmed expected relationships between the chemical and mineralogical composition of the stones, with the significant correlation between $F_{0,470nm}/F_{0,645nm}$ (as an indicator of the chlorophyta/cyanobacteria dominance) and the quartz and SiO_2 contents (r = 0.766, p < 0.001 and r = 0.685, p < 0.001, respectively).

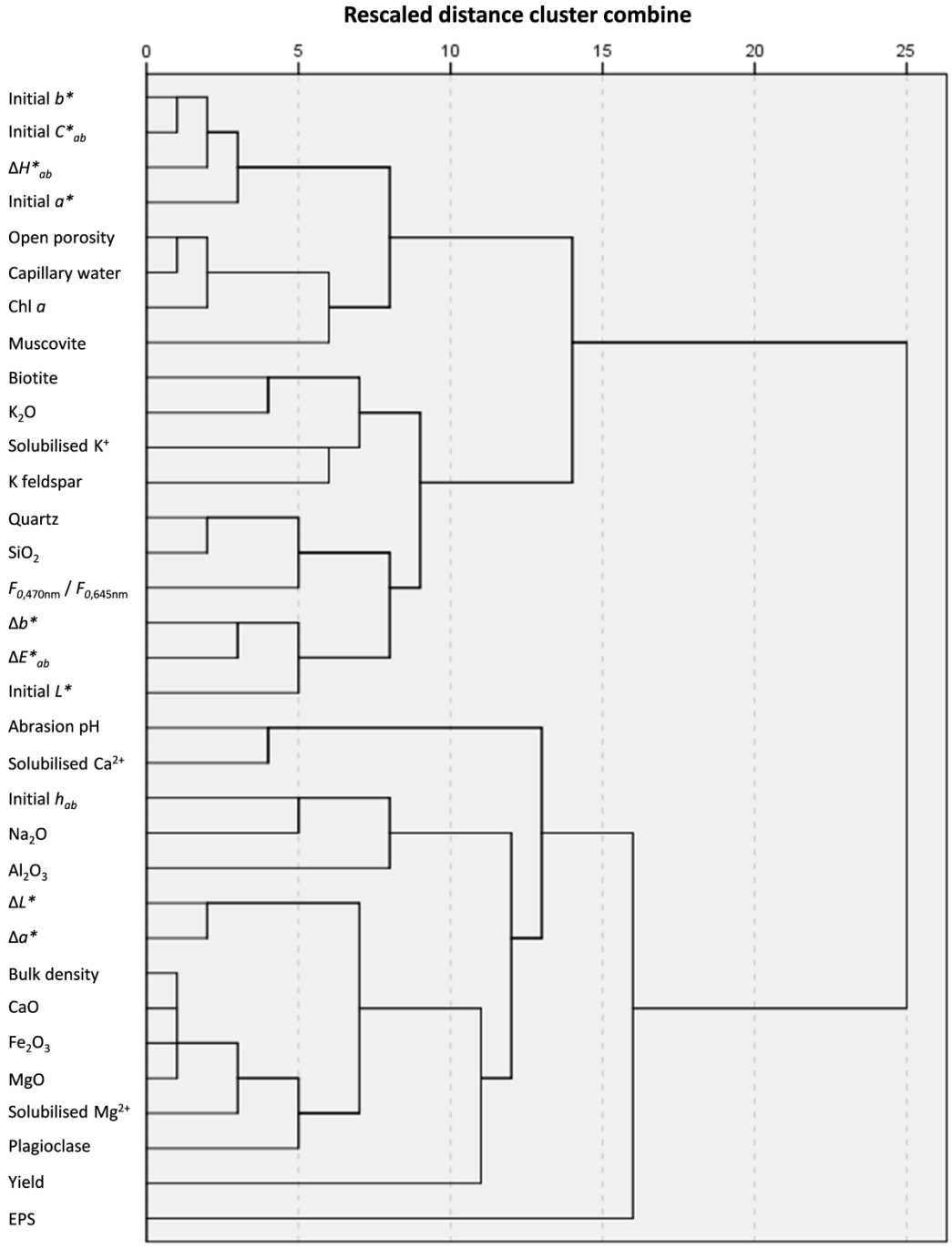

Figure 6.11 Dendrogram constructed by using between-groups average linkage of the standardised variables. Distances between clusters are based on Pearson's correlations.

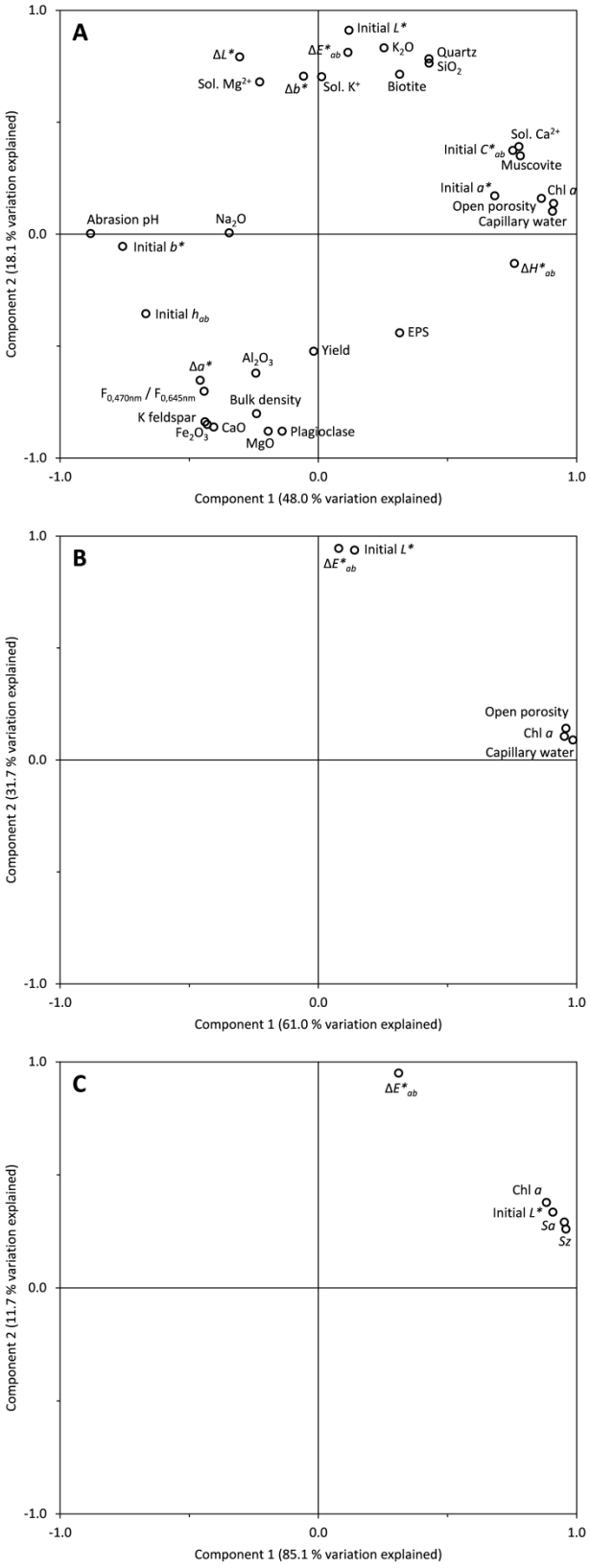

Figure 6.12 Graphical representation of PCA results. A) Including all the variables measured for the different lithotypes. B) After a selection of the most relevant variables. C) Including the variables measured for the different surface finishes studied for granite SIN.

A PCA was conducted to clarify the relationships between the stone properties and biofilm growth, (Figure 6.12). Initial screening including all the variables measured for the different lithotypes (Figure 6.12A) showed a similar pattern to that observed in the hierarchical clustering (Figure 6.11), as most of the variables included in one of the two large clusters formed also predominated over one of the first two components of the PCA. However, the two components only accounted for the 66.1 % of the total variance observed, and many of the variables did not contribute significantly to either of them. Careful selection of the most relevant variables, based on the maximisation of the variance explained and considering the least number of components possible, was therefore carried out in an attempt to simplify the bioreceptivity study (Figure 6.12B). Thus, a component mainly composed of the chl *a* content, the open porosity and the capillary water, and other component mainly formed by ΔE^*_{ab} and the initial L^* of the stone was able to explain 92.7 % of the variance (contributing to the 61.0 and 31.7 %, respectively). This is interesting as the biofilm growth (chl *a* content) was primarily affected by the open porosity and the capillary water in the stone (which are indeed closely correlated: $r = 0.956$, $p < 0.001$). However, the total colour change on the stone surface produced by the biofilm growth (ΔE^*_{ab}) was significantly correlated with the initial L^* (lightness) of the stone ($r = 0.796$, $p < 0.001$), rather than with the chl *a* content ($r = 0.191$, $p = 0.287$). These results suggest that the primary bioreceptivity of the different granites could be assessed by two separate components: the biofilm growth and colour change produced on the stone surface by the biofilm growth.

If the same statistical procedure is applied to the data derived from the granite (SIN) with different surface finishes (Figure 6.12C), the results differ from those observed for the different lithotypes (Figure 6.12B). The chl *a* contents were closely correlated with the roughness parameters *Sa* and *Sz* ($r = 0.939$, $p < 0.001$ and $r = 0.936$, $p < 0.001$, respectively). However, the initial L^* of the stone surface seems to be closely related to the roughness parameters *Sa* and *Sz* ($r = 0.961$, $p < 0.001$ and $r = 0.943$, $p < 0.001$, respectively), so that these four variables strongly influence the first component, which accounts for 85.1 % of the variance. The total colour change ΔE^*_{ab} thus remains as the only variable that dominates the second component, which now only explains 11.7 % of the variance. Moreover, the chl *a* content was significantly correlated with the ΔE^*_{ab} in these samples ($r = 0.627$, $p = 0.029$). This may indicate that the intrinsic physical properties of the different lithotypes (i.e. mainly open porosity and capillary

water) primarily affected the extent of the colonisation (i.e. chl *a* content) but do not necessarily determine the ΔE^*_{ab} produced by such colonisation, for which the initial L^* (lightness) of the stone surface is more important. However, considering a single lithotype with a different surface finish (i.e. the intrinsic physical properties of the stone remain constant), the roughness significantly affected both the chl *a* content and the initial L* of the stone surface, so that the ΔE^*_{ab} produced by the colonisation cannot be clearly separated from the extent of such colonisation. This interpretation is supported by the results of the one-way ANOVAs, in which the chl *a* content in the biofilms was significantly affected by the variety of granite (Table 6.7) and the surface finish (Table 6.12). However, the ΔE^*_{ab} was significantly affected by the variety of granite (Table 6.9) but not by the surface finish (Table 6.14), which could be attributed to the simultaneous effect of the roughness on the initial L^* of the stone (Table 6.5) in addition to on the chl *a* content in the biofilms.

6.3.5 Development of a bioreceptivity index (BI)

A bioreceptivity index for classifying the different granites studied on a scale according to their susceptibility to biological colonisation is proposed. Based on the above-described results, two different aspects of the biofilm growth were taken into account in developing the bioreceptivity index. The first aspect was the extent of the biological colonisation achieved, quantified by the chl *a* content, and mainly affected by the open porosity, capillary water and surface roughness of the stone, which can be considered as the bioreceptivity *sensu stricto*. The second aspect was the colour change produced on the stone surface by such colonisation, represented by ΔE^*_{ab}, and related to the initial clarity (L^*) of the stone, which can be considered as the bioreceptivity perceptible by the human eye. The bioreceptivity index (*BI*) can thus be divided in two components: a 'sub-index' for describing the extent of the susceptibility of the granite to biofilm growth (BI_{growth}) and a 'sub-index' for describing the potential colour change undergone by the stone because of a biofilm growth (BI_{colour}). Both components can be standardised to a range 0-10 for incorporation in a scale by the following formula:

$$A_{st} = 10\left(\frac{A - \min(A)}{\max(A) - \min(A)}\right)$$

where A_{st} is the standardised parameter; A is the real value of the parameter; min(A) is the minimum observed value of the parameter; and max(A) is the maximum observed value of the parameter. The reference parameter will be the chl *a* content or the ΔE^*_{ab} (for the calculation of BI_{growth} and BI_{colour}, respectively) achieved by the biofilm grown on a lithotype after the accomplishment of the standardised bioreceptivity experiment proposed. Both min(chl *a*) and min(ΔE^*_{ab}) will be assigned to a value of 0, since, although this value was not observed in any case, it can be considered as a total absence of colonisation. The value assigned for max(chl *a*) will be 4.14 µg cm^{-2} (sanded SIN, Table 6.12), and for max(ΔE^*_{ab}) it will be 24.25 (BCR, Table 6.9). Thus, the two components of the bioreceptivity index can be calculated as follows:

$$BI_{growth} = 10 \cdot \frac{chl\ a\ (\mu g\ cm^{-2})}{4.14\ \mu g\ cm^{-2}} \qquad \text{Equation 1}$$

$$BI_{colour} = 10 \cdot \frac{\Delta E^*_{ab}}{24.25} \qquad \text{Equation 2}$$

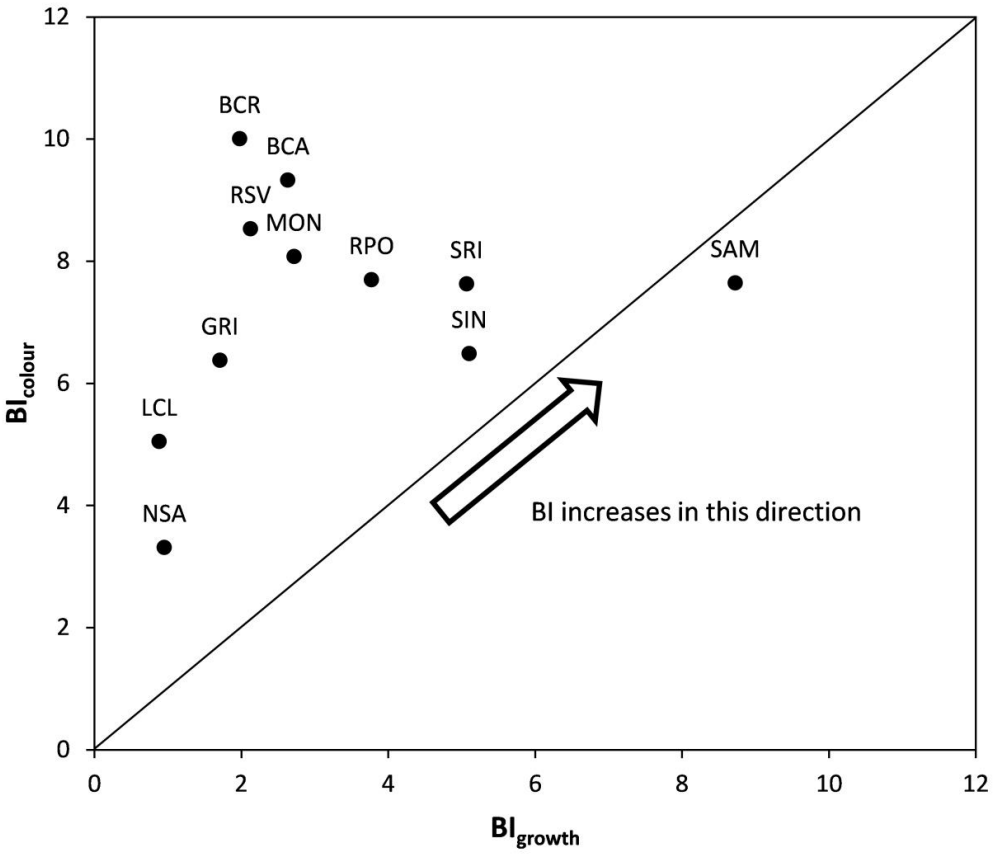

Figure 6.13 Values of BI_{growth} and BI_{colour} obtained for each of the different lithotypes studied.

The BI_{growth} and BI_{colour} values obtained for each of the different lithotypes studied (as mean values of three replicates) are depicted in Figure 6.13. The BI_{colour} values of some of the granites (e.g. BCR, BCA, RSV) were very high, indicating a considerable change in colour of the stone due to colonisation, even though the extent of the colonisation was relatively low, as indicated by the low BI_{growth} values. The opposite case, i.e. extensive biofilm growth and a slight colour change, did not occur to any of the granites, possibly because the darkest granites (NSA and LCL) were also those on which least microbial growth was observed.

The final *BI* will be calculated from the values obtained for BI_{growth} and BI_{colour}. As seen in Figure 6.13, if both components have an equal weight in the *BI*, the value of BI_{colour} will predominate over the value of BI_{growth} in almost all the cases. Therefore, in order to prevent this effect, the weight of BI_{growth} should be twice that of BI_{colour}. This produces more consistent results than with equal weighting, as the values of *BI* thus obtained for the different lithotypes are more homogeneously distributed on the 0-10 scale (Table 6.17). The bioreceptivity index (*BI*) can therefore be calculated as follows:

$$BI = \frac{2 \cdot BI_{growth} + BI_{colour}}{3} \qquad \text{Equation 3}$$

The values of *BI*, as well as the values of BI_{growth} and BI_{colour}, occur within an interval of 0-10, so that a qualitative classification, describing the associated primary bioreceptivity, can be assigned to each *BI* value. This enables use of the *BI* as a decision-making tool for rapid, simple selection of appropriate lithotypes (Table 6.16).

Table 6.16 Qualitative interpretation for the *BI* values.

Bioreceptivity index (*BI*)	Qualitative assignment
$BI \leq 2$	Very low bioreceptivity
$2 < BI \leq 4$	Low bioreceptivity
$4 < BI \leq 6$	Mild bioreceptivity
$6 < BI \leq 8$	High bioreceptivity
$BI > 8$	Very high bioreceptivity

The results of the *BI* calculated, for both the different granite varieties studied and the different surface finishes applied to granite SIN, are shown in Table 6.17. The *BI* enabled classification of the granites according to their primary bioreceptivity. Regarding the different lithotypes studied (all with honed surface finishes), SAM was the only granite classified as having 'very high bioreceptivity'. The SRI, SIN, RPO, BCA, BCR, MON and RSV were all classified as 'mildly bioreceptive', and GRI and LCL as having 'low bioreceptivity'. NSA was the only lithotype that showed 'very low bioreceptivity'. Comparing the different surface finishes studied for granite SIN, an increase in the *BI* from 'low bioreceptivity' to 'very high bioreceptivity' was observed in to the increase in the surface roughness, reflecting the strong influence of this parameter on the bioreceptivity.

Table 6.17 Classification of the different lithotypes and surface finishes studied according to their bioreceptivity index (*BI*).

Granite	BI_{growth}	BI_{colour}	*BI*	Classification
BCA	2.6	9.3	4.9	Mild bioreceptivity
BCR	2.0	10.0	4.7	Mild bioreceptivity
GRI	1.7	6.4	3.3	Low bioreceptivity
LCL	0.9	5.0	2.3	Low bioreceptivity
MON	2.7	8.1	4.5	Mild bioreceptivity
NSA	1.0	3.3	1.7	Very low bioreceptivity
RPO	3.8	7.7	5.1	Mild bioreceptivity
RSV	2.1	8.5	4.3	Mild bioreceptivity
SAM	8.7	7.6	8.4	Very high bioreceptivity
SIN	5.1	6.5	5.6	Mild bioreceptivity
SRI	5.1	7.6	5.9	Mild bioreceptivity
SIN polished	3.3	4.8	3.8	Low bioreceptivity
SIN honed	5.1	6.5	5.6	Mild bioreceptivity
SIN sawn	6.4	7.6	6.8	High bioreceptivity
SIN sanded	10.0	7.7	9.2	Very high bioreceptivity

6.4 DISCUSSION

6.4.1 Adaptation of the biofilms to the stone substratum

The extent of colonisation on the different granites was quantified by the chl *a* content, as a biomass estimator of the phototrophic biofilms formed. This proxy has been widely used in bioreceptivity studies (Saiz-Jimenez et al. 1995, Shirakawa et al. 2003, Prieto & Silva 2005, Escadeillas et al. 2009, Miller et al. 2009a, 2010b, Marques et al. 2015, Ferrándiz-Mas et al. 2016). Use of PAM fluorometry in the present study enabled reliable, non-destructive measurement of the chl *a* content (Figure 6.6). Other parameters such as the maximum quantum yield, the $F_{0,470nm}/F_{0,645nm}$ ratio and the EPS content of the biofilms also provided interesting information about the biological colonisation process.

Quantification of the EPS in the subaerial biofilms formed on the different lithotypes and surface finishes showed that neither the type of granite nor the surface roughness had significant effects on EPS production (Tables 6.10 and 6.15, Figures 6.8 and 6.10). The EPS content did not vary significantly over time (Tables 6.10 and 6.15), i.e. the EPS content at the end of the three-month colonisation period was not significantly different from that determined in the first month (Figures 6.8 and 6.10). The EPS content was not correlated with chl *a* content ($r = 0.261$, $p = 0.142$) (Figures 6.11 and 6.12), which suggests that microorganisms produce EPS during establishment on the stone surface, independently of their biomass. These results are consistent with the findings of an electron microscopy study showing that EPS production by biofilms growing on stone surfaces was not correlated with microbial growth and that EPS production reached maximum rates after the initial growth phase of the organisms (Kemmling et al. 2004). It therefore seems reasonable to assume that EPS production is required at the initial stage of stone colonisation for subsequent growth of the subaerial biofilms, and once the EPS matrix is formed, other factors will ultimately determine the extent of the growth. Moreover, we previously observed that the use of different multi-species phototrophic cultures (i.e. composed of different microbial communities) as inocula for biofilm formation on granite produced significantly different amounts of EPS (Chapter 5). The amounts of EPS produced by biofilm development therefore depend primarily on the requirements and/or capacities of the biofilm-forming microorganisms rather than on the bioreceptivity of the substratum. These findings are

especially important from the point of view of biodeterioration, in which the EPS matrix plays a central role, as water absorption and desiccation cause swelling and shrinkage of the biofilm matrix, exerting mechanical stresses on the mineral structure and finally leading to cracks and fissures in the stone (Warscheid & Braams 2000).

The photochemical efficiency of phototrophic organisms in the biofilm, assessed by measuring the maximum PSII quantum yield with a Phyto-PAM system, was affected by the incubation time, but not by the lithotype or surface finish (Tables 6.6 and 6.11). The quantum yield initially increased, from 0.55 to ca. 0.60-0.65, and then decreased until ca. 0.60 (Figures 6.7 and 6.9). This may be explained by adaptation of the culture from a planktonic to a biofilm state after inoculation, when only the more adaptable microorganisms survived, and then the global photosynthetic yield increased.

The $F_{0,470nm}$ / $F_{0,645nm}$ ratios were affected by incubation time, lithotype and surface finish (Tables 6.6 and 6.11), although the values at the end of the incubation period in the surface finishes studied were not significantly different (Table 6.12). This ratio can be considered as an indicator of the dominance of green algae (high values) or cyanobacteria (low values) and used to assess the adaptability of such microorganisms. Regarding the different granites studied, a decrease from the initial value was observed for LCL and NSA, while the ratio increased in the other lithotypes (Table 6.7 and Figure 6.7). BCR was unusual in that the values were low in the first half of the experiment but had increased notably by the end of the experiment. This indicates that the biofilm-forming microorganisms have different preferences for the different types of granite or variable capacity to adapt to the substrate. Unlike the chl *a* contents, the $F_{0,470nm}$ / $F_{0,645nm}$ ratios were more closely correlated with the chemical and mineralogical composition of the stone (r = 0.766, p < 0.001 for quartz, r = -0.687, p < 0.001 for plagioclase, r = 0.685, p < 0.001 for SiO_2, r = -0.673 for MgO, p < 0.001, r = -0.684, p < 0.001 for solubilised Mg^{2+}) rather than with the physical properties (r = 0.297, p = 0.094 for open porosity, r = 0.321, p = 0.069 for capillary water). Hence, chlorophyta seem to be more adaptable to acidic granite, while cyanobacteria seem to proliferate better on basic rocks. These relationships may involve the ecological characteristics and survival strategies of the different constituents of the biofilm (Villa et al. 2016), although more detailed research is needed to clarify this. Nonetheless, the observed adaptability in the multi-species phototrophic culture to the different varieties of granites demonstrates the advantage of the use of these types of inocula for

bioreceptivity studies, as previously stated by Miller et al. (2008). The capacity of the microbial community to adapt to different characteristics of the rocks enables evaluation of the bioreceptivity of the lithotypes to a wide range of pioneer colonisers, in a model resembling the complexity of natural colonisation.

6.4.2 Primary bioreceptivity of granitic rocks to phototrophic biofilms

The physical and chemical properties of the eleven varieties of granite under study differed significant (Tables 6.2-6.5, Figures 6.2-6.4), and relationships between these and the chl *a* content achieved were established (Figures 6.11 and 6.12). In relation to the physical properties of the granites, and based on Pearson's correlation coefficients, we found that biofilm growth was strongly affected by the open porosity ($r = 0.868$, $p < 0.001$) and the capillary water ($r = 0.929$, $p < 0.001$) of the stone and, to a lesser degree, by the bulk density ($r = -0.545$, $p = 0.001$). High open porosity could promote biofilm growth because the pores act as shelters where the microorganisms can easily attach, while high capillary water content can provide the moisture needed for proper biological development. The close correlation between these parameters ($r = 0.956$, $p < 0.001$) prevented evaluation of the relative weight of these effects. The influence of the surface roughness of the stone on its bioreceptivity was also assessed for one of the granites studied (SIN), and a very high correlation with the chl *a* content was observed ($r = 0.939$, $p < 0.001$ for *Sa* and $r = 0.936$, $p < 0.001$ for *Sz*). The open porosity, the capillary water and the bulk density are inherent properties of the stone and therefore cannot be manipulated. However, the surface roughness of building stones depends on the surface finish applied (Table 6.4). As the surface roughness has a very strong influence on bioreceptivity, the selection of smooth finishes could help to minimise the biological colonisation of highly susceptible lithotypes.

The chemical properties of the stones did not appear to affect the bioreceptivity as strongly as the physical properties. Abrasion pH, an indicator of the propensity of the rock to provide nutrients for the colonising organisms, was closely correlated with the chl *a* content of biofilms ($r = -0.804$, $p < 0.001$). However, the correlation was inverse, i.e. biofilm growth appeared to have been enhanced by low abrasion pH (within the range studied: 7.76 - 9.58). At low abrasion pH, fewer basic cations will be solubilised, as indicated by the direct correlation with the analytically measured amounts of solubilised cations ($r = 0.783$, $p < 0.001$ for Ca^{2+}; $r = 0.525$, $p = 0.002$ for Mg^{2+}). If the

solubilised cations act as nutrient sources for development of the biofilms, the correlation between the abrasion pH and the chl *a* should be direct rather than inverse. However, considering the abrasion pH as an indicator of weathering (Grant 1969, Taboada et al. 1996) helps in understanding the data. Granites SAM, SIN and SRI, in which mineral weathering processes were detected, also showed the lowest abrasion pH (Table 6.3) and the highest open porosity and capillary water content (Figure 6.3). We can therefore assume that abrasion pH is correlated with the bioreceptivity of the stone as it is also correlated with the physical properties of the stone (r = -0.768, $p < 0.001$ for open porosity; r = -0.855, $p < 0.001$ for capillary water); however, from a chemical point of view, the influence of abrasion pH is not important, or, at least, not as important as the physical properties related to the movement of water inside the stone. These observations are consistent with those of Prieto & Silva (2005), who stated that the bioreceptivity of granites is directly related to the degree of weathering of the rock rather than its capacity to supply cations or its 'potential fertility'. Similarly, neither the chemical nor the mineralogical composition of the granites seemed to have a significant influence on biofilm growth. Although muscovite was relatively closely correlated with chl *a* (r = 0.701, $p < 0.001$), its presence was limited to the three weathered granites (SAM, SIN and SRI), and a similar explanation to that proposed for abrasion pH is likely.

In general, although the crossed relationships between the parameters studied require careful interpretation of the results, the data suggest that the physical properties of the granites, mainly the open porosity, capillary water and surface roughness, have a stronger influence on the bioreceptivity than the chemical characteristics. Hence, weathered granites with high open porosity and capillary water contents are therefore the most susceptible to biological colonisation. These granites, which are commercialised in Spain under the denomination 'silvestre', are very popular for building restauration and also for ornamental purposes because their brownish colour is similar to that usually found in traditional buildings. The high bioreceptivity of these granites relative to that of sound granites must be highlighted.

The observed relationships between bioreceptivity and the properties of the granites, which can be graphically visualised in the dendrogram in Figure 6.11, are consistent with those observed by other authors. In a review of primary bioreceptivity studies carried out with several lithotypes, Miller et al. (2012) stated that, although the

findings were not conclusive, the porosity and the surface roughness of stones, along with their mineralogical nature, should be considered essential for assessing the bioreceptivity. In the particular case of granites, Prieto & Silva (2005) (to our knowledge, the only laboratory-based primary bioreceptivity study involving several varieties of granites carried out to date) related the bioreceptivity to surface roughness and four intrinsic properties of the stone: abrasion pH, bulk density, open porosity and capillary water. The findings of the present study are consistent with those of the aforementioned study, which showed a positive correlation between the amount of chl *a* measured and each of surface roughness, open porosity and capillary water and a negative correlation between the chl *a* and abrasion pH and bulk density. The authors developed an equation enabling estimation of the potential bioreceptivity of granite from the intrinsic properties of the stone. However, application of the equation to the data obtained in the present study produced some inconsistent results, such as extremely high chl *a* contents and negative values (data not shown). There are several possible explanations for this, including the fact that the authors used a cyanobacterial mixture as inocula, established different laboratory conditions for biofilm growth and, moreover, used stones with different properties from those used in the present study (e.g. the development of the equation involved granites with abrasion pH below 6 and open porosity above 10 %).

Comparison of the bioreceptivity of granites and of other types of rock revealed some findings contrasting with those of the present study. Marques et al. (2015) observed that only a small portion of the inoculated cyanobacteria was able to establish on the samples of granite and did not develop to the same extent as in schist samples. The abrasion pH of schists was lower and the bulk density was higher than in granite, while the open porosity and capillary water contents were similar in both lithotypes. Other factors, such as the chemical and mineralogical compositions of the stones, must therefore have been involved. Tiano et al. (1995) attributed the higher bioreceptivity of a granitic rock (than that of several limestones, sandstones and marbles) to its highly heterogeneous chemical composition. Miller et al. (2006) reported weaker colonization on granite than on carbonate rocks. The sensitivity of the microorganisms used as inoculum to the possible presence of toxic elements as minor components of the stone was suggested. These findings, unlike those of the present study, indicate that the chemical properties have a stronger influence on the bioreceptivity of granites than the

physical properties. This may be attributed to the very different chemical characteristics of the stones under study, which included granite, but also limestone, marble, sandstone and other construction materials. As the present study focuses on siliceous rocks with relatively similar chemical and mineralogical composition (Tables 6.1 and 6.2, Figure 6.2), the effect of very different chemical characteristics (e.g. those of carbonate rocks) on bioreceptivity could not be evaluated.

6.4.3 Bioreceptivity index

Several key features, such as the biological culture used as inoculum, the laboratory growth conditions, the properties of the materials to be tested and the techniques used for quantifying the biomass, should be carefully chosen for correct assessment of the primary bioreceptivity of stone. In the present study, we have tried to address these requirements fully in order to develop a bioreceptivity index, which has been identified as an essential tool in the fields of cultural heritage, ornamental stone and civil engineering (Guillitte 1995, Miller et al. 2012), but not yet established.

The multi-species phototrophic culture used as inoculum was representative of natural subaerial biofilms grown on stone substrata and capable of emulating environmental-like colonisation of granite in the laboratory (Chapter 3, Vázquez-Nion et al. 2016a and Chapter 5). This allows the results obtained to be consistently extrapolated to the real environment. The autotrophic nature of this culture also enabled assessment of the susceptibility of granite to pioneer colonisers, which provides an organic nutrient base for subsequent heterotrophic microflora, and the use of this type of culture can therefore be considered the most comprehensive way of evaluating the primary bioreceptivity of stones (Miller et al. 2008). The experimental set-up provided optimal conditions for the formation and growth of subaerial biofilms on granite in the laboratory (Chapter 5), enabling assessment of the intrinsic properties of the stone in relation to the bioreceptivity. Moreover, the conditions of temperature, light and moisture, as well as the incubation time, were clearly defined. The experiment was therefore reproducible and applicable to other types of material, representing a first step in standardising the protocols used in studying bioreceptivity.

The number and variety of granites tested was representative enough to involve wide ranges of the stone properties studied, for efficient evaluation of their effect on

bioreceptivity. All granite properties that may influence the bioreceptivity, within reason and on the basis of the results of previous studies (Tiano et al. 1995, Silva et al. 1997, Prieto & Silva 2005, Miller et al. 2006, 2012, Marques et al. 2015), were analysed. Wide ranges and significant differences between the lithotypes studied were observed for all of the properties (Tables 6.2-6.4, Figures 6.2-6.4). Finally, the techniques used to quantify the biomass should provide useful, reliable information about the stone colonisation process. Chlorophyll fluorescence and colour measurements have been extensively used for this purpose (Prieto et al. 2005, 2006a, Miller et al. 2009a, 2010b, Escadeillas et al. 2009, De Muynck et al. 2009b, Sanmartín et al. 2010, 2012, Tran et al. 2012, 2014, D'Orazio et al. 2014, Manso et al. 2014a, Marques et al. 2015). Both are non-destructive techniques and can be used for *in situ* measurements. Moreover, they provided complementary information concerning two different aspects of the biological colonisation. Chlorophyll fluorescence enabled estimation of the phototrophic biomass of subaerial biofilms, as well as assessment of their photosynthetic performance, while colour measurements were used to quantify the aesthetic impact of biofilm growth on granite surfaces (Prieto et al. 2006b). All of these important considerations were taken into account in the present study, enabling us to obtain consistent results regarding the primary bioreceptivity of granite and, thus, to propose a robust and well-founded bioreceptivity index.

The proposed *BI* (Equation 3) consists of two components related to two different aspects of biological colonisation: BI_{growth} (Equation 1) and BI_{colour} (Equation 2). BI_{growth} was calculated from the chl *a* content in the biofilms formed. It was designed to quantify the extent of the biological growth and was primarily affected by the open porosity, capillary water and surface roughness of the stones. BI_{colour} was calculated from ΔE^*_{ab}. It was designed to quantify the colour change undergone by the stone due to colonisation, which can be considered as the bioreceptivity perceptible by the human eye. BI_{colour} was included within *BI* because comparison of the results obtained for different lithotypes shows that the total colour change ΔE^*_{ab} is closely correlated with the initial lightness (L^*) of the stone but not with the biofilm biomass (chl *a*) (Figure 6.12). Light coloured stones can therefore undergo important colour changes due to biological colonisation, although the extent of such colonisation is low. This is an important factor for describing the bioreceptivity of stones used in construction, especially from the point of view of its aesthetically biodeteriorative effects. This is

consistent with the results obtained by Prieto et al. (2006b), who established ΔE^*_{ab} = 3.17 (corresponding to 0.04 µg chl *a* cm^{-2} of a cyanobacterial mixture) as the colour change from which the biological colonisation of granite can be appreciated by the human eye. The ΔE^*_{ab} values obtained in the present study (up to 24.25) are much higher than this threshold, indicating 'very intense' aesthetic impacts in some cases, following the qualitative classification developed by these authors. The important aesthetic impacts of biofilms on stone are thus considered within the *BI* through the component BI_{colour}.

The values of *BI*, BI_{growth} and BI_{colour} were adjusted to a scale of 0-10, to enable qualitative classification of the lithotypes on the basis of their primary bioreceptivity (Table 6.16). In cases where one of the two components of the *BI* is not required, as the information provided is not of interest, the bioreceptivity can be expressed within the same scale by the other component. For example, for enhancing the bioreceptivity of a facade, use of *BI* for selecting the most appropriate lithotype should focus on the potential biological growth, and the colour change produced may be considered an unimportant secondary effect. In this case, use of BI_{growth}, rather than *BI*, is recommended for selecting the stone. The qualitative classification proposed in Table 6.16 could be used in the same way, taking into account that only the biological growth is considered. Thus, BI_{growth}, BI_{colour} or *BI* can be used for selecting lithotypes, depending on the purpose of the selection, and qualitative interpretation of the values may be the same for all.

The experimental conditions used to obtain the chl *a* and ΔE^*_{ab} values, which are needed to calculate *BI*, were clearly defined in an attempt to standardise the method. The laboratory protocol could therefore be reproduced with other types of rock, in addition to granites, to enable comparison of the results. The bioreceptivity of eleven varieties of granite was assessed, revealing quite different degrees of bioreceptivity (Table 6.17). Calculation of *BI* for new granites will presumably fit within the scale proposed. However, calculation of the *BI* for other types of rocks (e.g. limestones, marbles, sandstones or artificial materials), which may vary more widely in their properties, may produce results that cannot be adapted to such a scale. For example, the *BI* values for rocks with higher open porosity than granites, and therefore presumably with higher bioreceptivity, may be much higher than 10. Thus, a rock with e.g. *BI* = 15 and a rock with e.g. *BI* = 9 would both be classified as having 'very high bioreceptivity'

despite showing quite different susceptibilities to colonisation. If this is observed in future bioreceptivity experiments, the qualitative interpretation of the *BI* values proposed in Table 6.16 must be adapted to the new values. This should be considered a strong point of the bioreceptivity index proposed, as the use of different scales to compare different types of rocks is possible. Thus, if necessary, specific scales could be developed for granitic rocks (that obtained in the present study), carbonate rocks, cements and even for different construction materials.

Finally, the main recommendations for correct calculation and application of the *BI* proposed are summarized as follows:

a) Calculation of the *BI* for a new lithotype should involve the following methodological considerations:

   i) Blocks of a new lithotype should be inoculated with a multi-species phototrophic culture that can adapt to the substratum and emulate environmental-like colonisation, and the amount of inoculum should be as similar as possible to that used in the present study (1.51 mg dry weight biomass in exponential growth phase for a surface of 16 cm^2, or equivalent).

   ii) Inoculated blocks should be incubated under the standardised growth conditions described in the present study (i.e. temperature 23 ºC; cool day light ~20 µmol photon m^{-2} s^{-1}, 12h light/dark photoperiod; ~95 % relative humidity and permanent access to water by capillarity) for three months.

   iii) The values of chl *a* content (µg cm^{-2}) and ΔE^*_{ab} derived from the biofilms formed at the end of the colonisation period should be used to calculate *BI*.

b) If the *BI* calculated for a new lithotype is much higher than 10, which will probably occur with materials that are more bioreceptive than granites, the qualitative interpretation of the *BI* values proposed in Table 6.16 will have to be adapted to the new values. If necessary, specific scales could be developed for the different types of rock and other construction materials, or for comparison between these.

c) If one of the two components of the *BI* (BI_{growth} and BI_{colour}) is not required, as the information provided by it is not of interest for whatever reason, the bioreceptivity can be expressed within the same scale by the other component. Hence, BI_{growth},

BI_{colour} or *BI* could be used to select lithotypes depending on the purpose of the selection. The same qualitative interpretation of the values could be used for all components.

6.5 CONCLUSIONS

Analysis of the chl *a* content, used to estimate the biomass of phototrophic biofilms formed on the stones, revealed significant differences in the extent of the colonisation on the different granites and surface finishes under study. Furthermore, the physical and chemical properties of the eleven varieties of granite studied, commonly used as construction material and ornamental stones, differed significantly, and relationships between these properties and their bioreceptivity were established. The primary bioreceptivity of the granites was affected by the physical characteristics of the stones rather than by the chemical composition, as biofilm growth was strongly enhanced by high open porosity, capillary water content and surface roughness. The amount of EPS produced by biofilms was not related to the extent of the colonisation, and EPS production primarily depended on the requirements and/or capacities of the biofilm-forming microorganisms rather than on the bioreceptivity of the substratum. This is particularly important from the point of view of biodeterioration, in which the EPS matrix plays a key role.

Use of a multi-species phototrophic culture as an inoculum (to represent a complex community of natural pioneer colonisers) and the application of a standardised laboratory protocol for growth of biofilms on stone, enabled us to develop a robust, well-founded bioreceptivity index (*BI*). The following equation (Equation 3) was proposed for calculating the *BI*:

$$BI = \frac{2 \cdot BI_{growth} + BI_{colour}}{3}$$

where (Equations 1 and 2, respectively):

$$BI_{growth} = 10 \cdot \frac{chl\ a\ (\mu g\ cm^{-2})}{4.14\ \mu g\ cm^{-2}} \qquad \text{and} \qquad BI_{colour} = 10 \cdot \frac{\Delta E^*_{ab}}{24.25}$$

and where BI_{growth} is the component of the *BI* that describes the susceptibility of the rock to biofilm growth; BI_{colour} is the component of *BI* that describes the potential colour

change undergone by the stone due to biofilm growth; chl *a* and ΔE^*_{ab} are the values reached by the biofilm grown on a stone on completion of the standardised bioreceptivity experiment. The values of *BI*, BI_{growth} and BI_{colour} are adjusted to a 0-10 scale, thus enabling qualitative classification of the granites depending on their primary bioreceptivity. The index can therefore be used as a decision-making tool for selecting appropriate lithotypes for building purposes.

CHAPTER 7
CONCLUDING REMARKS

7.1 CONCLUSIONS

The findings of this study have helped to improve our knowledge of the primary bioreceptivity of granites and other aspects related to the biological colonisation of stone surfaces. The proposed objectives were successfully accomplished, including the main purpose of the thesis: the development of a bioreceptivity index for granitic rocks. The most important conclusions reached are summarised below:

1. Analysis of five subaerial biofilms growing natural on the surface of historic granite buildings in Santiago de Compostela (NW Spain), by using next-generation sequencing (Pacific Biosciences) techniques for environmental barcoding, revealed complex microbial communities mainly composed of species of Chlorophyta (green algae) and Ascomycota (fungi) that are commonly associated with rocky substrata. The estimated species richness and diversity were higher for the fungal assemblages than for algae, and the fungal samples were more heterogeneous. The data supported the assumption that subaerial biofilms are ecosystems with relatively low algal diversity and that many of their common species are ubiquitous. The large number of unidentified OTUs also highlighted the need to enhance production of high-quality molecular datasets and increase the representation of subaerial biofilm-forming microorganisms in DNA sequence repositories.

2. Multi-species phototrophic cultures were obtained from natural subaerial biofilms. A period of one year was required to establish stable microbial communities in the

cultures, which can be used as inocula to reliably reproduce environmental-like colonization of granitic stone surfaces under laboratory conditions. Morphological characterization revealed that most taxa identified in the cultures, mainly members of Chlorophyta and Cyanobacteria, did not form part of the major biomass in the original biofilms, but can be considered common pioneer colonisers of building stone surfaces, including granite.

3. Comparison of the growth patterns of the different phototrophic multi-species cultures studied revealed that C5 was the most appropriate for use as an inoculum in experiments aimed at studying the bioreceptivity of granitic rocks. This culture, comprising several taxa including Bryophyta (*Syntrichia ruralis*), Charophyta (*Klebsormidium* sp.), Chlorophyta (*Bracteacoccus* sp., *Chlamydomonas* sp., *Chlorella* sp. and *Stichococcus bacillaris*) and Cyanobacteria (*Aphanocapsa* sp., *Leptolyngbya cebennensis*), proved particularly suitable for this purpose, mainly owing to its microbial richness, rapid adaptability to the substratum and high capacity for colonization.

4. The experimental protocol developed proved appropriate for inducing environmental-like colonisation on granite samples in the laboratory. The temperature (23ºC), light (~20 µmol photon m^{-2} s^{-1}, 12h light/dark photoperiod) and moisture (95% relative humidity and permanent access to water by capillarity) conditions contributed to successful growth of subaerial biofilms, induced by inoculation of multi-species phototrophic cultures on granite blocks. These conditions and the incubation time (three months) were clearly defined, in an attempt to standardise the protocols involved for the study of the bioreceptivity. The experiment is reproducible and applicable to other materials.

5. A method for extracting EPS from subaerial biofilms on rocky substrata was successfully developed. H_2SO_4 proved unsuitable as an extractant as it caused excessive cell lysis, while the optimisation of NaOH-mediated extraction by response surface methodology minimized cell lysis. Application of the proposed protocol provided the first (to our knowledge) quantitative data on EPS extracted from subaerial biofilms growing on stone: PN/PS ratio ranging between 0.06 and 0.60. This ratio is much lower than reported for other types of biofilm, suggesting

that subaerial biofilms may produce larger amounts of polysaccharides to enhance water retention and thus enable them to tolerate desiccation in dry environments.

6. The amounts of EPS produced by subaerial biofilms primarily depended on the requirements and/or characteristics of the biofilm-forming microorganisms, rather than on the bioreceptivity of the substratum, as neither the type of granite nor the surface roughness significantly affected EPS production in the phototrophic biofilms derived from culture C5. However, the use of different multi-species phototrophic cultures (i.e. composed of different microbial communities) as inocula for inducing biofilm formation produced significantly different amounts of EPS. Nonetheless, the EPS contents did not vary significantly over the incubation time (after the first month), suggesting that microorganisms produce the amounts of EPS required at the initial stage of establishment on the stone surface, independently of the subsequent biomass development.

7. The primary bioreceptivity of the granites was more strongly affected by the physical characteristics of the stones than by their chemical composition. Growth of phototrophic biofilms was strongly enhanced by high open porosity, capillary water content and surface roughness, and the bioreceptivity of weathered granites was higher than that of sound granites. The chl *a* content, derived from chlorophyll fluorescence measurements and used as a biomass estimator of the phototrophic biofilms formed on the stones, indicated significant differences in the extent of the colonisation achieved on the different granites and the granite with the different surface finishes. The physical and chemical properties of the eleven varieties of granite were also significantly different, and relationships between these and the primary bioreceptivity were established.

8. Chlorophyll fluorescence and colour measurements, the techniques used to monitor biofilm growth in the primary bioreceptivity experiment, provided complementary information concerning two different aspects of the biological colonisation. Chlorophyll fluorescence analysis enabled estimation of the phototrophic biomass of subaerial biofilms, and evaluation of their photosynthetic performance, while colour measurements enabled quantification of the aesthetic impact of the biofilm growth on granite surfaces, which was found to be more closely correlated with the initial lightness of the stone than with the final biofilm biomass.

9. The study findings enabled us to develop a robust and well-founded bioreceptivity index (*BI*) for granitic rocks. The proposed *BI* (Eq. 4) has two components: BI_{growth} (Eq. 2), which quantifies the extent of the biological growth, and BI_{colour} (Eq. 3), which quantifies the colour change undergone by the stone due to the colonisation, considered to be the bioreceptivity perceptible by the human eye. The values of *BI*, BI_{growth} and BI_{colour} were fitted to a scale of 0-10, for qualitative classification of the lithotypes according to their primary bioreceptivity (Table 16). The index can therefore be used as a decision-making tool for the selection of appropriate lithotypes for building purposes.

7.2. FUTURE PERSPECTIVES

The conclusions reached in this thesis, especially the development of the bioreceptivity index, lead to a number of possible new applications and future research. Two key challenges can be addressed in the future on the basis of the results obtained:

- The standardised experimental protocol developed in the study should be applied to as many different lithotypes as possible, both granites and other types of rocks or construction materials, in order to calculate the *BI* of each. This will improve our knowledge about bioreceptivity, as wider ranges in the physical and chemical properties of the materials would be taken into account under reproducible, and therefore comparable, conditions. The creation of a database concerning the primary bioreceptivity of a variety of construction materials would thus be possible. In this respect, the proposed *BI*, as well as the *BI* values obtained for the different lithotypes studied, should be exported to end-users (e.g. conservators/restorers, architects, engineers and distributors of ornamental or construction stone) for practical application. The *BI*, which classifies a stone within a scale of 0-10 associated with qualitative interpretation of the primary bioreceptivity, is simple to understand and could therefore be used as a decision-making tool for selecting appropriate lithotypes for use in new constructions and/or replacement in existing structures.

- The data on the primary bioreceptivity of the granites studied could also be used as reference values for the subsequent study of secondary and/or tertiary bioreceptivity. Several types of laboratory-induced weathering or artificial

treatments could be applied to the granites, causing alteration of their properties and, therefore, of their potential bioreceptivity. Application of the standardised protocol for inducing biological colonisation on sample blocks would enable comparison of the results thus obtained with the findings regarding primary bioreceptivity. These data could be used to quantify the effects of the alterations on the bioreceptivity and to evaluate whether the different types of granite respond in different ways to such alterations. This would provide useful additional information about the bioreceptivity of a particular type of stone. Application of the *BI* to the study of secondary and/or tertiary bioreceptivity is therefore possible.

USC
UNIVERSIDADE
DE SANTIAGO
DE COMPOSTELA

REFERENCES

Adav SS, Lee D-J. (2008) Extraction of extracellular polymeric substances from aerobic granule with compact interior structure. Journal of Hazardous Materials 154: 1120-1126.

Alcamo IE. (1997) Fundamentals of Microbiology. Menlo Park: Benjamin Cummings.

Anagnostidis K, Gehrmann CK, Gross M, Krumbein WE, Lisi S, Pantazidou A, Urzi C, Zagari M. (1991) Biodeterioration of marbles of the Parthenon and Propylaea, Acropolis, Athens - associated organisms, decay and treatment suggestions. In: Decrouez D, Chamay J, Zezza F. (Eds.) Proceedings of the 2nd International Symposium on the Conservation of Monuments in the Mediterranean Basin. Geneva: Ville de Genève - Muséum d'Histoire Naturelle & Musée D'Art et d'Histoire.

Barranguet C, van Beusekom SAM, Veuger B, Neu TR, Manders EMM, Sinke JJ, Admiraal W. (2004) Studying undisturbed autotrophic biofilms: still a technical challenge. Aquatic Microbial Ecology 34: 1-9.

Bartoli F, Casanova Municchia A, Futagami Y, Kashiwadanic H, Moond KH, Caneva G. (2014) Biological colonization patterns on the ruins of Angkor temples (Cambodia) in the biodeterioration vs bioprotection debate. International Biodeterioration & Biodegradation 96: 157-165.

Bezerra MA, Santelli RE, Oliveira EP, Villar LS, Escaleira LA. (2008) Response surface methodology (RSM) as a tool for optimization in analytical chemistry. Talanta 76: 965-977.

Box GEP, Wilson KB. (1954) The exploration and exploitation of response surfaces: some general considerations and examples. Biometrics 10: 16-60.

Burford EP, Kierans M, Gadd GM. (2003) Geomycology: fungi in mineral substrata. Mycologist 17: 98-107.

Burton K. (1956) Study of the conditions and mechanism of the diphenylamine reaction for the colorimetric estimation of deoxyribonucleic acid. Biochemical Journal 62: 315-323.

Caporaso JG, Kuczynski J, Stombaugh J, Bittinger K, Bushman FD, Costello EK, Fierer N, Peña AG, Goodrich JK, Gordon JI, Huttley GA, Kelley ST, Knights D, Koenig JE, Ley RE, Lozupone CA, McDonald D, Muegge BD, Pirrung M, Reeder J, Sevinsky JR, Turnbaugh PJ, Walters WA, Widmann J, Yatsunenko T, Zaneveld J, Knight R. (2010) QIIME allows analysis of high-throughput community sequencing data. Nature Methods 7: 335-336.

Chertov O, Gorbushina AA, Deventer B. (2004) A model for microcolonial fungi growth on rock surfaces. Ecological Modelling 177: 415-426.

CIE (1986) Colorimetry CIE Publication 15-2. Vienna: Central Bureau of the Commission Internationale l'Eclairage (CIE).

Comte S, Guibaud G, Baudu M. (2006) Relations between extraction protocols for activated sludge extracellular polymeric substances (EPS) and EPS complexation properties: Part I. Comparison of the efficiency of eight EPS extraction methods. Enzyme and Microbial Technology 38: 237-245.

Costerton JW. (2007) The biofilm primer. Heidelberg: Springer.

Crispim CA, Gaylarde CC. (2005) Cyanobacteria and biodeterioration of cultural heritage: a review. Microbial Ecolology 49: 1-9.

Cutler NA, Oliver AE, Viles HA, Whiteley AS. (2012) Non-destructive sampling of rock-dwelling microbial communities using sterile adhesive tape. Journal of Microbiological Methods 91: 391-398.

Cutler NA, Oliver AE, Viles HA, Ahmad S, Whiteley AS. (2013) The characterisation of eukaryotic microbial communities on sandstone buildings in Belfast, UK, using TRFLP and 454 pyrosequencing. International Biodeterioration & Biodegradation 82: 124-133.

De Muynck W, Maury Ramirez A, De Belie N, Verstraete W. (2009a) Evaluation of strategies to prevent algal fouling on white architectural and cellular concrete. International Biodeterioration & Biodegradation 63: 679-689.

De Muynck W, Maury A, De Belie N, De Bock J, Verstraete W. (2009b) Evaluation of anti-fouling strategies on aerated concrete by means of an accelerated algal growth test. In: Alexander MG, Beushausen HD, Dehn F, Moyo P. (Eds.) Concrete Repair, Rehabilitation and Retrofitting II, pp. 131-132.

D'Orazio M, Cursio G, Graziani L, Aquilanti L, Osimani A, Clementi F, Yéprémian C, Lariccia V, Amoroso S. (2014) Effects of water absorption and surface roughness on the bioreceptivity of ETICS compared to clay bricks. Building and Environment 77: 20-28.

Dubois M, Gilles KA, Hamilton JK, Rebers PA, Smith F. (1956) Colorimetric method for determination of sugars and related substances. Analytical Chemistry 28: 350-356.

Edgar RC. (2004) MUSCLE: multiple sequence alignment with high accuracy and high throughput. Nucleic Acids Research 32: 1792-1797.

Edgar RC. (2010) Search and clustering orders of magnitude faster than BLAST. Bioinformatics 26: 2460-2461.

Eggert A, Haubner N, Klausch S, Karsten U, Schumann R. (2006) Quantification of algal biofilms colonising building materials: chlorophyll a measured by PAM-fluorometry as a biomass parameter. Biofouling 22: 79-90.

EN 1925:1999. Natural stone test methods - determination of water absorption coefficient by capillarity. Belgium: European Committee for Standardization (CEN).

EN 1936:1999. Natural stone test method - determination of real density and apparent density, and of total and open porosity. Belgium: European Committee for Standardization (CEN).

Escadeillas G, Bertron A, Blanc G, Dubosc A. (2007) Accelerated testing of biological stain growth on external concrete walls. Part 1: Development of the growth tests. Materials and Structures 40: 1061-1071.

Escadeillas G, Bertron A, Ringot E, Blanc G, Dubosc A. (2009) Accelerated testing of biological stain growth on external concrete walls. Part 2: Quantification of growths. Materials and Structures 42: 937-945.

Ettl H, Gärtner G. (1995) Syllabus der Boden-, Luft- und Flechtenalgen. Stuttgart: Gustav Fischer Verlag.

Favero-Longo SE, Borghi A, Tretiach M, Piervittori R. (2009) In vitro receptivity of carbonate rocks to endolithic lichen-forming aposymbionts. Mycological Research 113: 1216-1227.

Fernández-Silva I, Sanmartín P, Silva B, Moldes A, Prieto B. (2011) Quantification of phototrophic biomass on rocks: optimization of chlorophyll-a extraction by response surface methodology. Journal of Industrial Microbiology & Biotechnology 38: 179-188.

Ferrándiz-Mas V, Bond T, Zhang Z, Melchiorri J, Cheeseman CR. (2016) Optimising the bioreceptivity of porous glass tiles based on colonization by the alga Chlorella vulgaris. Science of the Total Environment 563-564: 71-80.

Flemming HC, Wingender J. (2010) The biofilm matrix. Nature Reviews Microbiology 8: 623-633.

Gardes M, Bruns TD. (1993) ITS primers with enhanced specificity for Basidiomycetes - application to the identification of mycorrhizae and rusts. Molecular Ecology 2: 113-118.

Gaylarde CC, Gaylarde PM. (2005) A comparative study of the major microbial biomass of biofilms on exteriors of buildings in Europe and Latin America. International Biodeterioration & Biodegradation 55: 131-139.

Giannantonio DJ, Kurth JC, Kurtis KE, Sobecky PA. (2009) Effects of concrete properties and nutrients on fungal colonization and fouling. International Biodeterioration & Biodegradation 63: 252-259.

Gorbushina AA. (2007) Life on the rocks. Environmental Microbiology 9: 1613-1631.

Gorbushina AA, Broughton WJ. (2009) Microbiology of the atmosphere-rock interface: how biological interactions and physical stresses modulate a sophisticated microbial ecosystem. Annual Review of Microbiology 63: 431-450.

Grant WH. (1969) Abrasion pH, an index of chemical weathering. Clays and Clay Minerals 17: 151-155.

Gregor J, Jančula D, Maršálek B. (2008) Growth assays with mixed cultures of cyanobacteria and algae assessed by in vivo fluorescence: One step closer to real ecosystems? Chemosphere 70: 1873-1878.

Guillitte O. (1995) Bioreceptivity: a new concept for building ecology studies. Science of the Total Environment 167: 215-220.

Guillite O, Dreesen R. (1995) Laboratory chamber studies and petrographical analysis as bioreceptivity assessment tools of building materials. Science of the Total Environment 167: 365-374.

Gustavs L, Schumann R, Eggert A, Karsten U. (2009) In vivo growth fluorometry: accuracy and limits of microalgal growth rate measurements in ecophysiological investigations. Aquatic Microbial Ecology 55: 95-104.

Haaland PD. (1989) Experimental design in biotechnology. New York: Marcel Dekker.

Hoppert M, Berker R, Flies C, Kämper M, Pohl W, Schneider J, Ströbel S. (2002) Biofilms and their extracellular environment on geomaterials: methods for investigation down to nanometer scale. Geological Society of London, Special Publications 205: 207-215.

Jachlewski S, Jachlewski WD, Linne U, Bräsen C, Wingender J, Siebers B. (2015) Isolation of extracellular polymeric substances from biofilms of the thermoacidophilic archaeon Sulfolobus acidocaldarius. Frontiers in Bioengineering and Biotechnology 3: 123.

Kemmling A, Kämper M, Flies C, Schieweck O, Hoppert M. (2004) Biofilms and extracellular matrices on geomaterials. Environmental Geology 46: 429-435.

Keshari N, Adhikary SP. (2014) Diversity of cyanobacteria on stone monuments and building facades of India and their phylogenetic analysis. International Biodeterioration & Biodegradation 90: 45-51.

Kõljalg U, Nilsson RH, Abarenkov K, Tedersoo L, Taylor AFS, Bahram M, Bates ST, Bruns TD, Bengtsson-Palme J, Callaghan TM, Douglas B, Drenkhan T, Eberhardt U, Dueñas M, Grebenc T, Griffith GW, Hartmann M, Kirk PM, Kohout P, Larsson E, Lindahl BD, Lücking R, Martín MP, Matheny PB, Nguyen NH, Niskanen T, Oja J, Peay KG, Peintner U, Peterson M, Põldmaa K, Saag L, Saar I, Schüßler A, Scott JA, Senés C, Smith ME, Suija A, Taylor DL, Telleria MT, Weiß M, Larsson KH. (2013) Towards a unified paradigm for sequence-based identification of Fungi. Molecular Ecology 22: 5271-5277.

Komárek J, Anagnostidis K. (1999) Cyanoprokaryota. Part 1: Chroococcales. In: Ettl H, Gärtner J, Heynig H, Mollenhauer D. (Eds.) Süßwasserflora von Mitteleuropa 19/1. Stuttgart: Gustav Fisher, pp. 1-548.

Komárek J, Anagnostidis K. (2005) Cyanoprokaryota. Part 2: Oscillatoriales. In: Büdel BH, Gärtner J, Krienitz L, Schagerl M. (Eds.) Süßwasserflora von Mitteleuropa 19/2. München: Elsevier, Spektrum Akademischer Verlag, pp. 1-759.

Komárek J. (2013) Cyanoprokaryota. Part 3: Heterocytous Genera. In: Büdel BH, Gärtner J, Krienitz L, Schagerl M. (Eds.) Süßwasserflora von Mitteleuropa 19/3. München: Elsevier, Spektrum Akademischer Verlag, pp. 1-1130.

Lawrence JR, Nie TR, Swerhone GDW. (1998) Application of multiple parameter imaging for the quantification of algal, bacterial and exopolymer components of microbial biofilms. Journal of Microbiological Methods 32: 253-261.

Le Maitre RW. (2002) Igneous Rocks. A Classification and Glossary of terms. Recommendations of the IUGS Subcommission on the Systematics of Igneous Rocks. Cambridge: Cambridge University Press.

Liu H, Fang HHP. (2002) Extraction of extracellular polymeric substances (EPS) of sludges. Journal of Biotechnology 95: 249-256.

Lowry OH, Rosebrough NJ, Farr AL, Randall RJ. (1951) Protein measurement with the Folin phenol reagent. Journal of Biological Chemistry 193: 265-275.

Lozupone C, Knight R. (2005) UniFrac: a new phylogenetic method for comparing microbial communities. Applied and Environmental Microbiology 71: 8228-8235.

Macedo MF, Miller AZ, Dionísio A, Saiz-Jimenez C. (2009) Biodiversity of cyanobacteria and green algae on monuments in the Mediterranean Basin: an overview. Microbiology 155: 3476-3490.

Manso S, De Muynck W, Segura I, Aguado A, Steppe K, Boon N, De Belie N. (2014a) Bioreceptivity evaluation of cementitious materials designed to stimulate biological growth. Science of the Total Environment 481: 232-241.

Manso S, Mestres G, Ginebra MP, De Belie N, Segura I, Aguado A. (2014b) Development of a low pH cementitious material to enlarge bioreceptivity. Construction and Building Materials 54: 485-495.

Manso S, Calvo-Torras MA, De Belie N, Segura I, Aguado A. (2015) Evaluation of natural colonisation of cementitious materials: Effect of bioreceptivity and environmental conditions. Science of the Total Environment 512-513: 444-453.

Marques J, Vázquez-Nion D, Paz-Bermúdez G, Prieto B. (2015) The susceptibility of weathered versus unweathered schist to biological colonization in the Côa Valley Archaeological Park (north-east Portugal). Environmental Microbiology 17: 1805-1816.

McNamara CJ, Mitchell R. (2005) Microbial deterioration of historic stone. Frontiers in Ecology and the Environment 3: 445-451.

Miller AZ, Macedo MF. (2006) Mapping and characterization of a green biofilm inside of Vilar de Frades Church (Portugal). In: Fort R, Alvarez de Buergo M, Gomez-

Heras M, Vazquez-Calvo C. (Eds.) Heritage, Weathering and Conservation. London: Taylor & Francis, pp. 329-335.

Miller AZ, Dionísio A, Macedo MF. (2006) Primary bioreceptivity: a comparative study of different Portuguese lithotypes. International Biodeterioration & Biodegradation 57: 136-142.

Miller AZ, Laiz L, Gonzalez JM, Dionísio A, Macedo MF, Saiz-Jimenez C. (2008) Reproducing stone monument photosynthetic-based colonization under laboratory conditions. Science of the Total Environment 405: 278-285.

Miller AZ, Dionísio A, Laiz L, Macedo MF, Saiz-Jimenez C. (2009a) The influence of inherent properties of building limestones on their bioreceptivity to phototrophic microorganisms. Annals of Microbiology 59: 1-9.

Miller AZ, Laiz L, Dionísio A, Macedo MF, Saiz-Jimenez C. (2009b) Growth of phototrophic biofilms from limestone monuments under laboratory conditions. International Biodeterioration & Biodegradation 63: 860-867.

Miller AZ, Rogerio-Candelera MA, Laiz L, Wierzchos J, Ascaso C. Sequeira Braga MA, Hernandez-Marine M, Mauricio A, Dionisio A, Macedo MF, Saiz-Jimenez C. (2010a) Laboratory-induced endolithic growth in calcarenites: biodeteriorating potential assessment. Microbial Ecology 60: 55-68.

Miller AZ, Leal N, Laiz L, Rogerio-Candelera MA, Silva RJC, Dionisio A, Macedo MF, Saiz-Jimenez C. (2010b) Primary bioreceptivity of limestones used in Southern Europe monuments. In: Smith BJ, Gomez-Heras M, Viles HA, Cassar J. (Eds.) Limestone in the built environment: present day challenges for the preservation of the past. London: Geological Society, Special Publications, pp. 79-92.

Miller AZ, Sanmartín P, Pereira-Pardo L, Dionísio A, Saiz-Jimenez C, Macedo MF, Prieto B. (2012) Bioreceptivity of building stones: A review. Science of the Total Environment 426: 1-12.

Montgomery DC. (1997) Design and Analysis of Experiments. New York: John Wiley & Sons.

Ortega-Calvo JJ, Hernandez-Marine M, Saiz-Jimenez C. (1991) Biodeterioration of building materials by cyanobacteria and algae. International Biodeterioration 28: 165-185.

Ortega-Calvo JJ, Ariño X, Hernandez-Marine M, Saiz-Jimenez C. (1995) Factors affecting the weathering and colonization of monuments by phototrophic microorganisms. Science of the Total Environment 167: 329-341.

Papida S, Murphy W, May E. (2000) Enhancement of physical weathering of building stones by microbial populations. International Biodeterioration & Biodegradation 46: 305-317.

Pérez G, Coma J, Martorell I, Cabeza LF. (2014) Vertical Greenery Systems (VGS) for energy saving in buildings: A review. Renewable and Sustainable Energy Reviews 39: 139-165.

Perkins RG, Paterson DM, Sun H, Watson J, Player MA. (2004) Extracellular polymeric substances: Quantification and use in erosion experiments. Continental Shelf Research 24: 1623-1635.

Perry TD, Duckworth OW, McNamara CJ, Martin ST, Mitchell R. (2004) Effects of the biologically produced polymer alginic acid on macroscopic and microscopic calcite dissolution rates. Environmental Science & Technology 38: 3040-3046.

Price MN, Dehal PS, Arkin AP. (2010) FastTree 2 - Approximately Maximum - Likelihood Trees for Large Alignments. Plos One 5: e9490.

Prieto B, Rivas T, Silva B. (2002) Rapid quantification of phototrophic microorganisms and their physiological state through their color. Biofouling 18: 229-236.

Prieto B, Silva B, Lantes O. (2004) Biofilm quantification on stone surfaces: comparison of various methods. Science of the Total Environment 333: 1-7.

Prieto B, Silva B. (2005) Estimation of the potential bioreceptivity of granitic rocks from their intrinsic properties. International Biodeterioration & Biodegradation 56: 206-215.

Prieto B, Silva B, Aira N, Laiz L. (2005) Induction of biofilms on quartz surfaces as a means of reducing the visual impact of quartz quarries. Biofouling 21: 237-246.

Prieto B, Silva B, Aira N. (2006a) Methodological aspects of the induction of biofilms for remediation of the visual impact generated by quartz mining. Science of the Total Environment 370: 254-261.

Prieto B, Silva B, Aira N, Álvarez L. (2006b) Toward a definition of a bioreceptivity index for granitic rocks: Perception of the change in appearance of the rock. International Biodeterioration & Biodegradation 58: 150-154.

Prieto B, Sanmartín P, Silva B, Martínez-Verdú F. (2010) Measuring the Color of Granite Rocks: A Proposed Procedure. Color Research and Application 35: 368-375.

Prieto B, Sanmartín P, Silva C, Vázquez-Nion D, Silva B. (2014) Deleterious effect plastic-based biocides on back-ventilated granite facades. International Biodeterioration & Biodegradation 86: 19-24.

Prieto B, Sanmartín P. (2016) Air pollution and changes to the biology of urban fabric. In: Brimblecombe P. (Ed.) Urban pollution and changes to materials and building surfaces. London: Imperial college press, pp. 193-223.

Quast C, Pruesse E, Yilmaz P, Gerken J, Schweer T, Yarza P, Peplies J, Glöckner FO. (2013) The SILVA ribosomal RNA gene database project: improved data processing and web-based tools. Nucleic Acids Research 41: D590-D596.

Redmile-Gordon MA, Brookes PC, Evershed RP, Goulding KWT, Hirsch PR. (2014) Measuring the soil-microbial interface: Extraction of extracellular polymeric substances (EPS) from soil biofilms. Soil Biology and Biochemistry 72: 163-171.

Rifón-Lastra A, Noguerol-Seoane A. (2001) Green algae associated with the granite walls of monuments in Galicia (NW Spain). Cryptogamie Algologie 22: 305-326.

Rindi F. (2007) Diversity, distribution and ecology of green algae and cyanobacteria in urban habitats. In: Seckbach J. (Ed.) Algae and Cyanobacteria in Extreme Environments. Dordrecht: Springer, pp. 571-582.

Rippka R, Deruelles J, Waterbury JB, Herdman M, Stanier RY. (1979) Genetic assignments, strain histories and properties of pure cultures of cyanobacteria. Journal of General Microbiology 111: 1-61.

Saiz-Jimenez C, Ariño X, Ortega-Calvo JJ. (1995) Mechanisms of stone deterioration by photosynthesis-based epilithic biofilms. In: De Cleene M. (Ed.) Teractive physical weathering and bioreceptivity study on building stones, monitored by Computerized X-Ray Tomography (CT) as a potential non-destructive research tool. Protection and Conservation of the European Cultural Heritage. Ghent: Science Information Office, pp. 25-62.

Sánchez Delgado N, Rodríguez-Rey A, Calleja L, Ruiz de Argandoña VG, Camino C. (2014) Petrophysical interpretation of mechanical behaviour of ornamental stones from Galicia (Spain). In: Alejano R, Perucho A, Olalla C, Jiménez R. (Eds.) Rock Engineering and Rock Mechanics: Structures in and on Rock Masses. London: Taylor & Francis Group, pp. 257-260.

Sanmartín P, Aira N, Devesa-Rey R, Silva B, Prieto B. (2010) Relationship between color and pigment production in two stone biofilm-forming cyanobacteria (Nostoc sp. PCC 9104 and Nostoc sp. PCC 9025). Biofouling 26: 499-509.

Sanmartín P, Vázquez-Nion D, Silva B, Prieto B. (2012) Spectrophotometric color measurement for early detection and monitoring of greening on granite buildings. Biofouling 28: 329-338.

Scheerer S, Ortega-Morales O, Gaylarde C. (2009) Microbial Deterioration of Stone Monuments - An Updated Overview. Advances in Applied Microbiology 66: 97-139.

Schloss PD, Wescott SL, Ryabin T, Hall JR, Hartmann M, Hollister EB, Lesniewski RA, Oakley BB, Parks DH, Robinson CJ, Sahl JW, Stres B, Thallinger GG, Van Horn DJ, Weber CF. (2009) Introducing mothur: Open-source, platform-independent, community-supported software for describing and comparing microbial communities. Applied and Environmental Microbiology 75: 7537-7541.

Schreiber U, Gademann R, Bird P, Ralph PJ, Larkum AWD, Kuhl M. (2002) Apparent light requirement for activation of photosynthesis upon rehydration of desiccated beachrock microbial mats. Journal of Phycology 38: 125-134.

Seiffert F, Bandow N, Bouchez J, von Blanckenburg F, Gorbushina AA. (2014) Microbial colonization of bare rocks: laboratory biofilm enhances mineral weathering. Procedia Earth and Planetary Science 10: 123-129.

Sheng G-P, Yu H-Q, Yu Z. (2005) Extraction of extracellular polymeric substances from the photosynthetic bacterium Rhodopseudomonas acidophila. Applied Microbiology and Biotechnology 67: 125-130.

Sheng G-P, Yu H-Q, Li X-Y. (2010) Extracellular polymeric substances (EPS) of microbial aggregates in biological wastewater treatment systems: a review. Biotechnology Advances 28: 882-894.

Sherwood AR, Presting GG. (2007) Universal primers amplify a 23S rDNA plastid marker in eukaryotic algae and cyanobacteria. Journal of Phycology 43: 605-608.

Shirakawa MA, Beech IB, Tapper R, Cincotto MA, Gambale W. (2003) The development of a method to evaluate bioreceptivity of indoor mortar plastering to fungal growth. International Biodeterioration & Biodegradation 51: 83-92.

Silva B, Prieto B, Rivas T, Sánchez-Biezma MJ, Paz G, Carballal R. (1997) Rapid biological colonization of a granitic building by lichens. International Biodeterioration & Biodegradation 40: 263-267.

Taboada T, Romero R, García C. (1996) La disolución de abrasión en el estudio de los procesos de meteorización y edafogénesis. Nova Acta Científica Compostelana (Bioloxía) 6: 61-67.

Takahashi E, Ledauphin J, Goux D, Orvain F. (2009) Optimizing extraction of extracellular polymeric substances (EPS) from benthic diatoms: comparison of the efficiency of six EPS extraction methods. Marine and Freshwater Research 60: 1201-1210.

Tiano P, Accolla P, Tomaselli L. (1995) Phototrophic biodeteriogens on lithoid surfaces: an ecological study. Microbial Ecology 29: 299-309.

Tomaselli L, Lamenti G, Bosco M, Tiano P. (2000) Biodiversity of photosynthetic microorganisms dwelling on stone monuments. International Biodeterioration & Biodegradation 46: 251-258.

Tourney J, Ngwenya BT. (2014) The role of bacterial extracellular polymeric substances in geomicrobiology. Chemical Geology 386: 115-132.

Tran TH, Govin A, Guyonnet R, Grosseau P, Lors C, Garcia-Diaz E, Damidot D, Devès O, Ruot B. (2012) Influence of the intrinsic characteristics of mortars on biofouling by Klebsormidium flaccidum. International Biodeterioration & Biodegradation 70: 31-39.

Tran TH, Govin A, Guyonnet R, Grosseau P, Lors C, Damidot D, Devès O, Ruot B. (2014) Influence of the intrinsic characteristics of mortars on their biofouling by pigmented organisms: Comparison between laboratory and field-scale experiments. International Biodeterioration & Biodegradation 86: 334-342.

Urzì C, Realini M. (1998) Colour changes of Noto's calcareous sandstone as related to its colonisation by microorganisms. International Biodeterioration & Biodegradation 42: 45-54.

Urzì C, De Leo F. (2007) Evaluation of the efficiency of water-repellent and biocide compounds against microbial colonization of mortars. International Biodeterioration & Biodegradation 60: 25-34.

Vázquez-Nion D, Sanmartín P, Silva B, Prieto B. (2013) Reliability of color measurements for monitoring pigment content in a biofilm-forming cyanobacterium. International Biodeterioration & Biodegradation 84: 220-226.

Vázquez-Nion D, Rodríguez-Castro J, López-Rodríguez MC, Fernández-Silva I, Prieto B. (2016a) Subaerial biofilms on granitic historic buildings: microbial diversity and development of phototrophic multi-species cultures. Biofouling 32: 657-669.

Vázquez-Nion D, Echeverri-Díaz M, Silva B, Prieto B. (2016b) Extraction of extracellular polymeric substances (EPS) from subaerial biofilms developed on rocky substrata: optimization by response surface methodology. Analytical and Bioanalytical Chemistry (In press). doi: 10.1007/s00216-016-9752-0.

Viles HA. (2012) Microbial geomorphology: A neglected link between life and landscape. Geomorphology 157-158: 6-16.

Viles HA, Cutler NA. (2012) Global environmental change and the biology of heritage structures. Global Change Biology 18: 2406-2418.

Villa F, Pitts B, Lauchnor E, Cappitelli F, Stewart P. (2015) Development of a laboratory model of a phototroph-heterotroph mixed-species biofilm at the stone/air interface. Frontiers in Microbiology 6: 1251.

Villa F, Stewart PS, Klapper I, Jacob JM, Cappitelli F. (2016) Subaerial Biofilms on Outdoor Stone Monuments: Changing the Perspective Toward an Ecological Framework. BioScience 66: 285-294.

Wang Q, Garrity GM, Tiedje JM, Cole JR. (2007) Naive Bayesian classifier for rapid assignment of rRNA sequences into the new bacterial taxonomy. Applied and Environmental Microbiology 73: 5261-5267.

Warscheid T, Braams J. (2000) Biodeterioration of stone: a review. International Biodeterioration & Biodegradation 46: 343-68.

Wellburn AR. (1994) The spectral determination of chlorophylls a and b, as well as total carotenoids, using various solvents with spectrophotometers of different resolution, Journal of Plant Physiology 144: 307-313.

White TJ, Bruns T, Lee S, Taylor J. (1990) Amplification and direct sequencing of fungal ribosomal RNA genes for phylogenetics. In: Innis MA, Gelfand DH, Sninsky JJ, White TJ. (Eds.) PCR Protocols: a Guide to Methods and Applications. San Diego: Academic Press, pp. 315-322.

Whiting MF. (2002) Phylogeny of the holometabolous insect orders: molecular evidence. Zoologica Scripta 31: 3-15.

Wiktor V, Grosseau P, Guyonnet R. (2006) Biodétérioration d'une matrice cimentaire par les champignons: influence du vieillissement accéléré sur le développement fongique. Matériaux & Techniques 94: 507-515.

Wiktor V, De Leo F, Urzì C, Guyonnet R, Grosseau Ph, Garcia-Diaz E. (2009) Accelerated laboratory test to study fungal biodeterioration of cementitious matrix. International Biodeterioration & Biodegradation 63: 1061-1065.

Wiktor V, Grosseau Ph, Guyonnet R, Garcia-Diaz E, Lors C. (2011) Accelerated weathering of cementitious matrix for the development of an accelerated laboratory test of biodeterioration. Materials and Structures 44: 623-640.

Wingender J, Neu TR, Flemming HC. (1999) Microbial extracellular polymeric substances: characterisation, structure and function. Berlin: Springer.

Zhu L, Yu H, Liu Y, Qi H, Xu X. (2015) Optimization for extracellular polymeric substances extraction of microbial aggregates. Water Science and Technology 71: 1106-1112.

Zurita YP, Cultrone G, Castillo PS, Sebastián E, Bolívar FC. (2005) Microalgae associated with deteriorated stonework of the fountain of Bibatauín in Granada, Spain. International Biodeterioration & Biodegradation 55: 55-61.

USC
UNIVERSIDADE
DE SANTIAGO
DE COMPOSTELA

FIGURE INDEX

TABLE INDEX

AGRADECIMIENTOS / ACKNOWLEDGEMENTS

Quiero destacar el inestimable apoyo que he recibido durante esta etapa, tanto a nivel académico como personal, de mis directoras Bea y Beni. Esta tesis no hubiera sido posible sin la confianza que depositaron en mí desde el primer día y por ello les estaré siempre agradecido.

También me gustaría agradecer la ayuda y el buen ambiente ofrecido por todos los compañeros y compañeras del departamento, que hicieron del trabajo en el laboratorio una experiencia agradable y enriquecedora.

Por último, agradecer el apoyo de toda mi familia y amigos, siempre presentes, y en especial el de Micaela, quien ha conseguido mantener mi ánimo alto durante todos estos años.